Differentiation of effector and memory $CD8^+$ T cells during HSV1 infection

A Thesis

Submitted for the Degree of

Doctor of Philosophy

In the Faculty of Science

By

Dhaneshwar Kumar

Department of Biological Sciences,

Indian Institute of Science Education and Research (IISER) Mohali

Sector 81, Knowledge City, S. A. S. Nagar, Manauli PO, Mohali, 140306. Punjab, India.

2019

Dedicated to
Mummy and Papa

INDIAN INSTITUTE OF SCIENCE EDUCATION AND RESEARCH MOHALI

Sector - 81, Knowledge City, P.O. Manauli
S.A.S. Nagar, Mohali, Punjab - 140 306, India

DECLARATION

I hereby declare that the matter embodied in this thesis entitled "**Differentiation of effector and memory CD8$^+$ T cells during HSV1 infection**" is the result of investigations carried out by me under the supervision of **Dr. Sharvan Sehrawat** at the Department of Biological Sciences, Indian Institute of Science Education and Research (IISER) Mohali, SAS Nagar Mohali, India. This work has not been submitted in part or full for the award of any degree, a diploma or a fellowship to any other university or institute. Whenever contributions of others are involved, every effort is made to indicate it clearly with due acknowledgments. In keeping with the general practice of reporting scientific observations, acknowledgments have been made whenever the work was described based on the findings of other investigators. Any omission that might have occurred due to oversight or error in judgment is regretted. A complete bibliography of the books and journals referred to is given at respective section of the thesis.

Dhaneshwar Kumar

Date:

Place:

In my capacity as the supervisor of the candidate's thesis work, I certify that the above statements by the candidate are true to the best of my knowledge.

Dr. Sharvan Sehrawat
Assistant Professor
Department of Biological Sciences
Indian Institute of Science Education and Research Mohali

Date:

Place:

ACKNOWLEDGEMENTS

Writing this thesis has been fascinating and extremely rewarding. As I reached to the end of this journey, I recollect lot of memories of all the people who have helped me in bringing this journey to a fruitful end. Though the written words have a general tendency to mislead the feeling of gratitude to bland formality, it is the only means to make the feeling of "Thanks". I would like to thank a number of people who have contributed to the final result in many different ways:

To commence with, I pay my obeisance to the almighty ***GOD*** *to have bestowed upon me good health, courage, inspiration, zeal and the light. With high esteems and profound regards, I take this opportunity to express my indebtedness to my supervisor,* ***Dr. Sharvan Sehrawat****, for his invaluable expert guidance, unremitting encouragement, avid interest and outstanding help throughout the course of my study for carving another milestone in my academic journey. I would like to genuinely acknowledge his enlightening guidance and support and for being a tremendous mentor for me. I sincerely thank him for immense help in planning and execution of the research work.*

Apart from my mentor I will always be indebted to my doctoral committee members ***Dr. Rajesh Ramachandran*** *and* ***Dr. Mahak Sharma*** *for providing me their scholarly suggestions, scientific advice, encouragement and constant inspiration during my whole research work.*

I take it as an opportunity to thank the ***Director IISER Mohali*** *for providing all the necessary facilities required for a conducive research environment.*

I would like to extend my profound gratitude to the staff of animal house facility, ***Dr. Chander Shekhar****,* ***Bhavin Kansara, Devender Kumar*** *and* ***Guru Prasad*** *for their constant and timeless support.*

I also wish to thank ***Prateek Arora*** *for his timeless technical help in conducting my flow cytometry experiments.*

I extend my grateful thanks to my lab mates ***Manpreet Kaur****,* ***Sramona Kar, Roman Sarkar, Sudhakar Singh, Inamur Rahman, Surbhi Dahiya, Syed Azeez Tehseen, Yashu Sharma, Jasreen Kaur*** *and* ***Abhishek Dubey*** *for their cooperation and creating a wonderful working environment.*

*Apart from IISER Mohali, I express my thanks to **Dr. Ranjai Kumar, Dr. Parveen Kaushik, Dr. Manish Patel, Dr. Vijay Kumar, Dr. Ashish Dubey, Shubham Chauhan, Ramandeep Sharma, Paramveer Singh Dhillon** and **Amal Mathew** for their timely help and kind assistance during my research work simultaneously creating a stimulating and fun environment to learn and grow.*

*I wish to express my gratitude to my power backup **Abhishek, Swapnil, Anil, Dhiraj, Divya, Pooja, Narendra and Radha** who were there whenever I was in need, worked as stress relievers and played a crucial role in sustaining the zeal in my professional as well as personal life.*

I thank my friends for always backing me up and recharging me whenever I was down.

I acknowledge the Department of Science and Technology (DST) for providing me Scholarship to perform my work comfortably and a platform where I can scale the greatest heights in my carrier.

*Words are insufficient to express my indebtedness to my family who supported me all the way. All the blessings and inspiration from my **Mummy**, **Papa** and **Bhabhi** (**Sunita & Puja**) made it possible to complete the present work. A very special thanks to my niece **Harshit** and **Ishaan** for cheering my mood always**.** I thank to my elder brothers **Randhir** and **Pintu** for their constant care and love which acted as energy booster. I am also thankful to new member of our family **Aashi** as she brought the bundle of happiness back in our family.*

Apart from the above mentioned there are many hands, learned minds and good hearts that have helped me to walk on the right track of life. I shall ever remain indebted to all of them.

DHANESHWAR KUMAR

Preamble

All human population worldwide is infected with herpesviruses and most individuals develop one or the other immunopathological conditions manifested in critical organs. Such reactions are generally treated using glucocorticoids but their effects on virus-specific $CD8^+$ T cells remain less well explored. $CD8^+$ T cells are crucial for viral control. We show a dichotomy in the effects of dexamethasone, a synthetic analogue of glucocorticoid, on virus-specific quiescent (naive and memory) and effector $CD8^+$ T cells. Accordingly, dexamethasone induced apoptosis in naïve as well as virus-specific memory $CD8^+$ T cells but spared effector cells from killing as the latter population downregulated Nr3c1, a specific receptor for the glucocorticoids. Dexamethasone induced attrition of naïve and memory $CD8^+$ T cells compromised anti-viral $CD8^+$ T cells immunity against a subsequent infection but at the same time its transient exposure of effector cells augmented their function, inflammatory tissue homing potential as well as their transition into memory cells. The effects observed were generic as the differentiating $CD8^+$ T cells during both α-HSV1 and γ-MHV68 herpesvirus infections downregulated their Nr3c1. Surprisingly, dexamethasone also activated $CD8^+$ T cells in the absence of an overt TCR stimulation. Our study therefore calls into question the logic of corticosteroid therapy used for managing persistent inflammatory reactions. At the same time we also described a strategy to harness their untapped potential in promoting immunological memory.

In the second part of the study, we identified and characterized HSV1 specific $CD8^+$ T cells in experimentally infected zebrafish, a model system that offers a real time tracking of cellular dynamics *in vivo*. We generated class I MHC tetramer for probing the kinetics of virus-specific $CD8^+$ T cells during HSV1 infection and demonstrated a rapid expansion of virus-specific $CD8^+$ T cells both in the acute stage as well as upon their recall with a secondary homologous challenge. The expanded cells upregulated effector molecules and

helped control the viral growth. Therefore, zebrafish could potentially serve as a model system to decipher the differentiation pathways of antigen-specific $CD8^+$ T cells and their dynamics in live animals. Our results further suggest for an evolutionary conserved and functional adaptive immune cell homeostatic mechanisms activated during viral infection across vertebrates.

Table of Contents

PART – I …… 1

BACKGROUND AND OVERVIEW ……...……... 1

Herpes Simplex Virus Infection …… 2

HSV1 entry ……..…….... 3

Disease caused by HSV1 ..…….... 5

HSV1 recognition and response by immune cells ..…….... 5

Role of NK cells during HSV1 infection ...……..…. 8

Role of T cells in HSV1 infection and pathogenesis ……..…….. 9

TCR mediated T cell activation ...……...…… 11

Role of first signal …….……11

Role of second signal during T cell activation ...…… 12

Role of third signal during T cell induction …….……..……...… 13

Migration of activated $CD8^+$ T cells to infection site ...……..... 15

Role of $CD8^+$ T cells during HSV1 infection ……..…… 16

Immunopathology during/after HSV1 infection …….…….. 17

Immunoregulatory strategies to dampen immunopathology ……..……. 18

Immunosuppression by endogenous mechanisms …….……... 19

Strategies to boost immunosuppressive mechanisms …….…….. 21

Dexamethasone as an immunosuppressant …….…….. 22

The existing models of HSV1 infection and the resulting pathologies ……..…23

Zebrafish as a promising model for addressing unresolved questions …...…… 26

Conclusions ……...……..……...28

List of references ……..… 30

APPENDIX ……..……..…... 55

PART – II …… 57

DIVERGENT EFFECTS OF A TRANSIENT CORTICOSTEROID THERAPY ON QUUISCENT AND EFFECTOR VIRUS-SPECIFIC CD8$^+$ T CELLS …….. 57

Abstract ..……...…….... 58

Introduction ..……...…… 59

Materials and Methods ..……...…….…..... 61

Mice and viruses …….…….. 61

Antibodies, T cells isolation kits and other pharmacological reagents ……... 61

Cell staining for flow cytometry …….…… 62

Measuring the influence of neutralizing anti-CXCR3 antibody on cellular migration to inflammatory tissues in dexamethasone treated mice …...…….... 63

Intracellular cytokine staining (ICCS) of CD8$^+$ T cell ..……...… 63

Degranulation staining ..…….. 63

Ki67 staining ..…….…….…..... 64

Analysis of mRNA expression for different molecules in CD8$^+$ T cell subsets upon dexamethasone treatment ..……64

***Ex vivo* and *in vivo* assays to measure differential killing of CD8$^+$ T cell subsets ……..…….…… 65**

Measuring the influence of dexamethasone on immune cell population in HSV1 infected animals ..…….. 66

Measuring the responsiveness of dexamethasone pre-treated animals to a subsequent infection ..…….. 67

***In vivo* CTL assay ..……...……... 68**

Histopathology …...…….. 68

Plaque forming assays …...…….. 69

Statistical analysis …...……...…….. 69

Results ..…….. 70

Dexamethasone alters the distribution of $CD8^+$ T cells during herpesvirus Infection ..…….…... 70

Dexamethasone promotes CXCR3 mediated migration of $CD8^+$ T cells to inflammatory sites ……...…….. 72

Dexamethasone preferentially induces apoptosis of naive $CD8^+$ T cells ……...…75

A transient dexamethasone therapy compromised hosts' ability to respond to a subsequent infection ..……..76

Virus-specific $CD8^+$ T cells modulate the expression of glucocorticoid receptor, Nr3c1 during their differentiation ……. 78

A transient dexamethasone treatment causes bystander activation of $CD8^+$ T cells …….. 81

A brief exposure of activated $CD8^+$ T cells to dexamethasone alters their proliferative potential and conversion into effector memory cells …….. 83

Discussion …….. 85

List of References ……. 91

APPENDIX ……... 97

PART – III ……. 130

IDENTIFYING AND CHARACTERIZING VIRUS-SPECIFIC CD8$^+$ T CELLS IN HERPES SIMPLEX VIRUS 1 INFECTED ZEBRAFISH 130

Abstract ……..…….. 131

Introduction ……...……...…. 132

Materials and Methods ..……...…. 134

Zebrafish husbandry and their infection with HSV1 …… 134

***In vitro* proliferation assays …….. 134**

Sequence analysis of class I MHC molecules and their comparison with mouse H-2K^b ……...…… 134

Cloning, expression and purification of zebrafish class I MHC molecule ..….. 135

Generation of class I MHC tetramers …...……... 136

Analysis of single cell suspension using flow cytometry ……...……...….... 137

Detection and characterization of antigen specific T cell using flow cytometry …….…... 137

Quantitative PCR for effector molecules and viral load determination ....….... 137

Viral load determination using plaque assays …….…… 138

Statistical analysis ……..…….……... 139

Results and discussion ……..…….…… 139

HSV1 infection of zebrafishes ……...…… 139

Measuring anti-HSV1 immunity in infected zebrafishes ……...… 140

Generation of Uda-MHCI tetramer for detecting HSV1 specific CD8$^+$ T cell...141

Detecting and measuring the kinetics of HSV1 specific CD8$^+$ T cells during virus infection ……...…….. 144

HSV1 expanded lymphocytes express effector molecules ……..…… 146

Conclusions ……...……...…… 147

List of References ……..... 150

APPENDIX …….. 156

SUMMARY AND CONCLUSIONS ……... 169

Table of Figures

PART I

Figure 1. 1 HSV1 induced stromal keratitis and its management by immunosuppressive therapy. ……...56

PART II

Fig. 2.1 Dexamethasone therapy induces altered response in HSV1 infected animals. ..98

Fig. 2.2 Effect of glucocorticoid on immune cells. ……...…….100

Fig. 2.3 Effect of different dose of dexamethasone on virus specific $CD8^+$ T cells. …...101

Fig. 2.4 Dexamethasone modulates tissue homing molecules in $CD8^+$ T cells during HSV1 infection. ……..…….103

Fig. 2.5 Measuring chemokine receptors in $CD8^+$ T cells HSV1 infected mice that received either the diluent or dexamethasone. …….. 105

Fig. 2.6 A transient dexamethasone therapy induces CXCR3 mediated $CD8^+$ T cells migration to tissue sites. ……107

Fig. 2.7 Naive $CD8^+$ T cell are more susceptible to glucocorticoid-induced cell death. …….…...109

Fig. 2.8 Glucocorticoid treatment compromises the host's ability to mount an efficient $CD8^+$ T cells response to a subsequent infection. …….....…….…112

Fig. 2.9 Transcriptional profile of virus expanded $CD8^+$ T cells and susceptibility of memory $CD8^+$ T cells to dexamethasone. ……...…….…115

Fig. 2.10 mRNA expression on naive and activated $CD8^+$ T cells. …….117

Fig. 2.11 Dexamethasone therapy causes bystander activation of $CD8^+$ T cells. ……..119

Fig 2.12 Treatment of HSV1 infected mice with dexamethasone does not alter $CD8^+$ T cell memory generation. ……....…….121

Fig 2.13 A transient dexamethasone therapy induces enhanced proliferation and memory precursor phenotype in $CD8^+$ T cells. ……123

Fig 2.14 A demonstration that brief exposure of in vitro stimulated $CD8^+$ T cells enhances their proliferation potential. …….…...125

Fig 2.15 A brief exposure of activated $CD8^+$ T cells with dexamethasone enhance their survival and conversion into protective effector memory cells. ……...…...127

Fig 2.16 A proposed model to elucidate the role of glucocorticoids during differentiation of $CD8^+$ T cells. ……...…….....129

PART III

Fig. 3.1 HSV1 infection in zebrafish and viral reactivity of immune cells. ……...….157

Fig. 3.2 Identification of putative binding MHCI molecule for SSIEFARL peptide. ...159

Fig. 3.3 Generation of MHCI tetramer for HSV1 specific T cell detection. ……..……161

Fig. 3.4 Identifying virus-specific T cells in response to HSV1 infection in zebrafish. 163

Fig. 3.5 Cytokines production abilities of lymphocytes isolated from HSV1 infected zebrafish. ……165

Fig. 3.6 Uda monomer generation with other peptides. ……...167

List of Table/s

PART I

Table 1. Diseases caused by HSV1. ……..5

ABBREVIATIONS

HSV-1, 2	Herpes Simplex Virus 1, 2
MHV68	Murine Herpes Virus 68
HSK	Herpetic Stromal Keratitis
3-OS-HS	3-O-Sulfated Heparan Sulfate
HVEM	Herpes Virus Entry Mediator
gB, C, D, H, L	glycoprotein B, C, D, H, L
APC	Antigen Presenting Cell
NKG2D	Natural Killer Group 2D
XCR1	X Chemokine Receptor 1
XCL1	X Chemokine Ligand 1
Lck	Lymphocyte-specific protein tyrosine kinase
CXCR3, 4	CXC Chemokine Receptor 3, 4
CCR5, CCR7	CC Chemokine Receptor 5, 7
CXCL9, 10, 11	CXC Chemokine Ligand 9, 10, 11
CCL19, 20, 21	CC Chemokine Ligand 19, 20, 21
MHC	Major Histocompatibility Complex
IFN-α, β, γ, λ	Interferon alpha, beta, gamma, lambda
TNF-α	Tumor Necrosis Factor alpha
TGF-β	Transforming Growth Factor beta
IL-1, 2, 6, 8, 10, 12, 17	Interleukin 1, 2, 6, 8, 10, 12, 17, 18, 35
ATG	Anti-thymocyte Globulin
GC	Glucocorticoid
DEX	Dexamethasone
GR	Glucocorticoid Receptor
Nr3C1	Nuclear receptor subfamily 3 group C member 1
HPA axis	Hypothalamic Pituitary Adrenal axis
11β-HSD1, 2	11β-Hydroxysteroid Dehydrogenase 1, 2
KLRG1	Killer cell Lectin-Like Receptor subfamily G member 1
PD-1	Programmed cell death 1
TCR	T cell receptor
CFSE	Carboxyfluorescein succinimidyl ester

PBS	Phosphate Buffered Saline
BAL	Bronchoalveolar Lavage
MLN	Mediastinal Lymph node
PLN	Popliteal Lymph Node
PBMCs	Peripheral Blood Mononuclear Cells
MFI	Mean Fluorescence Intensity
Tg	Transgenic
T_x	Treatment
RAG	Recombination-activating gene
in	Intranasal
ip	Intraperitoneal
β_2m	β_2 microglobulin
DMEM	Dulbecco's Modified Eagle Media
RPMI	Roswell Park Memorial Institute media
LIL	Liver Infiltrating Cells
MWM	Molecular Weight Marker
qPCR	Quantitative Polymerase Chain Reaction
RT-PCR	Real Time Polymerase Chain Reaction
MOI	Multiplicity of Infection
HRP	Horseradish peroxidase
PAGE	Poly Acrylamide Gel Electrophoresis

PART - I

BACKGROUND AND OVERVIEW

Herpes simplex virus infection

Herpes simplex viruses are neurotropic viruses that belong to alphaherpesvirinae subfamily. More than 75% of human population worldwide is infected with these viruses. HSV1 and HSV2 are alphaherpesviruses that infect human beings. HSV1 causes skin, oral, ocular and also genital infections, whereas HSV2 predominantly causes genital infections. Both the viruses share approximately 74 of their homologous open reading frames, which allow them to infect both the sites i.e., orofacial and genitalia. As per the world health organization (WHO) report 2017, approximately 67% of human population (3.7 billion people) worldwide is infected with HSV1, and close to 11% population (417 million) is infected with HSV2. Most of the infected immunocompetent individuals remain asymptomatic. After primary infection both the viruses can adopt to an alternative life style known as latency established in the sensory nerve ganglia such as trigeminal ganglia (TG) or dorsal root ganglia (DRG) present in the lumbosacral region where these viruses remain hidden life-long. The latent virus can undergo reactivation that could be contributed by several factors such as stress, fever, menstrual cycle, radiation etc. HSV1 mainly reactivates from TG whereas HSV2 reactivates from DRG[1]. Both the primary and reactivated herpesviruses can migrate to CNS and cause encephalitis and/or meningitis particularly in immunocompromised individuals. HSV1 mainly causes encephalitis while HSV2 is primarily responsible for meningitis[2]. HSV1 can establish a successful infection in most of the cells types[3]. HSV1 has linear genome of 152 kb dsDNA rich in high GC content (~67%) and has ~84 open reading frames (ORFs)[4,5]. The core genomic material is encapsulated by nucleocapsid, which is surrounded by heterogeneous group of proteins referred to as tegument proteins. The tegument proteins are covered by lipid-protein (viral envelope) interspersed by several other glycoproteins. These glycoproteins help in the viral attachment and entry into the susceptible host cells[6,7]. HSV1 employs multiple entry

pathways for infection and spread. HSV1 can enter the host either by a pH independent, direct cell fusion with the plasma membrane or by the endocytic pathways. During endocytic entry HSV1 fuses with host cell membrane and this step follows its internalization. The process could either occur in a pH dependent or pH independent manner depending on the cell type involved. The same set of glycoproteins (gB, gD, gH/gL) are required for both of these processes. Glycoprotein D is critically required for the fusion process[8]. At low pH, gB undergoes conformational changes and might facilitate the process of virus fusion with the host cell[9]. Glycoprotein D internalizes nectin-1 and promotes the viral endocytosis, similarly the interaction of gB with paired immunoglobulin-like type 2 receptor-a (PILRa) facilitates the endocytic mode of entry[3,10].

The presence of multiple glycoproteins such as gB, gC, gD, gH/gL on the virus surface facilitate the adsorption, attachment, rolling and entry into the host cells.

HSV1 entry

HSV1 entry into the host cells involves multiple steps and requires the interaction of multiple viral glycoproteins (gB, gC, gD, gH and gL) with several receptors expressed by host cell surface. These include heparan sulfate proteoglycans (HSPG), herpesvirus entry mediator (HVEM), nectin-1, nectin-2, PILRα, Myelin associated glycoprotein (MAG), Non-muscle myosin heavy chain IIA (NMHC-IIA), B5 protein, αvβ3 integrin. The first step of viral entry is initiated by the attachment of viral gB and/or gC to the host cell's heparan sulfate proteoglycans (HSPG). The viral glycoproteins have positive charge and can efficiently interact with the negatively charged HSPG[11]. Although it is evident that the presence of gB/gC promotes the viral attachment and infection but the removal of gC and/or heparin sulphate (HS) do not abrogate the infectivity. As compared to gB, gC has more affinity to HSPG during the viral attachment, but gB is necessary

protein for the host cell-viral fusion step. The attachment of viral particles to the host cells concentrates the viral load on to the host cells. After initial attachment viral particles begins to surf (rolling) for additional receptors present on the host cell surface. Subsequently viral gD interacts with its different receptors (HVEM, nectin-1, nectin-2, 3-O-Sulfated heparan sulfate proteoglycan (3-OS-HS) present on the host cell surface. HVEM is a member of TNF (tumor necrosis factor) receptor family and expressed on a variety of cells such as leukocytes (including B and T lymphocytes), fibroblasts, epithelial cells and several human tissues (lungs, kidney, liver and some brain cells). Nectin-1 interacts with gD of both HSV1 and HSV2, whereas nectin-2 specifically recognizes the gD of HSV2 and promotes the viral entry. Nectin-1 is expressed in several tissues including skin, trachea, liver, ganglia and CNS. Another receptor which recognizes HSV1 gD is 3-OS-HS expressed in endothelial cells, liver, heart, kidney, pancreas and placenta. As opposed to nectin-2, 3-OS-HS specifically recognizes HSV1 gD. The interaction of gD with its receptor permits tight anchoring of viral envelope to the host cell membrane and helps bring both the virus and the host cells in juxtaposition. Crystal structure of gD ectodomain revealed that it has V-like immunoglobulin (IgV) core covered by N and C terminal extensions. The N terminus extension has distinct binding sites for different receptors whereas C terminus is involved in triggering the membrane and viral fusion[11]. The gD binding to its receptors induces some conformational changes and may also activate signal involving the gB and gH/gL molecules. These interactions eventually lead to the fusion of virus to the membrane[3,12]. Accordingly, it has been confirmed that the generation of a multiprotein complex (fusogen - comprised of glycoprotein D, gB and gH/gL) is required for the viral and host cells fusion. Some other molecules such as PILR-α, MAG and NMHC-IIA are additional known receptors for gB protein that facilitate the binding and fusion of the virus to cells.

Diseases caused by HSV1

After primary infection or the one precipitated by reactivated HSV1, asymptomatic or symptomatic clinical disease may result. The symptomatic diseases are manifested in various body parts of humans that involve skin, eye, oral, genitalia and central nervous system (CNS). The diseases caused by HSV1 infection are summarized in table 1.

Table 1.

Infection site	**Disease**
Skin	Cutaneous herpes Genital herpes
Ocular	HSK Uveitis Acute retinal necrosis
Orolabial	Oral ulcers Cold sores
Central nervous system	Encephalitis Meningitis Alzheimer

HSV1 recognition and response by immune cells

HSV1 is a double stranded DNA (dsDNA) virus and replicates in the nucleus. The virus has evolved several host immune response evading mechanisms. Virus recognition is an essential event to elicit strong immune responses for clearing the infection. The host

immune cells recognize several pathogens associated molecular patterns (PAMPs) expressed by HSV1. The PAMPs expressed by HSV1 include glycoproteins, tegument proteins, genomic DNA and RNAs expressed during productive infection. The receptors for recognizing PAMPs are termed as pattern recognition receptors (PRRs) and several such specific receptors for HSV1 recognition include: Toll like receptor (TLR) 2, TLR3, TLR9, Interferon gamma inducible protein 16 (IFI16), DAN-dependent activator of interferon-regulatory factors (DAI), DHX36, DEAH box 9 (DHX9), Ku70, DDX60, RNA polymerase III via retinoic acid-inducible gene I (RIG-I) and melanoma differentiation associated gene 5 (MDA5). Till date at least 6 different pathways have been suggested for HSV1 recognition by the host immune cells. These include:

(1) Interaction of host receptors with HSV1 surface proteins. TLR2 and mannose receptors (MR) interact with several glycoproteins present on viral surface, which ultimately induce an upregulation of several cytokines during HSV1 infection. The role of TLR2 signaling in HSV1 and HSV2 is well established. HSV1 infection is known to induce TLR2 in infected peritoneal cells[13]. Chinese hamster ovary cells that are normally resistant to HSV1 infection can respond to the virus upon their transfection with TLR2 leading to the activation of nuclear factor-κB (NF-κB) pathway[14,15]. The TLR2 interaction with the virus promotes apoptosis[16] and causes the induction of several chemokines and cytokines such as CCL2, IL-6[14], IFN-α/β and TNF-α[17–19].

(2) HSV1 proteins such as VP16, ICP0 and ICP27 induce several immune cells activation pathways. Thus, VP16 promotes c-Jun N-terminal kinase (JNK)-MAPK pathway[20] and ICP27 mediates the induction of p38/JNK and NF-κB pathways[21,22]. Similarly, the role of viral protein ICP0 in JNK, NF-κB as well as AP-1 activation has been reported[23–25].

(3) Viral DNA recognition either in the cytoplasm or nucleus by the host RNA polymerase III. The data obtained from HSV1 infection of RAW264.7 cells (macrophages) showed that the recognition of cytosolic DNA is mediated by RNA polymerase III and is followed by IFN-β production[26]. Another report showed that the interaction of PYHIN protein, IFI16 senses the cytosolic DNA and it is directly associated with IFN-β-inducible motifs to upregulate the IFN-β production[27]. In addition to RNA polymerase III, other proteins such as IFI16, DAI, DHX9, DHX36, DDX60 or Ku70 recognize cytoplasmic viral genomic DNA and mediate the induction of IFN-α/β/λ as well as TNF-α[28–31] after HSV1 infection.

(4) Viral RNA is recognized by MDA5 in the cytoplasm. In human macrophages, the recognition of viral RNA occurs via MDA5/MAVS dependent pathway that eventually produces type III IFN (IFN-λ1) as an effector molecule.

(5) HSV1 viral DNA is recognized by TLR9 in the endosome of infected cells. Since TLR9 is usually expressed by only some cell types such as, pDC (plasmacytoid dendritic cells), myeloid cells and B cells, it is not considered as the universal PRR for HSV1. Nonetheless, TLR9 recognizes HSV DNA at its unmethylated CpG motifs and induces the expression of IL-12, IFN-α and IFN-λ to generate an efficient immune responses[32–36].

(6) Viral dsRNA formed as an intermediary during replication is recognized by TLR3 expressed by endosome in the host cells. During active replication of HSV1, the dsRNA accumulates and is recognized by TLR3. This interaction induces the expression of various cytokines such as IL-6, type I IFN (IFN-α/β) and type III IFN (IFN-λ)[36–40]. HSV1 infected individuals lacking in TLR3 expression either because of a genetic deficiency or as a results of certain mutations are invariably more prone to encephalitis and exhibit an impaired expression of anti-viral cytokines[41]. Some studies focusing to elucidate the role of TLR3 in HSV1 infection suggest that the presence of TLR3 in antigen presenting cells

(DCs) help recognize the virus infected cells and induce signals to cytotoxic T cells by promoting antigen cross presentation, a process through which $CD8^+$ T cell response is induced as a result of exogenous antigen uptake[42].

Role of NK cells during HSV1 infection

Natural killer (NK) cells are one of the earlier cell types that respond to HSV1 infection. NK cells mediate their function by releasing effector molecules such as the preformed perforins and granzymes either by their direct contact with the virus leading to signaling in these cells or by an antibody-dependent cell-mediated cytotoxicity (ADCC) mechanism. In addition to presenting the antigenic peptide to the cytotoxic T cells, class I MHC molecule also serve as a ligand for the surface molecules of NK cells that include, Killer cell immunoglobulin-like receptors (KIRs), Ly49 and lectin-like receptor CD94/NKG2a. These molecules either act as activating or inhibitory receptors[43]. Since class I MHC molecule is ubiquitously present on most of the nucleated cells (except neurons), their ligation with inhibitory receptors present on NK cells prevents activation and therefore healthy cells are spared from killing[44]. US12 of HSV1 encodes for a soluble cytosolic protein (ICP47) that has 88 amino acids[45]. ICP47 forms helical hairpin structure and gets inserted into the central cavity of two TAP (transporter of antigen processing and presentation proteins) subunits and in so doing impairs the cytosolic peptide trafficking to the endoplasmic reticulum (ER). This results in the down regulation of peptide-class I MHC complex on the plasma membrane of infected cells[46]. The down regulation of class I MHC molecule during HSV1 infection particularly in humans release NK cells from self-inhibition and results in their activation for clearing the virus infected cells[47]. However, murine TAP subunits poorly interact with viral ICP47 protein and does not impair the class I MHC transport to the cell surface[48]. The β herpesviruses such as murine cytomegalovirus (MCMV) encoded m152 and human CMV (HCMV)

encoded US11 have been shown to down regulate class I MHC expression to activate NK cells. NKG2D, a receptor present on NK cells, is involved in the identification and elimination of tumor cells as well as virally infected cells[49]. It recognizes various ligands such as UL16-binding proteins 1-6 (ULBP1-6) and class I MHC polypeptide-related sequence A and B also known as MICA and MICB[50]. NK cells isolated from patients that have an active HSV1 replication display a higher level of NKG2D receptor expression[51]. In addition to the above-discussed contact mediated signaling events, NK cells exert anti-viral defense by ADCC mechanism. To perform this function NK cells use type I transmembrane protein CD16a, which binds at the hinge region (Fcγ portion) of antibodies generated against the pathogens[52]. The interaction transduces signal and induces tyrosine phosphorylation in CD3ζ chain to activate NK cells[53–55]. In well-established classical model of ADCC, NK cells expressed CD16a interacted with Fcγ portion of IgG1, IgG2 and IgG4 generated against the pathogen to induce cell killing. Antibody mediated cytotoxicity could be regulated by a mechanism known as antibody bipolar bridging wherein antibody IgG isotype generated against HSV1 infection could form a bipolar bridge between gE and gI proteins of the virus that are expressed on the surface of infected cells. Such an interaction could block the ligation of NK cells expressed CD16a to the Fcγ region of anti-HSV1 specific IgG antibody and in so doing abrogates ADCC[56]. This process could promote the viral resistance against the host defense mechanisms.

Role of T cells in HSV 1 infection and pathogenesis

T lymphocytes are the major player of adaptive immune response and contribute significant role by HSV1 mediated disease, viral clearance, establishing and maintaining viral latency as well as precipitating reactivation episodes. After any infection, T cells recognize pathogen derived peptides displayed by either class I or class II MHC

molecules present on the surface of infected and/or antigen presenting cells (APCs) to activate $CD8^+$ and $CD4^+$ T cells, respectively. Activated $CD8^+$ T cells mediate the efficient elimination of the pathogen whereas activated $CD4^+$ T cells help the former cells for their optimal activation and function. After HSV1 infection, cytotoxic T cells play a significant role in the pathogen elimination and also in blocking its reactivation form sensory ganglia.

T cells reside in the T cell zone of lymphoid organs in un-manipulated mice whereas DCs reside in the B cell follicles, T cell zone along with some areas of subcapsular sinus by forming extensive networks[57]. Although naive $CD8^+$ T cells mainly reside in the T cell zone but as soon as the presence of pathogens is detected in the lymph nodes, DCs and $CD8^+$ T cells populate the peripheral region[58,59]. Shortly after infection the pathogens/particulate antigen carried by APCs particularly those macrophages that express CD169 reach to the subcapsular sinus via lymphatics. Although a higher pathogen load is present in the macrophages but naive $CD8^+$ T cells preferentially make their initial contact with DCs and this process initiates the activation and differentiation of naïve $CD8^+$ T cells into effector cytotoxic T cells[60]. Although in the course of a primary infection with certain pathogens such as the one caused by *Toxoplasma gondii*, the relocation of naive $CD8^+$ T cell is antigen independent and is majorly dependent on chemokines build up as well as the lymph node architecture remodeling, the reinfection with *T. gondii* induces an antigen dependent migration of memory $CD8^+$ T cells to the subcapsular region to initiate their contacts with DCs for their re-stimulation[61]. On the other hand during vesicular stomatitis virus (VSV) and vaccinia virus (VV) infections, the activation and migratory behavior of $CD8^+$ T cells is majorly antigen driven[58]. Therefore, after any peripheral infection, the dramatic change in the lymphoid organs, chemokines and the gradient of cognate antigen induce the migration of naïve $CD8^+$ T

cells toward the subcapsular sinus region. At the same time $CD8^+$ DCs express XCR1 molecule a receptor for the XCL1 ligand specifically produced by recently activated $CD8^+$ T cells. The XCR1-XCL1 interaction helps induce the migration of DCs toward the lymph node region which then present pathogen derived peptide to naive $CD8^+$ T cell for their differentiation into effector cells[62].

TCR mediated T cell activation

The recognition of pathogen derived antigenic peptides by T cell receptor (TCR) transmits the first signal for the activation of $CD8^+$ T cells. The engagement of T cells expressed co-stimulatory molecules such as CD28 and the members of B7 family (B7.1 and B7.2) expressed by APCs provide the second signal, whereas the third signal for inducing efficient activation and differentiation of $CD8^+$ T cells comes from the ligation of various cytokine receptors by their respective cytokines that are initially produced by APCs and later on by T cells themselves. Once three signals are induced appropriately, T cells get activated optimally to eliminate the pathogen from the host.

Role of first signal

The T cell receptor expressed by αβ T cells comprises of one α and one β chain and the dimer directly interacts with cognate peptide displayed by either the class I or the class II MHC molecules for the activation of $CD8^+$ T cells and $CD4^+$ T cells, respectively. The TCR is associated with CD3 chains. CD3 molecule consists of one chain each of CD3ε, CD3δ and CD3γ and three chains of CD3ζ, the latter having immunoreceptor tyrosine-based activation motifs (ITAM) which are phosphorylated during T cell activation[63]. The formation of TCR-MHC-peptide complexes induce structural changes in cytoplasmic tail of CD3 and the TCR chains to make buried ITAM tyrosine molecules accessible for Lck (a Src kinase protein) mediated phosphorylation. Thereafter, CD8 or the CD4 molecules interact with the respective MHC chains outside

the peptide binding region to mediate Y(394) phosphorylation by CD8/CD4 associated Lck molecule either by trans or auto phosphorylation. This can also be brought about by the activity of Fyn (another Src kinase) expressed in T cells. The phosphorylation stabilizes the active conformation and helps facilitate in making its interaction with the catalytic domain of Zap70 protein[63]. Then Lck activates Zap70 by phosphorylating it at Y(319) in the interdomain B region, thereby relieving the Zap70 from auto-inhibition which in turn creates a binding site for the SH2 domain of Lck to stabilize Lck in active conformation[64]. Zap70 then phosphorylates it in either a trans or self manner to induce the catalytic activity. The activated Zap70 in turn phosphorylates the intracytoplasmic segment of Lat (linker for the activation of T cells) and CD6 to amplify the signal as well as diversify modules for an effective differentiation of the T cells so that such cells could exert their specific functions[63,65–67]. Recognition of foreign peptide-MHC complex by TCR transmit a very rapid signaling events and the induction of phosphorylation in TCR-proximal region begins within 4 seconds, the secondary messengers such as calcium and diacylglycerol are produced within 6-7 seconds and the cytoskeletal rearrangements start within 10 seconds of TCR engagement[68,69].

Role of second signal during T cell activation

The interaction of T cell expressed CD28 with CD80 (B7.1) and CD86 (B7.2) expressed on APCs, such as dendritic cells, macrophages and activated B cells constitute second signal during the activation of T cells. Both CD80 and CD86 are only highly expressed on fully activated but not by the unstimulated APCs, to keep a check on the activation of T cells during homeostatic conditions[70]. These molecules are induced on APCs by infection or the inflammation. The co-stimulation via CD28 is required for the optimal activation of T cells and such a step can lower down the activation threshold involving MHC-TCRs interactions[71] as well as prevents anergy in T cells. This is

achieved by enhancing the production of cytokines such as IL-2 to promote T cell proliferation[72]. Additionally, the co-stimulation can either interfere with or enhance multiple signaling pathways to fine tune several gene expression pathways[73,74]. The ligation of CD3/CD28 induces the phosphorylation of cytosolic region in CD28 that has highly conserved proline and tyrosine rich residues and thereby creating the docking sites for SH2 and/or SH3 domain of various downstream factors that include PI3K, Itk and Tec protein-tyrosine kinases, Lck, PKCθ, NF-κB inducing kinase, growth factor receptor bound protein 2(Grb2), Grb2-related adaptor protein (Gads), phosphatidylinositol 4,5-biphosphate kinase α (PIP5Kα) and guanine-nucleotide exchange factor Vav-1[75-83]. This signaling not only lowers the activation threshold through TCR but also enhances the production of cytokines but also promotes the membrane raft clustering via Vav-1 proteins to help facilitate the formation of immunological synapse for an optimal activation of T cells[84,85].

Role of third signal during T cell induction

The third signal for T cell activation is provided by the cytokines produced either from the neighboring cells; APCs or the T cells themselves. The availability of cytokines dictates the extent of activation, proliferation, effector function and survival of T cells. The cytokines that could provide signal 3 for cytotoxic T cell responses are IL-12, type I IFN (IFN-α and β) and type II IFN (IFN-γ). IL-12 either directly or in a synergy with IL-18 promotes immune function of $CD8^+$ T cells[86,87]. IL-12 mediated direct effects on $CD8^+$ T cell have been shown to enhance the proliferation, survival and differentiation of naïve cells into terminal effector cells that carry out their cytolytic function[88,89]. IL-12 could also induce T-bet engaging mTOR-dependent mechanisms[90]. The timing and the duration of IL-12 exposure determine the optimal effector function of $CD8^+$ T cells[91]. IL-12 signaling in $CD8^+$ T cells helps induce an effector function as well as upregulates the

anti-apoptotic protein Bcl-3[92] and inhibits the pro-apoptotic enzyme caspase-3[93] to promote their effector function.

An important role of IFN-α as a third signal in promoting $CD8^+$ T cell expansion and lytic function has been demonstrated. Adoptively transferred IFN-αβ receptor deficient LCMV specific $CD8^+$ T cells (P14 TCR-tg $CD8^+$ T cells) showed a severe defect in the expansion and memory generation during LCMV infection[94,95]. Similar to the role of type I IFN cytokines in T cell activation-differentiation, IFN-γR1 deficient P14 TCR-tg $CD8^+$ T and $CD4^+$ TCR-tg cells displayed an impaired expansion during LCMV infection[96,97]. Several members of TNFR family such as CD27, OX40 and 4-1BB transmit important co-stimulatory signals for the activation of $CD8^+$ T cells[98]. The roles of IL-2 in $CD8^+$ T cell effector function and memory generation are well documented. During initial stages of $CD8^+$ T cell activation, these cells produce IL-2 as one of their effector molecules but subsequently there is a loss of IL-2 production[99]. However, in order for their survival, $CD8^+$ T cells use IL-2 produced by $CD4^+$ T cells[100]. During the primary response IL-2 signaling in $CD8^+$ T cells is critical for their programming and generation of functional memory $CD8^+$ T cells[101,102]. $CD8^+$ T cells recognize and respond to IL-2 by three dynamically expressing surface receptor chains; IL-2Rα (CD25), IL-2Rβ (CD122) and IL-2Rγ (CD132). The impact of IL-2 during the differentiation of $CD8^+$ T cells has been elucidated using IL-2R deficient and wild type mixed chimeric experiments[102-104]. A deletion of IL-2Rα was shown to slightly diminish the expansion of $CD8^+$ T cells but the altered functionality and phenotype were significantly manifested during the memory generation[102,103]. The relative abundance of IL-2 during the activation of $CD8^+$ T cells had differential effects in the formation of effectors as compared to memory cells. The presence of high levels of IL-2 in the microenvironment during $CD8^+$ T cells activation enhanced the frequency of short-lived effector cells but compromised

memory precursor cells. Similarly the lower IL-2 levels in the microenvironment promoted effector cells to differentiate into memory precursors[104].

$CD8^+$ T cells are optimally activated when all three signals are induced appropriately and T cells subsequently divide extensively. Accordingly, such cells were shown to undergo more than 15 divisions in the week of pathogen-mediated stimulation thereby exhibiting up to 500,000-fold expansion. Although the rate of maximum cell division for $CD8^+$ T cell is thought to occur every 4-6 hrs, but one report estimated it to be shorter i.e., approximately 2 hr for one cycle[105]. After activation of $CD8^+$ T cells, there occurs a rapid metabolic change such as the enhanced utilization of amino acids, glucose and iron to meet out the sudden but enhanced demand for the building blocks such as nucleic acids, proteins, lipids. This is achieved by switching from oxidative phosphorylation to aerobic glycolysis[106]. After the activation, $CD8^+$ T cells differentiate into effector and/or memory cells depending on the relative abundance of various factors, such as the strength of TCR-MHC interaction, the level of different cytokines in the microenvironment, the expression profile of surface molecules and the transcription factors, metabolic regulators, the state of chromatin organization and their ability to undergo asymmetric division[107].

Migration of activated $CD8^+$ T cell to infection site

In an uninfected host, naïve $CD8^+$ T cells circulate between blood and lymph node via efferent lymphatics. The migratory behavior of $CD8^+$ T cells is dictated by several molecules such as the chemokine receptors and their ligands that includes the CC-chemokine receptor 7 (CCR7), L-selectin (CD62L) and sphingosine-1-phosphate receptor 1 (S1P1). Fibroblast reticular cells (FRCs) of the lymphoid organs produce ligands such as CC-chemokine ligand 19 (CCL19) and CCL21 which interact with CCR7 expressed by $CD8^+$ T cell and this helps their retention in the lymph node[108–110]. Whereas the

interaction of CD62L with P-selectin glycoprotein ligand 1 (PSGL-1) expressed on high endothelial venules (HEVs) helps promote $CD8^+$ T cell migration to lymph nodes[111].

During the viral infection induced activation of $CD8^+$ T cells there is a coordinated modulation of lymphoid tissue homing molecules (CCR7, CD62L and S1P1) and those that facilitate their migration to infected or the inflammatory tissue sites. Some of these molecules include CXCR3, CCR5, very late antigen 4 (VLA4) and the ligands for P-selectin and E-selectin[112–114]. Effector $CD8^+$ T cells upregulate the AKT activity which help downregulate the expression of Kruppel-like factor 2 (KLF2), a key regulatory transcription factor required for the expression of lymph node homing molecules (CD62L, S1P1 and CCR7) that ultimately helps retain activated T cells in the lymph nodes[111,115–119]. This provides enough time for activated cells to undergo a few rounds of divisions. Simultaneously the level of a transcription factor Tbx21 (T-bet) is upregulated in activated $CD8^+$ T cells which in turn upregulates CXC-chemokine receptor 3 (CXCR3)[113,120] a receptor for proinflammatory chemokines, such as CXC-ligand 9 (CXCL9), CXCL10 and CXCL11. The enhanced expression of CXCR3 helps promote the exit of activated cytotoxic T cells from lymph node to the infection/inflamed tissue site for viral clearance.

Role of $CD8^+$ T cells during HSV1 infection

Nash et al first indicated the involvement of $CD8^+$ T cells and their killing activity during HSV1 infection in 1980. They successfully collected cytotoxic T cells from the draining lymph node of infected mice as early as 4 dpi and reported maximum activity between 6 to 9 dpi. $CD8^+$ T cells recognize HSV1 specific peptides and differentiate into effector cells that produce effector molecules such as perforin, granzyme A (GrA), GrB, IFN-γ and TNF-α to help eliminate the virus infected cells from the host. After virus load declines, the activated $CD8^+$ T cells undergo contraction leaving behind a pool of ~5-10%

of the activated cells that further differentiate into memory $CD8^+$ T cells. Some of the residual cells exhibit CD103 expression and are preferentially retained at or near the infection tissue sites such as skin and/or trigeminal ganglia. Other $CD8^+$ T cell populations differentially express molecules such as CD103, CD62L and CD127. Of these cells some home to the lymph node as central memory (T_{CM}) cells, some remain in the circulation as effector memory (T_{EM}) and some at infection tissue site as resident memory (T_{RM}) cells to confer to the host a quick and efficient protection against the secondary infection with the virus. $CD8^+$ T cells retained in the sensory ganglia block/suppress the reactivation of viral particles from latency[121,122].

During some viral infections, a group of the activated $CD8^+$ T cells upregulate transcription factor Blimp1 and start producing an anti-inflammatory cytokine IL-10 which is likely to control their hyper-activation to prevent the host from excessive tissue damage[123–125]. However IL-10 producing $CD8^+$ T cells are shown to have superior killing activity and such cells also produce more IFN-γ, TNF-α and granzyme B level as compared to IL-10^{-ve} $CD8^+$ T cells. But such cells rapidly disappear after the clearance of viral load[126]. The transient superior activity of these cells could suggest that these cells are better at eliminating the pathogen from the system without causing extensive damage to the host.

Immunopathology during/after HSV1 infection

Initially after HSV1 infection, the innate immune cells such as neutrophils, NK cells and macrophages are recruited to the response. The primary and presumed roles of macrophages and NK cells are thought to achieve viral clearance[127]. Recognizing HSV1, innate immune cells begin to produce several proinflammatory cytokines, such as IFN-α/β/γ, TNF-α, TGF-β, IL-1α, IL-1β, IL-6, IL-8, IL-12 and IL-17[128,129] and in so doing play important roles in the disease control or its exacerbation. Among all the infiltrating

immune cells, Th17 $CD4^+$ T cells and neutrophils are the major known players in causing angiogenesis and corneal opacity that eventually lead to blindness. Studies measuring the infiltration of immune cells clearly demonstrated an enhanced infiltration of $CD4^+$ T cells and neutrophils in the cornea of infected animals. In a mouse model of HSK, a biphasic infiltration of Th17 cells to the infection site was demonstrated and this correlated with the disease appearance and progression[130]. Some proinflammatory molecules such as IL-6, IL-8, IL-17, CC-chemokine ligand 20 (CCL20), macrophage inflammatory protein 1α (MIP-1α) and MIP2 help in the migration of neutrophils and Th17 cells to the infected tissue site. IL-17 cytokine produced by Th17 cells and/or neutrophil not only help attract neutrophils but also promote their survival and their ability to produce matrix metalloproteinases (MMP) and oxy-radicals that cause tissue damage[130,131]. In normal cornea vesicular endothelial growth factor (VEGF) molecules remains bound to the soluble VEGF receptor 1 (sVEGFR-1) and thereby sequestering it from binding with the membrane tethered VEGF receptors. In so doing it abrogates the formation of new blood vessels. After HSV1 infection higher level of IL-17 induces the production of matrix metalloproteinases, such as MMP-2, MMP-7, MMP-8 and MMP-9 which degrade the soluble VEGF receptors and promote VEGF binding to bound VEGF receptors[130,132–135]. Simultaneously an enhanced level of IL-1, IL-6 and IL-17 cytokines promotes the production of VEGF which can then bind to its membranous receptors[130,135]. As a result of unavailability of enough soluble VEGF receptors and a higher level of the ligand the angiogenesis occurs in HSV1 infected corneal stroma.

Immunoregulatory strategies to dampen immunopathology

The immune cells detect and eliminate the pathogen, but their aberrant or uncontrolled activation lead to immunopathology. Immune regulatory mechanisms are put in place to regulate these immune responses and some such mechanisms include

different types of suppressor cells. The examples include $CD4^+$ regulatory T cells (Treg), $CD8^+$ regulatory T cells and myeloid derived suppressor cells (MDSCs). Anti-inflammatory molecules produced by different immune cells could also help dampen pro-inflammatory reactions. The examples of such molecules are IL-10, TGF-β, IL-35. Many such endogenous immunoregulatory mechanisms establish immune regulation to maintain homeostasis. This can be achieved by strategies such as promoting the functions of regulatory cells, infusing *in vitro* generated regulatory cells or by injecting immunosuppressive drugs or molecules from exogenous source in the host.

Immunosuppression by endogenous mechanisms

One of the most prominent and well characterized suppressive cell type of adaptive immune system is $CD4^+$ T cells and expresses the master transcription factor, forkhead box P3 (FoxP3). These cells additionally express some other surface receptors such as CD25, cytotoxic T-lymphocyte antigen 4 (CTLA4), lymphocyte-activation gene 3 (LAG3), CD39, CD73, OX40 (CD134), glucocorticoid induced tumor necrosis factor (GITR) and folate receptor 4 (FR4) in un-manipulated mice[136–138]. The constellation of molecules expressed by these regulatory T cells varies between humans and mice. Treg cells perform their suppressive function via several mechanisms that include the sequestration of available IL-2 and making it less available for the effector cells. Tregs express high affinity IL-2 receptor (CD25) on their surface in the absence of any antigenic stimulation[139,140]. The other mechanisms of inducing suppression include either a contact dependent or independent mechanisms between Tregs and the target cells. The contact dependent inhibition involves the interaction between cell surface expressed receptor and ligand pairs such as CTLA4 and CD80/CD86, LAG3 and class II MHC[141–145]. The contact independent inhibition includes the production of anti-inflammatory cytokines IL-10 and TGF-β[146–150] and/or molecules such as perforin and granzyme B by

the regulators that could inhibit the proliferation of effector cells or mediate killing of T cells, B cells, DCs and monocytes[151–153]. A recent study also showed that Tregs could suppress effector T cells in an antigen specific manner. Accordingly, Tregs downregulated cognate peptide displaying MHC II molecules on the surface of dendritic cells to cause an antigen specific inhibition while bystander activation of naive T cells remain unaffected[154].

$CD4^+$ regulatory T cells are broadly categorized into natural (nTreg) and induced (iTreg) regulatory T cells. Natural regulatory T cells originate in thymus and express surface CD25. Such cells circulate in the periphery to control self-reactive effector T or NK cells. The expression of intra nuclear transcription factor FoxP3 and surface CD25 serve as the key molecules for the identification of nTreg cells. Such cells constitute 5-10% of peripheral $CD4^+$ T cells in normal un-manipulated mice[155–158]. The protective roles of $CD25^+$ Tregs are well established during HSV1 pathogenesis and the corneal stromal keratitis[159]. Another type of T cells that are $CD25^{-ve}$ (in both $CD4^+$ and $CD8^+$) originates from thymus could differentiate into regulatory T cells upon their appropriate stimulation in an environment that consists of cytokines such as IL-2 and TGF-β. Such cells are referred to as inducible T regulatory (iTreg) cells and upon their activation these cells produce IL-10 and/or TGF-β to mediate immunosuppressive function by inhibiting the production of cytokines and proliferative capacity of effector T_H1, T_H2, $CD8^+$ T cells and NK cells[156,160,161]. $CD4^+CD25^-$ T cells activated upon recognition of self/foreign antigen could also differentiate into either TGF-β or IL-10 producing T helper 3 (T_H3) or T regulatory 1 (T_R1) cells respectively[158,162,163].

MDSCs develop from the cells of myeloid origin and comprise of a heterogeneous cell population that includes myeloid progenitor, immature macrophages, immature dendritic cells and immature granulocytes. MDSCs are usually characterized by

their expression of $CD11b^+CD33^+$ in human and $CD11b^+Gr1^+$ phenotypes in mice. MDSCs expand during tumor development and their involvement in the progression of tumorigenesis is well established and such cells are known to potently suppress T cell functionality. MDSCs mediate their immunosuppressive function in both innate and adaptive immune cells by producing various molecules such as argininase 1, inducible nitric oxide synthase (iNOS), reactive oxygen species (ROS) and IL-10[164,165]. Some studies suggest their potential role in converting Treg cells from non-Tregs to mediate long-term immunosuppression of $CD4^+$ and $CD8^+$ T cells[166] (**Sarkar et al., submitted**). The potential immunosuppressive function of MDSCs is reported in diseases such as multiple sclerosis, systemic lupus erythematosus, type 1 diabetes, inflammatory bowel disease and rheumatoid arthritis[167–172].

Strategies to boost immunosuppressive mechanisms

The situation where endogenous mechanisms fail to maintain a balance between immune reactions and immunosuppression necessitate the use of exogenous immunosuppressive strategies. This can be achieved either by promoting endogenous regulatory mechanisms, depleting effector cells or by blunting the activity of effector T cells. The common modalities include an administration of biological reagents such as antibodies or chemical compounds into the host. The generation and injection of antithymocyte globulin (ATG) polyclonal antibody preparations into patients are known to target a wide range of surface molecules expressed by various immune cells to dampen the hyperactivity of such cells. The antibodies against molecules such as CD2, CD3, CD8, CD11a, CD18, CD25, CD44, HLA-DR, HLA I expressed by various cells have been used to modulate the activity of different cells including T cells, B cells, NK cells, dendritic cells and endothelial cells[173]. In order to achieve specificity monoclonal antibodies generated against CD3 (moromonab - OKT3), CD20 (Rituximab), CD22

(epratuzumab), CD25 (basiliximab), CD40 (ASKP1240) CD52 (alemtuzumab), IL-6 (tocilizumab), IL-17 (secukinumab), TNF-α and complement C5 protein (eculizumab) have been shown to effectively manage various immunopathological conditions[174,175].

Not only antibodies but also chemical drugs that affect the cell fate and functions have been used to control inflammatory reactions. These include evrolimus, a rapamycin derivative, sirolimus (regulator of mTOR pathway), fingolimod (that impairs the cell trafficking and Treg induction), azacytidine (an anolog of purine in DNA synthesis to alter epigenetic architecture of nucleic acid), 2-deoxy-D-glucose (2DG - glycolysis inhibitor), cyclosporine and tacrolimus (calcineurin inhibitors) and leflunomide (inhibitor of dihydroorotate dehydrogenase - pyrimidine synthesizing enzyme) and cyclophosphamide. All these chemicals have been tested in preclinical studies to influence the outcome of immunopathological condition caused by HSV1 infections as well as other inflammatory conditions[175–178]. Additionally, glucocorticoids serve as potent inhibitor of inflammation and are used as the drug of choice for controlling disease conditions such as leukemia, autoimmune diseases and inflammatory reactions such as arthritis, multiple sclerosis, HSV1 induced corneal inflammation commonly known as herpetic stromal keratitis (HSK).

Dexamethasone as an immunosuppressant

Endogenous glucocorticoids such as corticosterone in rodents and cortisol in humans play essential role in the developmental and physiological processes[179–184]. Glucocorticoids (GC) are synthesized in mitochondria and are generally produced in the adrenal gland and to some extent in other tissues such as thymus, intestine, skin and lungs. Adrenal steroidogenesis induced via hypothalamic-pituitary-adrenal (HPA) axis, a neuro-endocrine network coordinates between physiological responses and the external stimuli. Physical strain, psychological stress, alteration in circadian rhythms and the

production of inflammatory cytokines such as IL-1, IL-6 and TNF-α trigger an enhanced glucocorticoid synthesis from the adrenal gland. Hypothalamus recognizes these signals and releases corticotropin-releasing hormone and arginine vasopressin (AVP), which in turn activate anterior pituitary gland to induce the production and release of adrenocorticotropin hormone (ACTH). ACTH then enters into the circulation and binds to their specific receptors on adrenocortical cells and induces the conversion of 11-dehydrocorticosterone and cortisone to corticosterone (in rodents) and cortisol (in human), respectively. Adrenocortical cells can also produce glucocorticoids upon their ligation of TLR2 and TLR4 agonists. Secreted glucocorticoids feed back to the hypothalamus, pituitary gland and inflammatory cytokines producing immune cells to exert inhibition of steroidogenesis[185]. The level of 11β-hydroxysteroid dehydrogenase enzymes (11β-HSD1 and 11β-HSD2) control the inter conversion of biologically active cortisol and inactive cortisone in the GC producing cells. 11β-HSD1 enzyme generates active form whereas 11β-HSD2 generates inactive form of glucocorticoids[186,187].

Dexamethasone, a synthetic glucocorticoid is resistant to inactivation by 11β-HSD2 and therefore exerts its immunosuppressive function for longer duration. It is internalized by the cells owing to its lipophilic nature and exhibits its function both through genomic and/or non-genomic mechanisms. While acting through its non-genomic mechanisms, GCs intercalate into the cells membrane and alter the cationic transport and in so doing promote the proton leakage from mitochondria[188,189]. Ligation of GCs to cytoplasmic GR-chaperone complex displaces the chaperone protein, thereafter the GC-GR complex translocates to the mitochondria to induce apoptosis[189,190].

Dexamethasone binds with the cytoplasmic glucocorticoid receptor (Nr3c1 – nuclear receptor subfamily 3 group C member 1) to cause immunosuppressive functions and performs its various activities through genomic mechanisms. The glucocorticoid

receptor (GR) has numerous sites for post translational modifications, such as acetylation, phosphorylation, sumoylation and ubiquitylation and such alterations play important roles in their cytoplasmic/nuclear transport, receptor degradation and gene regulation[190]. After internalization, GC interacts with cytosolic GR and the GC-GR complexes translocate to nucleus so as to modulate gene expression. Dexamethasone employs three different strategies to perform these functions. i) GC-GR complex could make direct interaction with GC response elements (GRE) in the genome for regulating the gene expression[191–193]. ii) The complex interacts first with the transcription factors (tethering) without making any direct contact with genomic DNA followed by an alteration in their respective gene expression[194]. The major immunosuppressive functions of GC are observed via second mode of regulation, where it interferes with various transcription factors responsible for pro-inflammatory cytokine production such as the activator protein (AP-1), nuclear factor-κB (NF-κB), signal transducer and activator of transcription (STAT) and nuclear factor of activated T cells (NFAT)[185]. iii) the third mode of GC response includes an alteration in the gene expression by involving composite GRE binding, where GC-GR complexes first bind with the transcription factor and then to the respective GRE to regulate the gene expression[195]. It is reported that all of the three modes of gene regulation by dexamethasone can cause immunosuppressive functions either by trans repression or by transactivation to enhance the expression of target genes, depending on the structure of downstream interacting partners[194,196–199]. Some of the known immunosuppressive effects of corticosteroids include a modulation of cytokine production by immune cells, apoptosis induction, an altered cellular trafficking, the promotion of phagocytosis as well as an enhancement of regulatory T cell functions.

The existing models of HSV1 infection and the resulting pathologies

HSV1 infection is a major cause of infectious blindness and encephalitis worldwide. The route of infection dictates the pathology caused, the disease outcome as well as the site of viral latency. HSV1 can infect a wide range of body parts such as cornea (to cause stromal keratitis and/or encephalitis) that eventually end up attaining latency in the trigeminal ganglia (TG) of the survived immunocompetent host, the intracerebral injection leads to encephalitis, oral/intranasal infection being the major cause of herpetic labialis and the virus resides in TG life long, cutaneous infection leads to zosteriform lesions and the subcutaneous foot pad infection causes peripheral infection[200]. After primary infection caused by both the cutaneous and subcutaneous infections, the virus remains in latency in lumbosacral dorsal root ganglia (DRG). Many animal model systems that include mice, rat, rabbit, guinea pig and macaques have been used for investigating virus induced pathological conditions and to elucidate the mechanisms of viral pathogenesis, the host responses triggered to clear/diminish the viral load, viral immune evasion mechanisms, latency establishment, maintenance and the viral reactivation from latency as well as the associated disease outcomes. The first report of HSV1 infection in any model system came from the experiments of Teague and Goodpasture in 1923. They demonstrated a zosteriform infection in the flank of rabbits and guinea pig and the vesicular lesion started to appear within 72hr of infection[201]. Later on the HSV1 infection in mice model[202] was shown by Sydiskis and Schultz in 1965. Thereafter, Simmons and Nash highlighted a significant role of T cells in controlling the zosteriform lesion spread and indicated the processes of latency establishment and maintenance[203]. Mouse model systems have been extensively studied because of its well-characterized genetic system, the availability and accessibility of immunological and molecular biological reagents, the availability and generation of number of multiple

genetic knock-in and knock-out strains and a low cost of maintenance. Despite having advantages, mouse models also suffer from some limitations as well. Thus, the phenotype of the disease or the lesion does not mimic the phenotype in humans. In HSV1 induced encephalitis, a focal patterns of viral and neuroinflammatory lesions is usually observed in humans but such lesions exhibit more diffusive pattern of viral load and inflammation the in mice brain[204,205]. Similarly the viral reactivation is not readily observed in mouse models. Guinea pig, rabbit and macaque provide better model of HSV1 reactivation and any recurrent ulcerative studies but suffer from other disadvantages such as the lack of reagents and ethical issues involved[206–208].

Zebrafish as a promising model for addressing unresolved questions

Zebrafish (*Danio rerio*) is an established model organism for investigating issues related to development, regeneration and drug discovery[209–211]. There are several unique advantages that zebrafish can offer as a model system[211–214]. Some are summarized below.

- Zebrafishes are prolific breeders and one breeding pair could give rise to ~200 offspring each week thereby making large numbers of animals available in short time scale.
- Zebrafish has high degree of similarity to the human at genomic level that facilitates understanding the mechanisms that could also be similar in pathophysiology of humans.
- The small size of animals allows for their easy maintenance and experimental designs and serves as a cost effective tool.
- Ex-utero fertilization allows for better understanding of developmental processes even in the early embryonic stages.

- Wild type animals are optically transparent upto an early adult stage and that could facilitate the direct visualization of internal organs and ongoing biological events.
- The development of transparent animals, such as casper (nacre$^{-/-}$; roy$^{-/-}$) and crystal (nacre$^{-/-}$; roy$^{-/-}$; alb$^{-/-}$) that do not produce any pigment and therefore could provide the accessibility of visual observation even in the adult stages.
- They have fully developed spatiotemporally distinct immune system. At early adult stage (upto ~30 days post fertilization) they do not have a developed adaptive immune system, which allow the investigators to study the role of innate immune cells in as any infection/disease condition.
- Morpholino based easier knock down (suppression) of specific protein function during early developmental stage help facilitate investigations involving target proteins in any biological pathway.

Since zebrafish has remarkable advantages over existing model systems therefore it has encouraged investigators to explore the immune reactions in a better way during various kinds of infections. Kidney marrow is the site of haematopoiesis and most of the immune cell lineages such as lymphoid, myeloid and erythroid have been discovered using transgenic approaches. After developing fluorescent or tractable T cells the origin and distribution of T cells have been discovered in zebrafish. Simultaneously the presence and the development of most of the immune organs (kidney marrow, thymus, spleen, pancreas - for B cells development) and immune cells, such as APC like cells, regulatory like T cells, B cells and neutrophils have been discovered. The immune cells produced in this animal model has the potential to generate various effector molecules such as IFN-γ, TNF-α, interleukins (IL), complement proteins, CC and CXC chemokines to mount an efficient immune response during infection and diseases[215–218].

For investigating immunity and lesions caused by infectious diseases such as tuberculosis induced granulomatous lesions, infected zebrafishes demonstrated close similarity to what is observed in the human patients[219,220]. The receptors required for causing patent infection upon HSV1 inoculation are present in zebrafishes. The entry receptors for HSV1 glycoprotein D, such as 3-O sulfated heparan sulfate (3-OS HS), herpesvirus entry mediator (HVEM) as a member of tumor necrosis factor receptor superfamily member 14 like receptor and nectins (nectin-1a and nectin-1b) have been described[221]. One study showed the HSV1 infectivity (by DNA content determination in dorsal-ventral mid body and encephalon) and the presence by immunostaining for the viral particles expressing VP16 protein in HSV1 injected zebrafish[222]. All these features and the associated advantages clued us to use zebrafish as a model system for investigating HSV1 pathogenesis and immune response induced. Moreover, the cellular dynamics of innate and antigen-specific immune cells could be deciphered and visualized in live animals.

Conclusions

Cytotoxic T cells serve as one of the critical constituents providing protection against HSV1 infection and can help clear or reduce the viral load in infected host. Apart from providing protection in the acute phase of response and controlling replicative viral particles, these cells also suppress the viral reactivation from sensory ganglia. Additionally other immune cells such as neutrophils and $CD4^+$ T cells that produce IFN-γ (Th1 cells) or IL-17 (Th17) cells also get activated during corneal infection and reach to the infection site to produce and secrete proinflammatory molecules and other tissue damaging enzymes to initiate new blood vessels formation (angiogenesis) leading to corneal tissue inflammation that can eventually results in blindness. In order to mitigate such situations, patients are prescribed immunosuppressive drugs.

The work reported in dissertation explored the cytotoxic T cell responses after HSV1 infection in mouse and zebrafish model system, and explored the effect of one of the immunosuppressive drugs (glucocorticoid) on differentiation of virus specific cytotoxic T cells. In first half, the impact of glucocorticoid (dexamethasone being a candidate drug) on differentiating $CD8^+$ T cells after HSV1 infection is explored using an established mouse model. The transient dexamethasone treatment exhibited duality of function on the quiescent and effector $CD8^+$ T cells. The immunosuppressive corticosteroid therapy specifically eliminated naive and memory $CD8^+$ T cells while activated cells were spared. This made the host more susceptible to subsequent infection. The drug treatment induced the tissue migratory molecules in persisting cells and promoted their migration toward infection tissue sites. Additionally dexamethasone treatment also promoted the bystander activation of naive cytotoxic T cells that were not eliminated. This suggests for a limited immunosuppressive potential of the drug. A brief exposure of dexamethasone to activated $CD8^+$ T cells promoted the proliferation that eventually formed more memory generation in the adoptively transferred animals. In second half the feasibility of using zebrafish as a model organism to study cytotoxic T cell responses against HSV1 infection was explored. MHCI-tetramer (Uda-tet) were generated and used for measuring the kinetics and dynamics of cytotoxic T cells responses. These experiments therefore developed zebrafish as a model organism to study virus-specific $CD8^+$ T cells response.

List of References

1. Lafferty, W. E., Coombs, R. W., Benedetti, J., Critchlow, C. & Corey, L. Recurrences after Oral and Genital Herpes Simplex Virus Infection. *N. Engl. J. Med.* **316**, 1444–1449 (1987).
2. Kleinschmidt-DeMasters, B. K. & Gilden, D. H. The expanding spectrum of herpesvirus infections of the nervous system. *Brain Pathol.* **11**, 440–51 (2001).
3. Karasneh, G. A. & Shukla, D. Herpes simplex virus infects most cell types in vitro: clues to its success. *Virol. J.* **8**, 481 (2011).
4. Kieff, E. D., Bachenheimer, S. L. & Roizman, B. Size, composition, and structure of the deoxyribonucleic acid of herpes simplex virus subtypes 1 and 2. *J. Virol.* **8**, 125–32 (1971).
5. Szpara, M. L., Parsons, L. & Enquist, L. W. Sequence variability in clinical and laboratory isolates of herpes simplex virus 1 reveals new mutations. *J. Virol.* **84**, 5303–13 (2010).
6. Egan, K. P., Wu, S., Wigdahl, B. & Jennings, S. R. Immunological control of herpes simplex virus infections. *J. Neurovirol.* **19**, 328–45 (2013).
7. Umene, K., Oohashi, S., Yoshida, M. & Fukumaki, Y. Diversity of the a sequence of herpes simplex virus type 1 developed during evolution. *J. Gen. Virol.* **89**, 841–852 (2008).
8. Akhtar, J. & Shukla, D. Viral entry mechanisms: cellular and viral mediators of herpes simplex virus entry. *FEBS J.* **276**, 7228–7236 (2009).
9. Dollery, S. J., Delboy, M. G. & Nicola, A. V. Low pH-Induced Conformational Change in Herpes Simplex Virus Glycoprotein B. *J. Virol.* **84**, 3759–3766 (2010).
10. Nicola, A. V & Straus, S. E. Cellular and viral requirements for rapid endocytic entry of herpes simplex virus. *J. Virol.* **78**, 7508–17 (2004).

11. Trybala, E., Liljeqvist, J. A., Svennerholm, B. & Bergström, T. Herpes simplex virus types 1 and 2 differ in their interaction with heparan sulfate. *J. Virol.* **74**, 9106–14 (2000).

12. Atanasiu, D., Saw, W. T., Cohen, G. H. & Eisenberg, R. J. Cascade of Events Governing Cell-Cell Fusion Induced by Herpes Simplex Virus Glycoproteins gD, gH/gL, and gB. *J. Virol.* **84**, 12292–12299 (2010).

13. Paludan, S. R., Melchjorsen, J., Malmgaard, L. & Mogensen, S. C. *European cytokine network. European Cytokine Network* **13**, (John Libbey Eurotext Ltd, 2002).

14. Kurt-Jones, E. A. *et al.* Herpes simplex virus 1 interaction with Toll-like receptor 2 contributes to lethal encephalitis. *Proc. Natl. Acad. Sci.* **101**, 1315–1320 (2004).

15. Kurt-Jones, E. A. *et al.* The Role of Toll-Like Receptors in Herpes Simplex Infection in Neonates. *J. Infect. Dis.* **191**, 746–748 (2005).

16. Aravalli, R. N., Hu, S. & Lokensgard, J. R. Toll-like receptor 2 signaling is a mediator of apoptosis in herpes simplex virus-infected microglia. *J. Neuroinflammation* **4**, 11 (2007).

17. Lebon, P. Inhibition of herpes simplex virus type 1-induced interferon synthesis by monoclonal antibodies against viral glycoprotein D and by lysosomotropic drugs. *undefined* (1985).

18. Ankel, H., Westra, D. F., Welling-Wester, S. & Lebon, P. Induction of Interferon-α by Glycoprotein D of Herpes Simplex Virus: A Possible Role of Chemokine Receptors. *Virology* **251**, 317–326 (1998).

19. Kanangat, S., Babu, J. S., Knipe, D. M. & Rouse, B. T. HSV-1-mediated modulation of cytokine gene expression in a permissive cell line: selective upregulation of IL-6 gene expression. *Virology* **219**, 295–300

20. Zachos, G., Clements, B. & Conner, J. Herpes simplex virus type 1 infection stimulates p38/c-Jun N-terminal mitogen-activated protein kinase pathways and activates transcription factor AP-1. *J. Biol. Chem.* **274**, 5097–103 (1999).

21. Hargett, D., McLean, T. & Bachenheimer, S. L. Herpes simplex virus ICP27 activation of stress kinases JNK and p38. *J. Virol.* **79**, 8348–60 (2005).

22. Hargett, D., Rice, S. & Bachenheimer, S. L. Herpes Simplex Virus Type 1 ICP27-Dependent Activation of NF-κB. *J. Virol.* **80**, 10565–10578 (2006).

23. Diao, L. *et al.* Herpes virus proteins ICP0 and BICP0 can activate NF-κB by catalyzing IκBα ubiquitination. *Cell. Signal.* **17**, 217–229 (2005).

24. Jang, K. L., Pulverer, B., Woodgett, J. R. & Latchman, D. S. Activation of the cellular transcription factor AP-1 in herpes simplex virus infected cells is dependent on the viral immediate-early protein ICPO. *Nucleic Acids Res.* **19**, 4879–83 (1991).

25. Diao, L. *et al.* Activation of c-Jun N-terminal kinase (JNK) pathway by HSV-1 immediate early protein ICP0. *Exp. Cell Res.* **308**, 196–210 (2005).

26. Chiu, Y.-H., MacMillan, J. B. & Chen, Z. J. RNA Polymerase III Detects Cytosolic DNA and Induces Type I Interferons through the RIG-I Pathway. *Cell* **138**, 576–591 (2009).

27. Unterholzner, L. *et al.* IFI16 is an innate immune sensor for intracellular DNA. *Nat. Immunol.* **11**, 997–1004 (2010).

28. Miyashita, M., Oshiumi, H., Matsumoto, M. & Seya, T. DDX60, a DEXD/H Box Helicase, Is a Novel Antiviral Factor Promoting RIG-I-Like Receptor-Mediated Signaling. *Mol. Cell. Biol.* **31**, 3802–3819 (2011).

29. Kim, T. *et al.* Aspartate-glutamate-alanine-histidine box motif (DEAH)/RNA helicase A helicases sense microbial DNA in human plasmacytoid dendritic cells. *Proc. Natl. Acad. Sci. U. S. A.* **107**, 15181–6 (2010).

30. Megjugorac, N. J., Gallagher, G. E. & Gallagher, G. Modulation of human plasmacytoid DC function by IFN-λ1 (IL-29). *J. Leukoc. Biol.* **86**, 1359–1363 (2009).

31. Zhang, X. *et al.* Cutting Edge: Ku70 Is a Novel Cytosolic DNA Sensor That Induces Type III Rather Than Type I IFN. *J. Immunol.* **186**, 4541–4545 (2011).

32. Krug, A. *et al.* Herpes simplex virus type 1 activates murine natural interferon-producing cells through toll-like receptor 9. *Blood* **103**, 1433–1437 (2003).

33. Megjugorac, N. J., Gallagher, G. E. & Gallagher, G. Modulation of human plasmacytoid DC function by IFN-λ1 (IL-29). *J. Leukoc. Biol.* **86**, 1359–1363 (2009).

34. Megjugorac, N. J., Young, H. A., Amrute, S. B., Olshalsky, S. L. & Fitzgerald-Bocarsly, P. Virally stimulated plasmacytoid dendritic cells produce chemokines and induce migration of T and NK cells. *J. Leukoc. Biol.* **75**, 504–514 (2004).

35. Takeshita, F. *et al.* Signal transduction pathways mediated by the interaction of CpG DNA with Toll-like receptor 9. *Semin. Immunol.* **16**, 17–22 (2004).

36. Wagner, H. The immunobiology of the TLR9 subfamily. *Trends Immunol.* **25**, 381–386 (2004).

37. Karikó, K., Ni, H., Capodici, J., Lamphier, M. & Weissman, D. mRNA Is an Endogenous Ligand for Toll-like Receptor 3. *J. Biol. Chem.* **279**, 12542–12550 (2004).

38. Jacquemont, B. & Roizman, B. RNA synthesis in cells infected with herpes simplex virus. X. Properties of viral symmetric transcripts and of double-stranded RNA prepared from them. *J. Virol.* **15**, 707–13 (1975).

39. Alexopoulou, L., Holt, A. C., Medzhitov, R. & Flavell, R. A. Recognition of double-stranded RNA and activation of NF-κB by Toll-like receptor 3. *Nature* **413**, 732–738 (2001).

40. SEN, G. & SARKAR, S. Transcriptional signaling by double-stranded RNA: role of TLR3. *Cytokine Growth Factor Rev.* **16**, 1–14 (2005).

41. Zhang, S.-Y. *et al.* TLR3 Deficiency in Patients with Herpes Simplex Encephalitis. *Science (80-.).* **317**, 1522–1527 (2007).

42. Schulz, O. *et al.* Toll-like receptor 3 promotes cross-priming to virus-infected cells. *Nature* **433**, 887–892 (2005).

43. Long, E. O. Negative signaling by inhibitory receptors: the NK cell paradigm. *Immunol. Rev.* **224**, 70–84 (2008).

44. Orr, M. T. & Lanier, L. L. Natural killer cell education and tolerance. *Cell* **142**, 847–56 (2010).

45. Herbring, V., Bäucker, A., Trowitzsch, S. & Tampé, R. A dual inhibition mechanism of herpesviral ICP47 arresting a conformationally thermostable TAP complex. *Sci. Rep.* **6**, 36907 (2016).

46. Ahn, K. *et al.* Molecular mechanism and species specificity of TAP inhibition by herpes simplex virus ICP47. *EMBO J.* **15**, 3247–55 (1996).

47. Oldham, M. L. *et al.* A mechanism of viral immune evasion revealed by cryo-EM analysis of the TAP transporter. *Nature* **529**, 537–540 (2016).

48. Tomazin, R. *et al.* Herpes simplex virus type 2 ICP47 inhibits human TAP but not mouse TAP. *J. Virol.* **72**, 2560–3 (1998).

49. Sauer, M. *et al.* CBP/p300 acetyltransferases regulate the expression of NKG2D ligands on tumor cells. *Oncogene* **36**, 933–941 (2017).

50. Groh, V., Wu, J., Yee, C. & Spies, T. Tumour-derived soluble MIC ligands impair expression of NKG2D and T-cell activation. *Nature* **419**, 734–738 (2002).

51. Schepis, D. *et al.* Herpes Simplex Virus Infection Downmodulates NKG2D Ligand Expression. *Scand. J. Immunol.* **69**, 429–436 (2009).

52. Sondermann, P., Huber, R., Oosthuizen, V. & Jacob, U. The 3.2-Å crystal structure of the human IgG1 Fc fragment–FcγRIII complex. *Nature* **406**, 267–273 (2000).

53. O'Shea, J. J., Weissman, A. M., Kennedy, I. C. & Ortaldo, J. R. Engagement of the natural killer cell IgG Fc receptor results in tyrosine phosphorylation of the zeta chain. *Proc. Natl. Acad. Sci. U. S. A.* **88**, 350–4 (1991).

54. Lanier, L. L., Yu, G. & Phillips, J. H. Co-association of CD3ζ with a receptor (CD16) for IgG Fc on human natural killer cells. *Nature* **342**, 803–805 (1989).

55. Anderson, P. *et al.* Fc gamma receptor type III (CD16) is included in the zeta NK receptor complex expressed by human natural killer cells. *Proc. Natl. Acad. Sci. U. S. A.* **87**, 2274–8 (1990).

56. Dubin, G., Socolof, E., Frank, I. & Friedman, H. M. Herpes simplex virus type 1 Fc receptor protects infected cells from antibody-dependent cellular cytotoxicity. *J. Virol.* **65**, 7046–50 (1991).

57. Lindquist, R. L. *et al.* Visualizing dendritic cell networks in vivo. *Nat. Immunol.* **5**, 1243–1250 (2004).

58. Hickman, H. D. *et al.* Direct priming of antiviral CD8+ T cells in the peripheral interfollicular region of lymph nodes. *Nat. Immunol.* **9**, 155–165 (2008).

59. John, B. *et al.* Dynamic Imaging of CD8+ T Cells and Dendritic Cells during Infection with Toxoplasma gondii. *PLoS Pathog.* **5**, e1000505 (2009).

60. Zhang, N. & Bevan, M. J. Review CD8 + T Cells: Foot Soldiers of the Immune System. (2011). doi:10.1016/j.immuni.2011.07.010

61. Chtanova, T. *et al.* Article Dynamics of T Cell, Antigen-Presenting Cell, and Pathogen Interactions during Recall Responses in the Lymph Node. *Immunity* **31**, 342–355

62. Dorner, B. G. *et al.* Article Selective Expression of the Chemokine Receptor XCR1 on Cross-presenting Dendritic Cells Determines Cooperation with CD8 + T Cells. *Immunity* **31**, 823–833

63. Chakraborty, A. K. & Weiss, A. Insights into the initiation of TCR signaling. *Nat. Immunol.* **15**, 798–807 (2014).

64. Pelosi, M. *et al. Tyrosine 319 in the Interdomain B of ZAP-70 Is a Binding Site for the Src Homology 2 Domain of Lck* Downloaded from*. *THE JOURNAL OF BIOLOGICAL CHEMISTRY* **274**, (1999).

65. Roncagalli, R. *et al.* Quantitative proteomics analysis of signalosome dynamics in primary T cells identifies the surface receptor CD6 as a Lat adaptor–independent TCR signaling hub. *Nat. Immunol.* **15**, 384–392 (2014).

66. Malissen, B., Grégoire, C., Malissen, M. & Roncagalli, R. Integrative biology of T cell activation. *Nat. Immunol.* **15**, 790–797 (2014).

67. Navarro, M. N. & Cantrell, D. A. Serine-threonine kinases in TCR signaling. *Nat. Immunol.* **15**, 808–814 (2014).

68. Brodovitch, A., Bongrand, P. & Pierres, A. Minute Seconds and Make a Decision within One T Lymphocytes Sense Antigens within. *J Immunol* **191**, 2064–2071 (2013).

69. Huse, M. *et al.* Article Spatial and Temporal Dynamics of T Cell Receptor Signaling with a Photoactivatable Agonist. doi:10.1016/j.immuni.2007.05.017

70. Salomon, B. T. *et al. B7/CD28 Costimulation Is Essential for the Homeostasis of the CD4 CD25 Immunoregulatory T Cells that Control Autoimmune Diabetes*. *Immunity* **12**, (2000).

71. Viola, A. & Lanzavecchia, A. T cell activation determined by T cell receptor number and tunable thresholds. *Science* **273**, 104–6 (1996).

72. Harding, F. A., McArthur, J. G., Gross, J. A., Raulet, D. H. & Allison, J. P. CD28-mediated signalling co-stimulates murine T cells and prevents induction of anergy in T-cell clones. *Nature* **356**, 607–609 (1992).

73. Porciello, N. & Tuosto, L. CD28 costimulatory signals in T lymphocyte activation: Emerging functions beyond a qualitative and quantitative support to TCR signalling. *Cytokine Growth Factor Rev.* **28**, 11–19 (2016).

74. Viola, A., Contento, R. L. & Molon, B. Signaling Amplification at the Immunological Synapse. in *Current topics in microbiology and immunology* **340**, 109–122 (2010).

75. Esensten, J. H., Helou, Y. A., Chopra, G., Weiss, A. & Bluestone, J. A. Review CD28 Costimulation: From Mechanism to Therapy. (2016). doi:10.1016/j.immuni.2016.04.020

76. Pagès, F. *et al.* Binding of phosphatidyl-inositol-3-OH kinase to CD28 is required for T-cell signalling. *Nature* **369**, 327–329 (1994).

77. August, A. *et al.* CD28 is associated with and induces the immediate tyrosine phosphorylation and activation of the Tec family kinase ITK/EMT in the human Jurkat leukemic T-cell line. *Proc. Natl. Acad. Sci. U. S. A.* **91**, 9347–51 (1994).

78. Holdorf, A. D. *et al. Proline Residues in CD28 and the Src Homology (SH)3 Domain of Lck Are Required for T Cell Costimulation*. *J. Exp. Med* **190**, (1999).

79. Yokosuka, T. *et al.* Spatiotemporal Regulation of T Cell Costimulation by TCR-CD28 Microclusters and Protein Kinase C θ Translocation. *Immunity* **29**, 589–601 (2008).

80. Muscolini, M., Sajeva, A., Caristi, S. & Tuosto, L. A novel association between filamin A and NF-κB inducing kinase couples CD28 to inhibitor of NF-κB kinase α and NF-κB activation. *Immunol. Lett.* **136**, 203–212 (2011).

81. Raab, M. *et al.* p56Lck and p59Fyn regulate CD28 binding to phosphatidylinositol 3-kinase, growth factor receptor-bound protein GRB-2, and T cell-specific protein-tyrosine kinase ITK: implications for T-cell costimulation. *Proc. Natl. Acad. Sci. U. S. A.* **92**, 8891–5 (1995).

82. Toma, H. *et al.* CD28-Mediated Costimulation with CD28 and Play Distinct Roles in Grb2 and Gads Exhibit Different Interactions. *J Immunol* **177**, 1085–1091 (2006).

83. Capuano, C. *et al.* Phosphatidylinositol 4–Phosphate 5–Kinase α and Vav1 Mutual Cooperation in CD28-Mediated Actin Remodeling and Signaling Functions. *J. Immunol.* **194**, 1323–1333 (2014).

84. Villalba, M. *et al.* Vav1/Rac-dependent actin cytoskeleton reorganization is required for lipid raft clustering in T cells. *J. Cell Biol.* **155**, 331–338 (2001).

85. Chan, G. *et al.* Vav is a regulator of cytoskeletal reorganization mediated by the T-cell receptor. *Curr. Biol.* **8**, 554-S3 (2004).

86. Berg, R. E., Crossley, E., Murray, S. & Forman, J. Memory CD8 T Cells Provide Innate Immune Protection against Listeria monocytogenes in the Absence of Cognate Antigen. *J. Exp. Med. J. Exp. Med.* □ **198**, 1583–1593 (2003).

87. Beadling, C. & Slifka, M. K. Differential regulation of virus-specific T-cell effector functions following activation by peptide or innate cytokines. *Blood* **105**, 1179–1186 (2005).

88. Schmidt, C. S. & Mescher, M. F. *In Vivo T Cells + Tolerizing to Immunizing for CD8 Peptide Antigen Administration from Adjuvant Effect of IL-12: Conversion of*. *J Immunol References* **163**, (1999).

89. Lins, M. C. *et al. T Cells + and CD8 + Signal for Activation of Naive CD4 Inflammatory Cytokines Provide a Third*. (1999).

90. Rao, R. R., Li, Q., Odunsi, K. & Shrikant, P. A. The mTOR Kinase Determines Effector versus Memory CD8 + T Cell Fate by Regulating the Expression of Transcription Factors T-bet and Eomesodermin. *Immunity* **32**, 67–78

91. Mescher, J. M., Curtsinger, C. M. & Johnson, M. F. Costimulation, and Signal 3 Cytokine Prolonged Exposure to Antigen, Development of Effector Function Require CD8 T Cell Clonal Expansion and. *J Immunol Ref.* **171**, 5165–5171 (2003).

92. Mescher, M. F., Valenzuela, J. O. & Hammerbeck, C. D. Antigen-Activated CD8 T Cells 3 Cytokine (IL-12) Prolongs Survival of Cutting Edge: Bcl-3 Up-Regulation by Signal. (2005). doi:10.4049/jimmunol.174.2.600

93. van Seventer Ellen M Palmer, G. A., Farrokh-Siar, L. & Maguire van, J. Enzyme Function IL-12 Alters Caspase Processing and Inhibits by Intercellular Adhesion Molecule-1. I. Costimulated Death in Human Naive Th Cells IL-12 Decreases Activation-Induced Cell. *J Immunol* **167**, 749–758 (2001).

94. Kolumam, G. A., Thomas, S., Thompson, L. J., Sprent, J. & Murali-Krishna, K. Type I interferons act directly on CD8 T cells to allow clonal expansion and memory formation in response to viral infection. **202**, 637–650 (2005).

95. Schweier, U. *et al.* Type I IFN Receptor for Clonal Expansion Require Lymphocytic Choriomeningitis Virus Cutting Edge: CD8 T Cells Specific for. (2006). doi:10.4049/jimmunol.176.8.4525

96. Whitmire, J. K., Tan, J. T. & Whitton, J. L. BRIEF DEFINITIVE REPORT Interferon-acts directly on CD8 T cells to increase their abundance during virus infection. **201**, 1053–1059 (2005).

97. Whitmire, J. K., Benning, N. & Whitton, J. L. Signaling Directly γ Cutting Edge: Early IFN. (2005). doi:10.4049/jimmunol.175.9.5624

98. Watts, T. H. TNF/TNFR FAMILY MEMBERS IN COSTIMULATION OF T CELL RESPONSES. *Annu. Rev. Immunol.* **23**, 23–68 (2005).

99. Deeths, M. J., Kedl, R. M. & Mescher, M. F. *Presence of Costimulation (Anergic) Following Activation in the T Cells Become Nonresponsive + CD8. J Immunol References* **102**, (1999).

100. Tham, E. L. & Mescher, M. F. CTL Response Th-Dependent Regulatory Checkpoint in the Activation-Induced Nonresponsiveness: A. (2002). doi:10.4049/jimmunol.168.3.1190

101. Bachmann, M. F., Wolint, P., Walton, S., Schwarz, K. & Oxenius, A. Differential role of IL-2R signaling for CD8+ T cell responses in acute and chronic viral infections. *Eur. J. Immunol.* **37**, 1502–1512 (2007).

102. Williams, M. A., Tyznik, A. J. & Bevan, M. J. Interleukin-2 signals during priming are required for secondary expansion of CD8+ memory T cells. *Nature* **441**, 890–893 (2006).

103. Obar, J. J. *et al.* CD4+ T cell regulation of CD25 expression controls development of short-lived effector CD8+ T cells in primary and secondary responses. *Proc. Natl. Acad. Sci.* **107**, 193–198 (2009).

104. Cox, M. A., Harrington, L. E. & Zajac, A. J. Cytokines and the Inception of CD8 T Cell Responses The Pluripotency of Naïve CD8 T cells. *Trends Immunol* **32**, 180–186 (2011).

105. Yoon, H., Kim, T. S. & Braciale, T. J. The Cell Cycle Time of CD8 + T Cells Responding In Vivo Is Controlled by the Type of Antigenic Stimulus. (2010). doi:10.1371/journal.pone.0015423

106. Vander Heiden, M. G., Cantley, L. C. & Thompson, C. B. Understanding the Warburg Effect: The Metabolic Requirements of Cell Proliferation NIH Public Access. *Science (80-.).* **324**, 1029–1033 (2009).

107. Chang, J. T., Wherry, E. J. & Goldrath, A. W. Molecular regulation of effector and memory T cell differentiation. *Nat. Immunol.* **15**, 1104–1115 (2014).

108. Katakai, T., Hara, T., Sugai, M., Gonda, H. & Shimizu, A. Lymph Node Fibroblastic Reticular Cells Construct the Stromal Reticulum via Contact with Lymphocytes. *J. Exp. Med. J. Exp. Med* **200**, 783–795 (2004).

109. Woolf, E. *et al.* Lymph node chemokines promote sustained T lymphocyte motility without triggering stable integrin adhesiveness in the absence of shear forces. *Nat. Immunol.* **8**, 1076–1085 (2007).

110. Real, E., Donnadieu, E., Asperti-Boursin, F., Trautmann, A. & Bismuth, G. CCR7 ligands control basal T cell motility within lymph node slices in a phosphoinositide 3–kinase– independent manner. *J. Exp. Med.* (2007). doi:10.1084/jem.20062079

111. Finlay, D. & Cantrell, D. A. Metabolism, migration and memory in cytotoxic T cells. *Nat. Rev. Immunol.* **11**, 109–117 (2011).

112. Mora, J. R. & von Andrian, U. H. T-cell homing specificity and plasticity: new concepts and future challenges. *Trends Immunol.* **27**, 235–243 (2006).

113. Lichtman, A. H. *et al.* Effector Activity Heart by Separable Effects on Migration and T-bet Controls Pathogenicity of CTLs in the. (2006). doi:10.4049/jimmunol.177.9.5890

114. Bankovich, A. J., Shiow, L. R. & Cyster, J. G. CD69 Suppresses Sphingosine 1-Phosophate Receptor-1 (S1P 1) Function through Interaction with Membrane Helix 4 * □ S Downloaded from. *J. Biol. Chem.* **285**, 22328–22337 (2010).

115. Sebzda, E., Zou, Z., Lee, J. S., Wang, T. & Kahn, M. L. Transcription factor KLF2 regulates the migration of naive T cells by restricting chemokine receptor expression patterns. *Nat. Immunol.* **9**, 292–300 (2008).

116. Bai, A., Hu, H., Yeung, M. & Chen, J. Transcription and Sphingosine-1-Phosphate Receptor 1 (CD62L) Trafficking by Activating L-Selectin Krüppel-Like Factor 2 Controls T Cell. *J Immunol Ref.* **178**, 7632–7639 (2007).

117. Carlson, C. M. *et al.* Kruppel-like factor 2 regulates thymocyte and T-cell migration. *Nature* **442**, 299–302 (2006).

118. Cyster, J. G. CHEMOKINES, SPHINGOSINE-1-PHOSPHATE, AND CELL MIGRATION IN SECONDARY LYMPHOID ORGANS. *Annu. Rev. Immunol* **23**, 127–59 (2005).

119. Pham, T. H. M., Okada, T., Matloubian, M., Lo, C. G. & Cyster, J. G. Article S1P 1 Receptor Signaling Overrides Retention Mediated by Ga i-Coupled Receptors to Promote T Cell Egress. doi:10.1016/j.immuni.2007.11.017

120. Lord, G. M. *et al.* T-bet is required for optimal proinflammatory CD4 T-cell trafficking. (2005). doi:10.1182/blood-2005-04-1393

121. Liu, T., Khanna, K. M., Chen, X., Fink, D. J. & Hendricks, R. L. CD8 T Cells Can Block Herpes Simplex Virus Type 1 (HSV-1) Reactivation from Latency in Sensory Neurons. *J. Exp. Med* **191**, 1459–1466 (2000).

122. Simmons, A. Anti-CD8 impairs clearance of herpes simplex virus from the nervous system: implications for the fate of virally infected neurons. *J. Exp. Med.* **175**, 1337–1344 (2004).

123. Palmer, E. M., Holbrook, B. C., Arimilli, S., Parks, G. D. & Alexander-Miller, M. A. IFNγ-producing, virus-specific CD8 + effector cells acquire the ability to produce IL-10 as a result of entry into the infected lung environment. *Virology* **404**, 225–230 (2010).

124. Kathryn Trandem, P., Zhao, J. & Fleming, E. Coronavirus-Induced Encephalitis Express Protective IL-10 at the Peak of Highly Activated Cytotoxic CD8 T Cells. (2011). doi:10.4049/jimmunol.1003292

125. Sun, J., Madan, R., Karp, C. L. & Braciale, T. J. Effector T cells control lung inflammation during acute influenza virus infection by producing IL-10. *Nat. Med.* **15**, 277–284 (2009).

126. Zhang, N. & Bevan, M. J. Review CD8 + T Cells: Foot Soldiers of the Immune System. *Immunity* **35**, 161–168 (2011).

127. Kaye, S. & Choudhary, A. Herpes simplex keratitis. *Prog. Retin. Eye Res.* **25**, 355–380 (2006).

128. Rouse, B. T. & Sehrawat, S. Immunity and immunopathology to viruses: what decides the outcome? *Nat. Rev. Immunol.* **10**, 514–26 (2010).

129. Rolinski, J. & Hus, I. Immunological aspects of acute and recurrent herpes simplex keratitis. *J. Immunol. Res.* **2014**, 513560 (2014).

130. Suryawanshi, A. *et al.* Role of IL-17 and Th17 cells in herpes simplex virus-induced corneal immunopathology. *J. Immunol.* **187**, 1919–30 (2011).

131. Azher, T. N., Yin, X.-T. & Stuart, P. M. Understanding the Role of Chemokines and Cytokines in Experimental Models of Herpes Simplex Keratitis. *J. Immunol. Res.* **2017**, 1–5 (2017).

132. Yang, Y.-N., Wang, F., Zhou, W., Wu, Z.-Q. & Xing, Y.-Q. TNF-α Stimulates MMP-2 and MMP-9 Activities in Human Corneal Epithelial Cells via the Activation of FAK/ERK Signaling. *Ophthalmic Res.* **48**, 165–170 (2012).

133. Xue, M. L. *et al.* Regulation of MMPs and TIMPs by IL-1β during Corneal Ulceration and Infection. *Investig. Opthalmology Vis. Sci.* **44**, 2020 (2003).

134. Farooq, A. V & Shukla, D. Herpes Simplex Epithelial and Stromal Keratitis: An Epidemiologic Update. (2012). doi:10.1016/j.survophthal.2012.01.005

135. Reddy, N. K., Rajasagi, B. T., Rouse, A., Suryawanshi, T. & Veiga-Parga, P. B. J. Infection Angiogenesis after Herpes Simplex Virus Expression and Promotes Corneal (VEGF)-A and Soluble VEGF Receptor 1 Vascular Endothelial Growth Factor IL-17A Differentially Regulates Corneal. *J Immunol Ref.* **188**, 3434–3446 (2012).

136. Yamaguchi, T. *et al.* Control of Immune Responses by Antigen-Specific Regulatory T Cells Expressing the Folate Receptor. *Immunity* **27**, 145–159 (2007).

137. Deaglio, S. *et al.* Adenosine generation catalyzed by CD39 and CD73 expressed on regulatory T cells mediates immune suppression. *J. Exp. Med.* **204**, 1257–1265 (2007).

138. Shevach, E. M. *et al.* The lifestyle of naturally occurring CD4+CD25+Foxp3+ regulatory T cells. *Immunol. Rev.* **212**, 60–73 (2006).

139. de la Rosa, M., Rutz, S., Dorninger, H. & Scheffold, A. Interleukin-2 is essential for CD4+CD25+ regulatory T cell function. *Eur. J. Immunol.* **34**, 2480–2488 (2004).

140. von Boehmer, H. Mechanisms of suppression by suppressor T cells. *Nat. Immunol.* **6**, 338–344 (2005).

141. Ghiringhelli, F. *et al.* CD4 $^{+}$ CD25 $^{+}$ regulatory T cells inhibit natural killer cell functions in a transforming growth factor–β–dependent manner. *J. Exp. Med.* **202**, 1075–1085 (2005).

142. Nakamura, K. *et al.* TGF-beta 1 plays an important role in the mechanism of CD4+CD25+ regulatory T cell activity in both humans and mice. *J. Immunol.* **172**, 834–42 (2004).

143. Kingsley, C. I., Karim, M., Bushell, A. R. & Wood, K. J. CD25+CD4+ regulatory T cells prevent graft rejection: CTLA-4- and IL-10-dependent immunoregulation of alloresponses. *J. Immunol.* **168**, 1080–6 (2002).

144. Fallarino, F. *et al.* The combined effects of tryptophan starvation and tryptophan catabolites down-regulate T cell receptor zeta-chain and induce a regulatory phenotype in naive T cells. *J. Immunol.* **176**, 6752–61 (2006).

145. Huang, C.-T. *et al.* Role of LAG-3 in Regulatory T Cells. *Immunity* **21**, 503–513 (2004).

146. Chen, W. *et al.* Conversion of Peripheral CD4 $^{+}$ CD25 $^{-}$ Naive T Cells to CD4 $^{+}$ CD25 $^{+}$ Regulatory T Cells by TGF-β Induction of Transcription Factor *Foxp3*. *J. Exp. Med.* **198**, 1875–1886 (2003).

147. Huber, S. *et al.* Cutting edge: TGF-beta signaling is required for the in vivo expansion and immunosuppressive capacity of regulatory CD4+CD25+ T cells. *J. Immunol.* **173**, 6526–31 (2004).

148. McGeachy, M. J., Stephens, L. A. & Anderton, S. M. Natural recovery and protection from autoimmune encephalomyelitis: contribution of CD4+CD25+ regulatory cells within the central nervous system. *J. Immunol.* **175**, 3025–32 (2005).

149. Uhlig, H. H. *et al.* Characterization of Foxp3+CD4+CD25+ and IL-10-secreting CD4+CD25+ T cells during cure of colitis. *J. Immunol.* **177**, 5852–60 (2006).

150. Kryczek, I. *et al.* Cutting edge: induction of B7-H4 on APCs through IL-10: novel suppressive mode for regulatory T cells. *J. Immunol.* **177**, 40–4 (2006).

151. Grossman, W. J. *et al.* Human T Regulatory Cells Can Use the Perforin Pathway to Cause Autologous Target Cell Death. *Immunity* **21**, 589–601 (2004).

152. Zhao, D.-M., Thornton, A. M., DiPaolo, R. J. & Shevach, E. M. Activated CD4+CD25+ T cells selectively kill B lymphocytes. *Blood* **107**, 3925–3932 (2006).

153. Gondek, D. C., Lu, L.-F., Quezada, S. A., Sakaguchi, S. & Noelle, R. J. Cutting edge: contact-mediated suppression by CD4+CD25+ regulatory cells involves a granzyme B-dependent, perforin-independent mechanism. *J. Immunol.* **174**, 1783–6 (2005).

154. Akkaya, B. *et al.* Regulatory T cells mediate specific suppression by depleting peptide–MHC class II from dendritic cells. *Nat. Immunol.* **20**, 218–231 (2019).

155. Hori, S., Nomura, T. & Sakaguchi, S. Control of regulatory T cell development by the transcription factor Foxp3. *Science* **299**, 1057–61 (2003).

156. Bluestone, J. A. & Abbas, A. K. Natural versus adaptive regulatory T cells. *Nat. Rev. Immunol.* **3**, 253–257 (2003).

157. Sakaguchi, S., Sakaguchi, N., Asano, M., Itoh, M. & Toda, M. Immunologic self-tolerance maintained by activated T cells expressing IL-2 receptor alpha-chains (CD25). Breakdown of a single mechanism of self-tolerance causes various autoimmune diseases. *J. Immunol.* **155**, 1151–64 (1995).

158. Mills, K. H. G. Regulatory T cells: friend or foe in immunity to infection? *Nat. Rev. Immunol.* **4**, 841–855 (2004).

159. Suvas, S., Azkur, A. K., Kim, B. S., Kumaraguru, U. & Rouse, B. T. CD4+CD25+ regulatory T cells control the severity of viral immunoinflammatory lesions. *J. Immunol.* **172**, 4123–32 (2004).

160. Garba, M. L., Pilcher, C. D., Bingham, A. L., Eron, J. & Frelinger, J. A. HIV antigens can induce TGF-beta(1)-producing immunoregulatory CD8+ T cells. *J. Immunol.* **168**, 2247–54 (2002).

161. Seo, N., Tokura, Y., Takigawa, M. & Egawa, K. Depletion of IL-10- and TGF-beta-producing regulatory gamma delta T cells by administering a daunomycin-conjugated specific monoclonal antibody in early tumor lesions augments the activity of CTLs and NK cells. *J. Immunol.* **163**, 242–9 (1999).

162. Marshall, N. A., Vickers, M. A. & Barker, R. N. Regulatory T Cells Secreting IL-10 Dominate the Immune Response to EBV Latent Membrane Protein 1. *J. Immunol.* **170**, 6183–6189 (2014).

163. Accapezzato, D. *et al.* Hepatic expansion of a virus-specific regulatory CD8+ T cell population in chronic hepatitis C virus infection. *J. Clin. Invest.* **113**, 963 (2004).

164. Li, M. *et al.* Roles of Myeloid-Derived Suppressor Cell Subpopulations in Autoimmune Arthritis. *Front. Immunol.* **9**, 2849 (2018).

165. Gabrilovich, D. I. & Nagaraj, S. Myeloid-derived suppressor cells as regulators of the immune system. *Nat. Rev. Immunol.* **9**, 162–174 (2009).

166. Huang, B. *et al.* Gr-1 $^{+}$ CD115 $^{+}$ Immature Myeloid Suppressor Cells Mediate the Development of Tumor-Induced T Regulatory Cells and T-Cell Anergy in Tumor-Bearing Host. *Cancer Res.* **66**, 1123–1131 (2006).

167. Haile, L. A. *et al.* Myeloid-Derived Suppressor Cells in Inflammatory Bowel Disease: A New Immunoregulatory Pathway. *Gastroenterology* **135**, 871–881.e5 (2008).

168. Fujii, W. *et al.* Myeloid-Derived Suppressor Cells Play Crucial Roles in the Regulation of Mouse Collagen-Induced Arthritis. *J. Immunol.* **191**, 1073–1081 (2013).

169. Kim, Y.-J., Chang, S.-Y. & Ko, H.-J. Myeloid-derived suppressor cells in inflammatory bowel disease. *Intest. Res.* **13**, 105–11 (2015).

170. Hu, C., Du, W., Zhang, X., Wong, F. S. & Wen, L. The role of Gr1+ cells after anti-CD20 treatment in type 1 diabetes in nonobese diabetic mice. *J. Immunol.* **188**, 294–301 (2012).

171. Park, M.-J. *et al.* Myeloid-Derived Suppressor Cells Induce the Expansion of Regulatory B Cells and Ameliorate Autoimmunity in the Sanroque Mouse Model of Systemic Lupus Erythematosus. *Arthritis Rheumatol.* **68**, 2717–2727 (2016).

172. Zhu, B. *et al.* CD11b+Ly-6C(hi) suppressive monocytes in experimental autoimmune encephalomyelitis. *J. Immunol.* **179**, 5228–37 (2007).

173. Mueller, T. F. Mechanisms of Action of Thymoglobulin. *Transplantation* **84**, S5–S10 (2007).

174. Wiseman, A. C. Immunosuppressive Medications. *Clin. J. Am. Soc. Nephrol.* **11**, 332–43 (2016).

175. Hartono, C., Muthukumar, T. & Suthanthiran, M. Immunosuppressive drug therapy. *Cold Spring Harb. Perspect. Med.* **3**, a015487 (2013).

176. Varanasi, S. K. *et al.* Azacytidine Treatment Inhibits the Progression of Herpes Stromal Keratitis by Enhancing Regulatory T Cell Function. *J. Virol.* **91**, (2017).

177. Knight, D. A. *et al.* Inhibition of herpes simplex virus type 1 by the experimental immunosuppressive agent leflunomide. *Transplantation* **71**, 170–4 (2001).

178. American Association of Immunologists., S. K. & Rouse, B. T. *The journal of immunology : official journal of the American Association of Immunologists. The Journal of Immunology* **198**, (Williams & Wilkins, 1950).

179. Turkay, E., Ozmen, A., Unek, G. & Mendilcioglu, I. The Effects of Glucocorticoids on Fetal and Placental Development. in *Glucocorticoids - New Recognition of Our Familiar Friend* (InTech, 2012). doi:10.5772/50103

180. Wilson, K. S. *et al.* Physiological roles of glucocorticoids during early embryonic development of the zebrafish (Danio rerio). *J. Physiol.* **591**, 6209–20 (2013).

181. Nesan, D. & Vijayan, M. M. Role of glucocorticoid in developmental programming: Evidence from zebrafish. *Gen. Comp. Endocrinol.* **181**, 35–44 (2013).

182. Fowden, A. L. & Forhead, A. J. Glucocorticoids as regulatory signals during intrauterine development. *Exp. Physiol.* **100**, 1477–1487 (2015).

183. HAUNER, H., SCHMID, P. & PFEIFFER, E. F. Glucocorticoids and Insulin Promote the Differentiation of Human Adipocyte Precursor Cells into Fat Cells. *J. Clin. Endocrinol. Metab.* **64**, 832–835 (1987).

184. Goodyer, I. M., Park, R. J., Netherton, C. M. & Herbert, J. Possible role of cortisol and dehydroepiandrosterone in human development and psychopathology. *Br. J. Psychiatry* **179**, 243–249 (2001).

185. Cain, D. W. & Cidlowski, J. A. Immune regulation by glucocorticoids. *Nat. Rev. Immunol.* **17**, 233–247 (2017).

186. Stewart, P. M. & Krozowski, Z. S. 11 beta-Hydroxysteroid dehydrogenase. *Vitam. Horm.* **57**, 249–324 (1999).

187. Draper, N. & Stewart, P. M. 11 -Hydroxysteroid dehydrogenase and the pre-receptor regulation of corticosteroid hormone action. *J. Endocrinol.* **186**, 251–271 (2005).

188. Buttgereit, F. & Scheffold, A. Rapid glucocorticoid effects on immune cells. *Steroids* **67**, 529–34 (2002).

189. Boldizsar, F. *et al.* Emerging pathways of non-genomic glucocorticoid (GC) signalling in T cells. *Immunobiology* **215**, 521–526 (2010).

190. Sionov, R. V., Cohen, O., Kfir, S., Zilberman, Y. & Yefenof, E. Role of mitochondrial glucocorticoid receptor in glucocorticoid-induced apoptosis. *J. Exp. Med.* **203**, 189–201 (2006).

191. Surjit, M. *et al.* Widespread Negative Response Elements Mediate Direct Repression by Agonist- Liganded Glucocorticoid Receptor. *Cell* **145**, 224–241 (2011).

192. Luisi, B. F. *et al.* Crystallographic analysis of the interaction of the glucocorticoid receptor with DNA. *Nature* **352**, 497–505 (1991).

193. Strähle, U., Klock, G. & Schütz, G. A DNA sequence of 15 base pairs is sufficient to mediate both glucocorticoid and progesterone induction of gene expression. *Proc. Natl. Acad. Sci. U. S. A.* **84**, 7871–5 (1987).

194. Ratman, D. *et al.* How glucocorticoid receptors modulate the activity of other transcription factors: a scope beyond tethering. *Mol. Cell. Endocrinol.* **380**, 41–54 (2013).

195. Diamond, M. I., Miner, J. N., Yoshinaga, S. K. & Yamamoto, K. R. Transcription factor interactions: selectors of positive or negative regulation from a single DNA element. *Science* **249**, 1266–72 (1990).

196. Teurich, S. & Angel, P. The glucocorticoid receptor synergizes with Jun homodimers to activate AP-1-regulated promoters lacking GR binding sites. *Chem. Senses* **20**, 251–5 (1995).

197. Lechner, J., Welte, T. & Doppler, W. Mechanism of Interaction between the Glucocorticoid Receptor and Stat5: Role of DNA-Binding. *Immunobiology* **198**, 112–123 (1997).

198. Kerppola, T. K., Luk, D. & Curran, T. Fos is a preferential target of glucocorticoid receptor inhibition of AP-1 activity in vitro. *Mol. Cell. Biol.* **13**, 3782–91 (1993).

199. Biddie, S. C. *et al.* Transcription Factor AP1 Potentiates Chromatin Accessibility and Glucocorticoid Receptor Binding. *Mol. Cell* **43**, 145–155 (2011).

200. Kollias, C. M., Huneke, R. B., Wigdahl, B. & Jennings, S. R. Animal models of herpes simplex virus immunity and pathogenesis. *J. Neurovirol.* **21**, 8–23 (2015).

201. TEAGUE, O. & GOODPASTURE, E. W. EXPERIMENTAL HERPES ZOSTER. *J. Am. Med. Assoc.* **81**, 377 (1923).

202. SYDISKIS, R. J. & SCHULTZ, I. HERPES SIMPLEX SKIN INFECTION IN MICE. *J. Infect. Dis.* **115**, 237–46 (1965).

203. Simmons, A. & Nash, A. A. *Zosteriform Spread of Herpes Simplex Virus as a Model of Recrudescence and Its Use to Investigate the Role of Immune Cells in Prevention of Recurrent Disease Downloaded from*. *JOURNAL OF VIROLOGY* (1984).

204. Meyding-Lamadé, U. K. *et al.* Experimental Herpes Simplex Virus Encephalitis: A Combination Therapy of Acyclovir and Glucocorticoids Reduces Long-Term Magnetic Resonance Imaging Abnormalities. *J. Neurovirol.* **9**, 118–125 (2003).

205. Barker, K. R. *et al.* Encephalitis in an immunocompetent man. *J. Clin. Virol.* **59**, 1–3 (2014).

206. Wagner, E. K. & Bloom, D. C. *Experimental Investigation of Herpes Simplex Virus Latency †*. **10**, (1997).

207. Valencia, F., Veselenak, R. L. & Bourne, N. In Vivo Evaluation of Antiviral Efficacy Against Genital Herpes Using Mouse and Guinea Pig Models. in 315–326 (2013). doi:10.1007/978-1-62703-484-5_24

208. Fan, S. *et al.* The Characteristics of Herpes Simplex Virus Type 1 Infection in Rhesus Macaques and the Associated Pathological Features. *Viruses* **9**, 26 (2017).

209. Lieschke, G. J. & Currie, P. D. Animal models of human disease: zebrafish swim into view. *Nat. Rev. Genet.* **8**, 353–367 (2007).

210. Dooley, K. & Zon, L. I. Zebrafish: a model system for the study of human disease. *Curr. Opin. Genet. Dev.* **10**, 252–6 (2000).

211. Kari, G., Rodeck, U. & Dicker, A. P. Zebrafish: an emerging model system for human disease and drug discovery. *Clin. Pharmacol. Ther.* **82**, 70–80 (2007).

212. White, R. M. *et al.* Transparent Adult Zebrafish as a Tool for In Vivo Transplantation Analysis. *Cell Stem Cell* **2**, 183–189 (2008).

213. Langenau, D. M. & Zon, L. I. The zebrafish: a new model of T-cell and thymic development. *Nat. Rev. Immunol.* **5**, 307–317 (2005).

214. Antinucci, P. & Hindges, R. A crystal-clear zebrafish for in vivo imaging. *Sci. Rep.* **6**, 29490 (2016).

215. Renshaw, S. A. & Ingham, P. W. Zebrafish models of the immune response: taking it on the ChIn. *BMC Biol.* **8**, 148 (2010).

216. Trede, N. S., Langenau, D. M., Traver, D., Look, A. T. & Zon, L. I. The use of zebrafish to understand immunity. *Immunity* **20**, 367–79 (2004).

217. Yoder, J. A., Nielsen, M. E., Amemiya, C. T. & Litman, G. W. Zebrafish as an immunological model system. *Microbes Infect.* **4**, 1469–78 (2002).

218. Meeker, N. D. & Trede, N. S. Immunology and zebrafish: Spawning new models of human disease. *Dev. Comp. Immunol.* **32**, 745–757 (2008).

219. Lesley, R. & Ramakrishnan, L. Insights into early mycobacterial pathogenesis from the zebrafish. *Curr. Opin. Microbiol.* **11**, 277–83 (2008).

220. Prouty, M. G., Correa, N. E., Barker, L. P., Jagadeeswaran, P. & Klose, K. E. Zebrafish- *Mycobacterium marinum* model for mycobacterial pathogenesis. *FEMS Microbiol. Lett.* **225**, 177–182 (2003).

221. Antoine, T. E., Jones, K. S., Dale, R. M., Shukla, D. & Tiwari, V. Zebrafish: modeling for herpes simplex virus infections. *Zebrafish* **11**, 17–25 (2014).

222. Burgos, J. S., Ripoll-Gomez, J., Alfaro, J. M., Sastre, I. & Valdivieso, F. Zebrafish as a New Model for Herpes Simplex Virus Type 1 Infection. *Zebrafish* **5**, 323–333 (2008).

APPENDIX

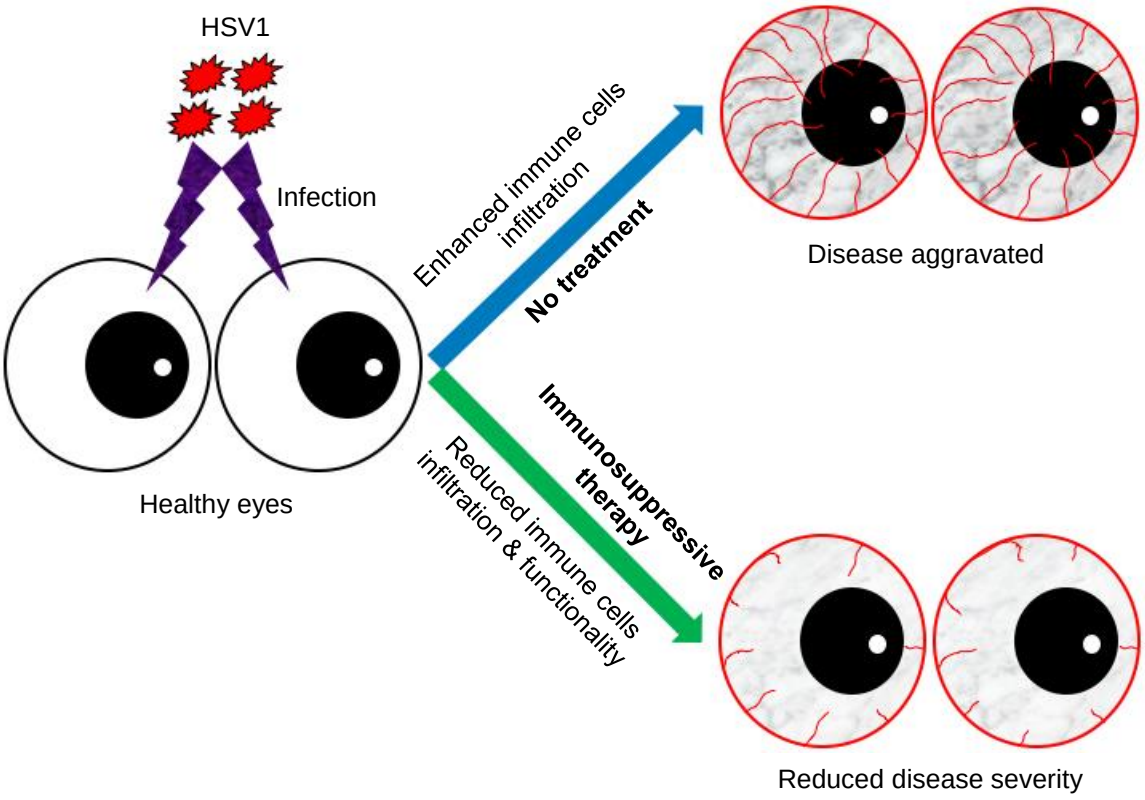

Figure 1. 1 HSV1 induced stromal keratitis and its management by immunosuppressive therapy.

Following ocular HSV1 infection, immune cells (polymorphonuclear leukocyts (PMN) and $CD4^+$ T lymphocytes) infiltration help induce neovascularization and various immunosuppressive therapies have been used to ameliorate the disease condition.

PART II

Divergent effects of a transient corticosteroid therapy on quiescent and effector virus-specific $CD8^+$ T cells

The research work described in this part is a slight modification of a paper submitted for publication in Frontiers in Immunology by Dhaneshwar Kumar and Sharvan Sehrawat. Divergent effects of a transient corticosteroid therapy on quiescent and effector virus-specific CD8 T cells.

In this chapter the words “our” and “we” allude to me and co-author. My contribution in the project includes (1) Selection of the topic (2) Designing and performing the experiments (3) Preparation of figures and graphs (4) Results interpretation (5) Compiling and elucidation of the literature (6) Writing and editing of the literature (7) Bestowing comprehensive structure to the paper

Abstract

We investigated the influence of a transient treatment of immunosuppressive corticosteroid in determining the fate and function of $CD8^+$ T cells during herpesvirus infections. Dexamethasone, a synthetic corticosteroid, induced apoptosis of naïve and virus-specific memory $CD8^+$ T cells but spared effector cells as the latter down regulated Nr3c1, a specific receptor for glucocorticoids. Dexamethasone induced attrition of naïve $CD8^+$ T cells compromised anti-viral $CD8^+$ T cells immunity against a subsequent infection but augmented the effector functions, inflammatory tissue homing potential as well as transition of effector cells into memory. Antibody-neutralization of CXCR3 drastically diminished dexamethasone mediated $CD8^+$ T cells migration to tissue sites that led to poor virus control. $CD8^+$ T cells expanded during both α-(HSV1) and γ-(MHV68) herpesvirus infections down regulated Nr3c1. Dexamethasone also activated $CD8^+$ T cells in the absence of an overt TCR stimulation. Our study therefore calls into question the logic of corticosteroid therapy used to manage persistent inflammatory conditions but at the same time also describes the strategy to harness untapped potential of corticosteroids in promoting differentiation of immune memory cells.

Introduction

Natural and synthetic glucocorticoids cause immunosuppression and are used to ameliorate inflammation resulting from infections, autoimmunities and leukemia[1]. Synthetic glucocorticoids are also administered in patients to ensure the success of tissue transplantations procedures[2,3]. Synthetic analogs of glucocorticoids such as dexamethasone, prednisolones are used clinically because of their prolonged activity, which is due to their resistance to 11 β-hydroxysteroid dehydrogenase 2 (11 β-HSD2), the enzyme that can easily inactivate endogenous glucocorticoids. These drugs act primarily through intracellular glucocorticoid receptors (GR), encoded by *nr3c1* gene. GRs normally reside in the cytosol and upon binding to the ligands are translocated to nucleus to alter gene expression[2,4,5]. Glucocorticoid drugs have pleotropic effects on most cell types and organ systems[5]. Endogenous glucocorticoids are induced during infections, cancer development as well as in various stress responses and are involved in regulating neuroendocrine processes via hypothalamic pituitary adrenal axis (HPA) that maintains homeostasis[6]. During some systemic herpesviruses and influenza virus infection, the HPA axis could help reduce the disease severity by balancing the immunity and immunopathological responses[7–9]. Some of the known immunosuppressive effects of corticosteroids include a modulation of cytokine production by immune cells, an altered cellular trafficking, the promotion of phagocytosis as well as an enhancement of regulatory T cell functions[2,10]. The mechanism by which corticosteroids dictate the fate and function of virus-specific $CD8^+$ T cells still remain less well explored and therefore we investigated this issue in the current study. As synthetic analogs of glucocorticoids are commonly used to reduce inflammatory responses during herpesvirus infections, we focused our analysis to measure the influence of such a therapy using dexamethasone as the candidate drug in dictating virus-specific $CD8^+$ T cells fate and functionality. $CD8^+$ T

cells are critically involved in controlling the primary infection as well as maintaining the viral latency[11–14].

We showed that the expression of nr3c1 is tightly regulated during the differentiation of naïve $CD8^+$ T cells into effector and memory cells during herpesvirus infections. Both α-(HSV1) and γ-(MHV68) herpesvirus infections expanded $CD8^+$ T cells down regulated their nr3c1 expression in the acute phase of response but the differentiated memory cells regained the expression. Nr3c1 expression levels in $CD8^+$ T cells enhanced the susceptibility of naïve and memory cells to dexamethasone-induced apoptosis. This led to a skewed virus-specific $CD8^+$ T cell response in the acute phase of response. Dexamethasone mediated preferential killing of naïve $CD8^+$ T cells compromised anti-viral $CD8^+$ T cell immunity during a subsequent infection. The residual $CD8^+$ T cells however exhibited enhanced effector functions and preferentially homed to inflammatory tissue sites due to their expression of molecules such as CD103 and CXCR3 as well as the transcription factor, Tbet that regulates CXCR3 and IFN-γ expression in $CD8^+$ T cells. Additionally, in the absence of an overt TCR ligation, $CD8^+$ T cells exposed to dexamethasone up regulated molecules such as CD69, KLRG1, CXCR3, PD1 and the transcription factor, Tbet. These molecules are associated with TCR stimulation and therefore suggest for a bystander activation of $CD8^+$ T cells. Activated $CD8^+$ T cells that were briefly exposed to dexamethasone proliferated more and survived longer as memory cells. Our results therefore suggest that the distinct homing pattern induced in $CD8^+$ T cells as well as their elevated functionality might limit the utility of immunosuppressive corticosteroids in managing chronic inflammatory diseases. Furthermore, corticosteroids could enhance hosts' susceptibility to subsequent infections as a result of preferential elimination of as naïve as well as memory $CD8^+$ T

cells. While dexamethasone depletes pre-existing memory, the transition of effector cells into memory could actually be promoted by its brief exposure.

Materials and Methods

Mice, and viruses

C57BL/6, TCR Tg OT-IxRag1$^{-/-}$ and CD45.1 mice were procured from Jackson laboratory, USA and bred in individual ventilated caging system at the Small Animal Facility for Experimentation (SAFE), IISER Mohali. HSV1-KOS and MHV68-M2-SIINFEKL viruses were grown and titrated using Vero cells (ATCC) as described earlier[15]. Institutional Animal Ethics Committee (IAEC) of IISER Mohali set up by the Committee for the Purpose of Control and Supervision of Experiments on Animals (CPCSEA), which is established under Chapter 4, Section 15(1) of the Prevention of Cruelty to Animals Act 1960. IAEC approved all the animal experimental protocols. The numbers of protocols are IISERM/SAFE/PRT/2016/09 and 011. All the procedures performed were strictly according to the approved protocols.

Antibodies, T cells isolation kits and other pharmacological reagents

MHC class I tetramers used in this study were synthesized in house, where H-2K^{b} heavy chain protein was loaded with SIINFEKL and SSIEFARL peptide as described earlier[15–17]. Dexamethasone, Mifepristone, 2,2,2- tribromoethanol, hematoxylin and eosin Y were purchased from Sigma Aldrich. Tissue OCT compound was procured from Fischer Scientific. CD8^{+} T cell untouched Dynabeads kit, CFSE, Intracellular fixation-permeabilization buffer, annexin V and streptavidin-PE were purchased from thermofisher. Antibodies against CD45.1 (A20), CD45.2 (104), CD8 (53-6.7), CD44 (IM7), KLRG1 (2F1), CD11b (M1/70) and TNF-α (TN3-19) and the propidium iodide were purchased from BD pharmingen. Antibodies against CD45 (30-F11), CD69

(H1.2F3), CD11c (N418), PD1 (J43.1), CD16/32 (2.4G2), CD127 (A7R34) and IFN-γ (XMG1.2) were purchased from Tonbo Biosciences. Monensin, Brefeldin A, purified anti-CD3 (17A2) and anti-CD28 (37.51), antibodies against CXCR3 (173), CXCR4 (2B11), CCR7 (4B12) and CD103 (2E7) were procured from eBioscience. CXCR3 neutralizing antibody (CXCR3-173) was purchased from BioXcell.

Cell staining for flow cytometry

Blood samples were collected from different mice in heparin containing micro centrifuge tubes. 50 µl blood was aliquoted directly in a centrifuge tube and 10 µl of antibody mix along with SSIEFARL-tetramer (the final concentration should be 1:100 in 60 µl) was added followed by the incubation of cells at 4 ^{o}C for 45 min in dark. After incubation 640 µl of 1x ACK solution (155 mM NH4Cl, 12 mM NaHCO3, 0.1 mM EDTA, pH 7.3) was added to lyse RBCs. The cocktail was kept at room temperature for 15 min. Then 600 µl PBS was added into it and cells were centrifuged at 1500 rpm at 4 ^{o}C for 5 min. After 2 more washing in cold PBS, cells were suspended in 200 µl of PBS and 100 µl of total volume was acquired and analyzed. Similarly, after HSV1 infection through footpad route, mice were treated with dexamethasone and diluent from 4 to 6 dpi. Peripheral blood samples at 6 dpi and PLNs at 7 dpi were collected and analyzed using antibodies against a panel of antibodies against CD8, KLRG1, CD103, CXCR3, CXCR4 and CCR7. Additionally, the cells were stained with HSV1 H-2K^{b}-gB$_{498\text{-}505}$ tetramers measuring the phenotypic profile of differentiating antigen specific CD8^{+} T cell. The levels of different migratory receptors (CXCR3, CXCR4 and CCR7) were measured on HSV1 specific H2-K^{b}-gB$_{498\text{-}505}$-tetramer positive CD8^{+} T cells. Similarly staining of cells from different lymphoid organs was performed and stained cells were analyzed using BD Accuri C6 flow cytometer.

Measuring the influence of neutralizing anti-CXCR3 antibody on cellular migration to inflammatory tissues in dexamethasone treated mice

$10x10^3$ OT-I cells (from OT-I TCR tg mice) were adoptively transferred in C57BL/6 mice, which were then infected one day later with MHV68-SIINFEKL via intranasal route. The animals were then divided into three groups. One groups was injected with dexamethasone and anti-CXCR3 antibody on 6 and 7 days post infection and other group received only dexamethasone. The lymphoid organs, lung tissues and bronchoalveolar lavage were analyzed one day later for cellular analysis and viral load determination.

Intracellular cytokine staining (ICCS) of $CD8^+$ T cell

Single cell suspension was prepared from the lymphoid organs of HSV1 or MHV68-M2 SIINFEKL infected animals. $1x10^6$ cells were incubated with 1x brefeldin A and 20 ng/ml of IL-2 in the absence or presence of cognate peptide (1 µg/ml of SSIEFARL or SIINFEKL) for 4 hrs. After incubation period was over, cells were surface stained with anti-CD8 and anti-CD44 antibodies as described earlier. After 3 washings, cells were fixed in IC fixation buffer for 25 min at room temperature and then permeablized in 1x permeabilization buffer for 5 min at room temperature (RT). After 2 more washings and Fc blocking, cells were stained with anti-IFN-γ and anti-TNF-α antibodies for 25 mins in dark at RT. To remove unbound antibodies, cells were washed thrice and acquired using a flow cytometer.

Degranulation staining

For measuring the degranulation of $CD8^+$ T cells, anti-CD107a antibody (1:500 dilution) was added to the SSIEFARL peptide pulsed cells having 1x monensin solution in complete RPMI. Similarly controls cells were cultured in the absence of SSIEFARL peptide. After 4 hrs of incubation cells were surface stained with anti-CD8 and HSV1 H-

$2K^b$-$gB_{498-505}$ tetramers at 4 ^oC in dark for 45 mins. Thereafter cells were acquired for degranulation.

Ki67 staining

PBMCs and lymph node cells were surface stained with anti-CD45, anti-CD8 antibodies and H-$2K^b$-$gB_{498-505}$-tetramers as described earlier. The unbound antibody was washed off and cells were fix-permeabilized. Thereafter Fc blocking was done and then the cells were stained with anti-Ki67 antibody for 25 mins in dark at RT and acquired using BD Accuri C6 flow cytometer.

Analysis of mRNA expression for different molecules in $CD8^+$ T cell subsets upon dexamethasone treatment

$1x10^5$ OT-I cells were adoptively transferred into gender matched C57BL/6 mice. The recipient mice were intraperitoneally infected next day with $1x10^6$ pfu of MHV68-SIINFEKL virus. At 9 dpi, spleens were removed from euthanized mice to prepare splenocytes which were then stained with fluorescent H-$2K^b$-SIINFEKL-tetramers, anti-CD44 and anti-CD8 antibodies. The stained cells were FACS sorted to isolate RNA for measuring the expression of different molecules. Similarly endogenous H-$2K^b$-SSSIFERAL-tet $^{+ve}$ cells reactive to HSV1 were analyzed for mRNA analysis of different genes. RNA was isolated from sorted $CD8^+$ T cells using a kit from Promega (Cat. No. Z6011). After DNAse treatment of the RNA samples, cDNA was synthesized using 50ng of RNA using SuperScript IV first strand synthesis system cDNA synthesis kit from Invitrogen (Cat. No.18091050). Qualitative real time PCR (qPCR) reaction was setup using 2x-DyNamo ColorFlash SYBR Green qPCR kit from Thermofisher (Cat. F416L). The reaction was carried out using QuantStudio Real-Time PCR system from Thermofisher. GAPDH gene primers were used as endogenous control and the relative expression of different genes were calculated by $2^{-\Delta\Delta}$ CT values. The reaction conditions

for qPCR were as following: initial denaturation (95^{o}C for 7 min), denaturation (95^{o}C for 10 sec), annealing and extension (60^{o}C for 30 sec) for 40 cycles. Subsequently melt curve analysis was performed. The primers used and the products size were; nr3c1 (FP: 5'-AGTGATTGCCGCAGTGAAAT-3' & RP: 5'-GCCATGAGAAACATCCATGA-3') = 105bp, Tbet (FP: 5' CAATGTGACCCAGATGATCG 3' & RP: 5' GCGTTCTGGTAGGCAGTCAC 3') = 168bp, Eomesodermin (FP: 5' TCCTAACACTGGCTCCCACT 3' & RP 5' GTCACTTCCACGATGTGCAG 3') = 153bp, PD1 (FP: 5' CCAAGGAACCTGCTTTTCAA 3' & RP: 5' GGCATTCTTGGGAACTGTGT 3') = 144bp, Bcl2 (FP: 5' GCAGATTGCCCTGGATGTAT 3' & RP: 5' AGAAAAGTCAGCCAGCCAGA 3') = 156bp, CXCR3 (FP: 5' TACCTTGAGGTTAGTGAACGTCA 3' & RP: 5' CGCTCTCGTTTTCCCCATAATC 3') = 100bp, GAPDH (FP: 5'-AAATGGTGAAGGTCGGTGTGAAC-3' & RP: 5'-CAACAATCTCCACTTTGCCACTG-3') = 90bp.

***Ex vivo and in vivo* assays to measure differential killing of CD8^{+} T cell subsets**

C57BL/6 female mice were infected with 5x10^{5} pfu of HSV1-KOS per footpad. Draining popliteal lymph nodes (PLNs) were collected on 6 dpi or 30 dpi to prepare single cell suspension. Single cell suspensions thus prepared were incubated with graded doses of dexamethasone (0.1 to 10 µM) in the presence or absence of 5 µM mifepristone, a specific inhibitor for dexamethasone. Subsequently, the kinetics of cell killing activity for 1 µM of dexamethasone for cells that were either pretreated with 5 µM of mifepristone or not exposed to mifepristone was measured. Diluent controls were invariably included in such experiments. The mifepristone treatment was preceded one hour by dexamethasone treatment. Cell death was measured by staining of cells with annexin V at indicated time points. Naive CD8^{+} T cells were isolated from CD45.1 mice

using untouched Dynabeads and subsequently activated with 1µg/ml of anti-CD3 (plate bound) and anti-CD28 (soluble) antibodies at 37 ^{o}C in CO_2 incubator for 20 hours. Thereafter, some cells were analyzed for their activation profile using anti-CD69 antibody and rest of the cells were stained with low concentration of CFSE (0.1 µM). Simultaneously, naive $CD8^+$ T cells isolated and purified from CD45.1 mice were stained with a high concentration of CFSE (5 µM). Both the activated ($CFSE^{lo}$) and naive ($CFSE^{hi}$) $CD8^+$ T cells were mixed in 1:1 ratio and $4x10^6$ cells were injected in gender matched CD45.2 mice. After 30 minutes of cell transfer one group of animals was treated with 10 mg/kg of dexamethasone and another group with diluent. After 36 hr of treatment the frequencies of transferred ($CD45.1^{+ve}$) naive and activated $CD8^+$ T cells were measured in different lymphoid organs and peripheral circulation from sham and dexamethasone treated animals. Equivalent numbers of naive ($CFSE^{hi}$) $CD8^+$ T cells and activated ($CFSE^{lo}$) $CD8^+$ T cells were injected and determined post transfer. The altered frequencies of naive cells in dexamethasone treated mice was determined as follows.

(Average frequency of naive $CD8^+$ T cells in sham treated group – frequency of naive $CD8^+$ T cells in dexamethasone treated mice).

In dexamethasone treated (compared to sham treatment) animals the percent specific elimination of naive $CD8^+$ T cells was calculated as:

% Killing of naïve cells = [(Reduced frequency of naive $CD8^+$ T cells in dexamethasone group / average frequency of naive $CD8^+$ T cells in sham group) x 100].

Measuring the influence of dexamethasone on immune cell population in HSV 1 infected animals

C57BL/6 female mice were infected in footpad with HSV1-KOS as described earlier. Six mice were treated intraperitoneally with dexamethasone (10 mg/Kg body weight), whereas 6 mice received diluent on 4, 5 and 6 dpi. To determine the distribution of

different cellular populations and their phenotype in peripheral blood circulation, blood samples were collected. The PBMCs were stained for different surface molecules using fluorochrome labelled antibodies and were then analyzed by Accuri C6 flow cytometer. At 7 dpi all the animals were sacrificed and draining PLNs were processed to isolate cells which were then analyzed by H-2K^{b}-SSIFERAL-tetramer for antigen-specific CD8^{+} T cells. The functionality of the cells was determined by intracellular cytokine staining assays (ICCS) for the production of cytokines. Surface staining for different molecules was performed cytofluorimetrically. The virus titers in footpad tissues were measured by plaque forming assays.

For some experiments, we *in vitro* stimulated OT-I cells with anti-CD3 and anti-CD28 for 16 hours and thereafter a fraction of these cells were treated with 1 µM of dexamethasone and the other fraction with only the diluent for 1 hour. The cells were then washed extensively and transferred in separate groups of animals to measure the survival of these cells. The recipient animals were then analyzed for analyzing donor cells for different parameters. A recall response of the surviving cells was analyzed by infecting recipient animals intranasally with MHV68-M2-SIINFEKL after 30 days of transfer. The expanding cells were analyzed 8 days later by flow cytometry. The lung samples were analyzed histologically and the virus titration was done.

Measuring the responsiveness of dexamethasone pre-treated animals to a subsequent infection

Gender matched CD45.1 C57BL/6 mice received 10000 naive and purified OT-I cells. The next day these mice were injected with CFA in hind footpad to induce the non-specific inflammation. After transient (4-6 dpi) treatment of dexamethasone (10 mg/Kg body weight) and sham, at day 30 post cell transfer these mice were infected intranasally with 2x10^{5} pfu of MHV68-SIINFEKL virus and simultaneously CFA was injected in the

hind foot pad. At 10 dpi of MHV68 infection the cell types were analyzed in blood circulation and these mice were sacrificed at 11 dpi to collect BAL, mediastinal lymph nodes and spleens for cellular analysis.

***In vivo* CTL assay**

Splenocytes were collected from naïve gender matched C57BL/6 mice, to make target cells. 50% of splenocytes were incubated with 5 µM SSIEFARL peptide at 37 ^{o}C for 45 min. After 2 times of washing, the peptide pulsed cells were stained with high CFSE (5 µM) whereas un-pulsed splenocytes were stained with low CFSE (0.5 µM). After counting both the cell populations were mixed in 1:1 proportion and a total of $1x10^{7}$ cells were injected intravenously into uninfected and 4 dpi of memory recalled gender matched C57BL/6 mice. Peripheral blood was collected from recipient mice after 1 hr of transfer and analyzed for target cells killing. Assuming that equal numbers of unpulsed and peptide-pulsed cells were injected.

The percent killing of target cells in uninfected animals was determined as:

$[(\%CFSE^{low} - \%CFSE^{high}) \times 100]/\% CFSE^{low}]$

In infected animals the percent killing of target cells was calculated as:

Ratio = $(\% CFSE^{low} / \% CFSE^{high})$.

% specific lysis = [1- (ratio uninfected/ratio infected) x 100].

Histopathology

Lungs samples were collected from infected mice that were injected with diluent or dexamethasone treated cells. The caudal right lobes of lungs from each group of mice were fixed overnight at 4 ^{o}C in 4% PFA prepared in 10 mM PBS. On next day the lung tissues were dehydrated using sucrose gradient (5 - 20% prepared in 10 mM PBS) at room temperature and embedded in tissue blocks in OCT compound and frozen at -80^{o}C. 10 µM tissue sections were prepared using Leica cryotome and slides were stored at -

20^{o}C until further use. H&E staining were performed. The stained sections were dried at room temperature and coverslip were mounted with medium. After drying, the sections were photographed on Leica DMi8 microscope and the images were analysed for size and scale bar using ImageJ software.

Plaque forming assays

To determine the viral load in mice organs (foot pad and lungs), Vero cells were plated in 24 well plates. Next day, when cells attained 90-100% confluency, tissues were homogenized in serum free DMEM. After centrifugation, supernatants were collected and different dilutions prepared in serum free DMEM were added onto the monolayers of Vero cells. After two hrs, the supernatants were removed and low melting agar prepared in 10% DMEM was gently poured on the surface of cells. The plates were incubated at 37 ^{o}C in CO_2 incubator for 4-5 days. Once plaques were visible under microscope, cells were fixed with 10% paraformaldehyde overnight at RT. Next day the fixation buffer and agar plugs were removed to stain the fixed cells with 0.2% crystal violet and the numbers of plaques were counted for each dilution. The number plaque forming units per ml of solution were calculated as:

pfu/ml = (No. of plaques/volume plated) x dilution factor

pfu/ml in target tissue was represented as pfu/gm of the tissue.

Statistical analysis

Graph pad prism software version 7 was used for statistical analysis. Data with similar variances and having Gaussian distribution were analyzed with two tailed unpaired Student's t-tests. Data not following Gaussian distribution were analyzed with two tailed Mann-Whitney U tests. For multiple comparisons two-way ANOVA test with Bonferroni post hoc analysis were used. The P value below 0.05 considered as significant. * <0.05, ** <0.01 and *** <0.001.

Results

1. Dexamethasone alters the distribution of $CD8^+$ T cells during herpesvirus infection.

Dexamethasone is commonly used as an immunosuppressive therapy for managing inflammatory reactions caused by infections. The mechanism by which the differentiation of virus-specific $CD8^+$ T cells is affected by such therapies is not known. We investigated how a transient treatment with dexamethasone influences different immune cell populations in HSV1 infected mice. We observed reduced frequencies and numbers of leukocytes ($CD45^+$ cells and $CD8^+$ T cells) in the peripheral circulation (Fig 2.1A-C and Fig 2.2A-B). The frequencies of $CD11b^+$ myeloid cells within leukocytes ($CD45^{+ve}$ cells) were two fold higher in the peripheral circulation of dexamethasone treated mice as compared to controls (Fig 2.2A-E). The total numbers of virus-specific $CD8^+$ T cells (K^b-$gB_{498-505}$-$tetramer^{+ve}$ cells) in the peripheral blood were lower but the frequencies of $tetramer^{+ve}CD8^+$ T cells were more than two fold higher in the dexamethasone treated animals as compared to control animals (Fig 2.1A-C). The frequencies of $tetramer^+$ $CD8^+$ T cells were more than two fold higher (Fig 2.1D and E), but the absolute numbers of $CD8^+$ T cells as well as $tetramer^+$ $CD8^+$ T cells were reduced in the draining popliteal lymph nodes (PLNs) at 7dpi in treated group as compared to control (Fig 2.1F). We also measured the frequencies and total numbers of cytokine producing $CD8^+$ T cells that responded to an immunodominant H-$2K^b$ restricted $gB_{498-505}$-(SSIEFARL) peptide of HSV1 using intracellular cytokine staining (ICCS) assays. While the frequencies of IFN-γ^+CD8^+ T cells were more than two fold higher in drug treated animals as compared to controls, there were no significant differences in the frequencies of either the TNF-α^+CD8^+ T cells or the double positive (IFN-γ^+TNF-α^+) $CD8^+$ T cell population between two groups (Fig 2.1G-I). More $CD8^+$ T cells produced

IFN-γ on a per cell basis in dexamethasone group as compared to control (Fig 2.1M). The frequencies of total degranulating ($CD107a^+$) $CD8^+$ T cells as well as $tetramer^{+ve}CD107a^+$ were higher in dexamethasone treated animals as compared to controls (Fig 2.1J-K). The expression of CD107a was also higher on a per cell basis in dexamethasone group as compared to control (Fig 2.1L). The expression of CD107a as well as cytokine production by $CD8^+$ T cells are associated with their superior functionality[18]. Our data suggests that under the influence of a transient dexamethasone therapy, residual herpesvirus specific $CD8^+$ T cells exhibit greater functionality. We therefore investigated whether or not the better functionality of surviving virus-specific $CD8^+$ T cells controls viral infection. We quantified the virus loads in the footpads of animals from two groups. More replicating virus particles were observed at 7dpi in dexamethasone treated animals in comparison to controls (Fig 2.1N). However, by 10 dpi all the animals cleared the replicating virus from footpad tissues. Therefore, we conclude that the dexamethasone skews the response towards greater frequencies of functional virus-specific $CD8^+$ T cells but their total numbers were reduced, which resulted in a delayed viral control.

Experiments aimed at measuring the influence of different doses of dexamethasone on various immune cell population revealed that a 1000 fold lower dose (0.01 mg/Kg B Wt) did not change the function and phenotype of different subsets of $CD8^+$ T cells, but 100 fold lower doses (0.1 mg/Kg B Wt) demonstrated a trend similar to what was observed for 1x dose (10 mg/kg B Wt) in the total numbers and frequencies of virus-specific $CD8^+$ T cells. The results were not significantly different for the associated effector functions and phenotype of $CD8^+$ T cells isolated from the peripheral circulation as well as PLNs (Fig 2.3A-N). Therefore, the observed effects of dexamethasone on differentiating herpesvirus specific $CD8^+$ T cells are highly dose dependent.

2. Dexamethasone promotes CXCR3 mediated migration of $CD8^+$ T cells to inflammatory sites.

We observed greater frequencies of virus-specific $CD8^+$ T cells but not the numbers in HSV1 infected mice receiving a transient dexamethasone treatment as compared to diluent controls. We therefore speculated that the observed effects could be either because of the drug induced distinct homing pattern in $CD8^+$ T cells or their differential survival or a combination of two. That dexamethasone treatment enhances CXCR4 mediated migration of naive T cells as well as monocytes was shown earlier, but such effects on virus-expanded $CD8^+$ T cells remain unexplored[19,20]. We therefore investigated whether or not dexamethasone modulates the expression of homing molecules such as CXCR3, CXCR4, CCR7 and CD103 in virus expanded $CD8^+$ T cells. These molecules either help $CD8^+$ T cells to preferentially migrate to tissue sites (CXCR3, CXCR4, CD103) or sequester them to lymphoid organs (CCR7). The MFI of CXCR4 and CCR7 on HSV1 reactive cells as well as their frequencies were unchanged (~11% for CXCR4 and ~1% for CCR7) in the peripheral blood and (~6% for CXCR4 and 45% for CCR7) in the PLNs of both the groups (Fig 2.5). The frequencies of $CXCR3^+K^b$-$gB_{495\text{-}505}$-$tetramer^{+ve}CD8^+$ T cells were significantly higher in dexamethasone treated mice (83%) as compared to controls (72.4%) in PBMCs and so were the MFI values for CXCR3 on K^b-$gB_{495\text{-}505}$-$tetramer^{+ve}$ (~1.5 fold higher) (Fig 2.4A-C). Interestingly, the proportions of $CXCR3^+K^b$-$gB_{495\text{-}505}$-$tetramer^{-ve}CD8^+$ T cells were also higher in dexamethasone (46%) as compared to control (33%) group (Fig 2.4A-B). The expression of CXCR3 on a per cells basis was also higher on K^b-$gB_{495\text{-}505}$-$tetramer^{+ve}CD8^+$ T cells in PBMCs of dexamethasone group as compared to control (Fig 2.4C). Not only in the peripheral blood but also in the draining popliteal LN, more frequencies of $CXCR3^+K^b$-$gB_{495\text{-}505}$-$tetramer^{+ve}CD8^+$ T cells (66% in dexamethasone group vs 49% in sham group)

as well as higher MFI values for CXCR3 expression were observed for dexamethasone group (Fig 2.4D-F). K^b-$gB_{495-505}$-tetramer$^{-ve}CD8^+$ T cells also had higher expression of CXCR3 on a per cell basis in dexamethasone treated mice as compared to controls (Fig 2.4F). The moderate alteration in the percent positive cells in draining LNs $CD8^+$ T cells could suggest that a majority of $CXCR3^+CD8^+$ T cells might have migrated to tissue sites. A further phenotypic analysis of virus-specific $CD8^+$ T cells in HSV1 infected mice revealed a greater proportions of KLRG1$^-$CD103$^+$$K^b$-$gB_{498-505}$-tetramer$^{+ve}CD8^+$ T cells in the draining LNs of dexamethasone treated animals as compared to those of controls (~1.5 fold higher, Fig 2.4G-I). Similarly, the MFI values for CD103 integrin were higher but for KLRG1 were lower in K^b-$gB_{498-505}$-tetramer$^{+ve}CD8^+$ T cells isolated from dexamethasone group (Fig 2.4J). Some have showed that activated $CD8^+$ T cells that are likely to give rise to tissue resident memory precursor cells display a similar phenotype (i.e. CD103$^+$KLRG1$^-$)[21]. Therefore, a transient treatment with dexamethasone causes virus-expanded $CD8^+$ T cells to preferentially home to tissue sites.

The migration of $CD8^+$ T cells to inflammatory tissues was promoted by their expression of CXCR3 was elucidated by our additional experiments that involved administration of neutralizing anti-CXCR3 antibody in infected and dexamethasone treated mice (Fig 2.6). $10x10^3$ OT-I cells were transferred into mice followed by their intranasal infection with MHV68 SIINFEKL. On 6 and 7dpi mice were treated with dexamethasone. Some of the dexamethasone treated animals were additionally injected with a neutralizing anti-CXCR3 antibody[22]. The responses were measured in the peripheral circulation, bronchoalveolar lavage samples, draining mediastinal LNs and spleens (Fig 2.6A). Upto 3 fold more K^b-SIINFEKL-tetramer$^{+ve}CD8^+$ T cells (13% in dexamethasone gp vs 4% in sham T_x gp) were recovered from the peripheral blood (Fig 2.6B and C) and upto 3 fold more from the bronchoalveolar tissue lavages (Fig 2.6D and

E) of dexamethasone treated animals as compared to the sham group (26% in dexa T_x vs 9% in sham T_x gp). The frequencies of K^b-SIINFEKL-tet^{+ve} $CD8^+$ T cells increased moderately in the spleens of dexamethasone treated group as compared to control but no significant differences were observed in their frequencies in the draining mediastinal LNs of two groups of animals (Fig 2.6F-I). This further corroborated our findings that specific upregulation of chemokine receptors by dexamethasone treated $CD8^+$ T cells induces their exit from lymphoid organs and migration to periphery. The administration of anti-CXCR3 antibodies alongside dexamethasone drastically reduced the frequencies of antigen-specific (K^b-SIINFEKL-$tetramer^{+ve}$) $CD8^+$ T cells in peripheral blood and bronchoalveolar lavages and the frequencies reached similar levels as observed for sham treated group (Fig 2.6B-E). The antibody therapy simultaneously increased the frequencies of K^b-SIINFEKL-$tetramer^{+ve}CD8^+$ T cells in spleens and draining mediastinal LNs (Fig 2.6F-I). Therefore our data strongly suggest that dexamethasone induced upregulation of CXCR3 mediated $CD8^+$ T cells migration to inflammatory tissue site. We also considered the possibility that a reduced migration of $CD8^+$ T cells would lead to an inefficient viral control. The replicating virus was quantified in lung tissues of animals from different groups. While significantly different, but slightly more replicating virus load was present in the lung tissues of dexamethasone group as compared to sham treated group (more than 2 fold), the viral burden increased greatly (more than 20 fold) in antibody-injected animals (Fig 2.6J).

Taken together, our results demonstrate that dexamethasone enhances the expression of chemokine receptors CXCR3, on $CD8^+$ T cells to facilitate their migration to the infection sites.

3. Dexamethasone preferentially induces apoptosis of naive $CD8^+$ T cells.

The observed skewed frequencies of $CD8^+$ T cell subsets in the dexamethasone treated mice could also be due to their differential survivability. To explore this possibility we isolated draining popliteal LN cells from HSV1 infected animals in the acute phase of response and exposed these cells to graded doses of dexamethasone (0.1, 1 and 10 μM). Some of the cells were pretreated with mifepristone, a specific competitive inhibitor of glucocorticoid receptors[23]. Dexamethasone induced the apoptosis of $CD8^+$ T cells in a dose dependent manner and the effect was significantly rescued by their pre-treatment with mifepristone (Fig 2.7A and B). We then measured the apoptosis (annexin V^{+ve}) in different subsets of $CD8^+$ T cells isolated from HSV1 infected mice and subsequently exposed to dexamethasone. While the virus-specific activated $CD8^+$ T cells (tetramer^{+ve}CD44^{hi} $CD8^+$ T cells) were not affected by dexamethasone (84.8 ± 3.45% in sham vs 83.3 ± 2.5% annexin V^{+ve} in dexa gp), a significant proportion of naive $CD8^+$ T cells (tetramer^{-ve}CD44^{lo}$CD8^+$ T cells) exhibited an enhanced apoptosis (48.5 ± 7.1% in sham vs 89.9 ± 1.2% annexin V^{+ve} in dexa group) after 24 hrs (Fig 2.7C upper and lower panel, 2.7D-F). Tetramer^{-ve}CD44^{hi}$CD8^+$ T cells were also killed to a greater extent in similar experiments (57.3 ± 4.7% annexin V^{+ve} cells in sham vs 81.7 ± 1.2% annexin V^{+ve}cells in dexamethasone group) (Fig 2.7C middle panel and F). We however observed differences in the kinetics of apoptosis among tetramer^{+ve}CD44^{hi}$CD8^+$ T cells and tetramer^{-ve}CD44^{hi}$CD8^+$ T cells (Fig 2.7E and F). Tetramer^{-ve}CD44^{hi}$CD8^+$ T cells constitute a heterogeneous population of cells with some reactive to the viral epitopes other than SSIEFARL, or other cells in different stages of their activation and differentiation states. Therefore, some of these cells could exhibit relatively different susceptibility to dexamethasone-induced apoptosis (Fig 2.7E and F). A prior treatment of mifepristone greatly rescued susceptible $CD8^+$ T cells from drug induced for both CD44^{lo}

and $CD44^{hi}$ but $tetramer^{-ve}$ at all the time points investigated (Fig 2.7B-F). This suggested that the receptor ligation is crucial for the observed effects.

In order to test whether or not *ex vivo* results could be recapitulated *in vivo,* we measured the dexamethasone induced differential killing of naïve and activated $CD8^+$ T cells using an adoptive transfer approach. $CD8^+$ T cells were activated *in vitro* using co-receptor stimulation. More than 80% cells were $CD69^+$. The activated cells and the freshly isolated naïve $CD8^+$ T cells (both being $CD45.1^{+ve}$) were labeled with two different concentrations of CFSE ($CFSE^{hi}$ and $CFSE^{lo}$) and their equal numbers were transferred into CD45.2 congenic mice. One group of recipient mice was administered with dexamethasone and the surviving $CD45.1^{+ve}$ cells frequencies were measured (Fig 2.7G). Only a single dose of dexamethasone (10 mg/Kg B Wt) significantly reduced transferred naïve $CD8^+$ T cells as compared to their activated counterparts (Fig 2.7H-I). This confirms the enhanced susceptibility of naïve cells to dexamethasone-induced apoptosis. Varying frequencies of surviving naive cells in different lymphoid organs could be due to differential bioavailability of the injected drug. However this issue was not investigated further.

We conclude that the susceptibility of naive cells to dexamethasone-induced apoptosis could contribute to a skewed response pattern towards virus-specific $CD8^+$ T cells in HSV1 infected mice that received a transient dexamethasone therapy. While the virus expanded $CD8^+$ T cells resist apoptosis, naïve cells are more prone to dexamethasone induced apoptosis.

4. A transient dexamethasone therapy compromised hosts' ability to respond to a subsequent infection.

Having demonstrated that dexamethasone preferentially kill naive $CD8^+$ T cells, we tested whether such a scenario would have functional consequences and compromises

host's ability to generate an efficient antigen-specific $CD8^+$ T cells immunity to a subsequent infections. A schematic of these experiments is shown in Figure 2.8A. We transferred $10x10^3$ OT-I cells ($CD45.2^{+ve}$) in $CD45.1^+$ mice one day prior to injecting with complete Freund's adjuvants (CFA) in their hind footpads to induce a non-specific inflammatory response whose severity could be controlled by dexamethasone therapy. This could serve as a surrogate mimic to clinical situations that would call for a corticosteroids therapy. One group of mice was then given a transient dexamethasone treatment on 4-6 day post CFA injection and another group was injected with the diluent only. We hypothesized that if indeed a prior administration of dexamethasone for a short duration reduced the frequencies of naïve OT-I cells and in the absence of their *de novo* generation by hematopoiesis, a subsequent MHV68-SIINFEKL virus infection would inefficiently expand such cells. After 30 day of OT-I cell transfer, we infected these animals with MHV68-SIINFEKL virus through intranasal route to measure the response of persisting donor cells. CFA was again injected in their hind footpads to neutralize the effect of a local inflammation induced by the virus in the respiratory tract that could potentially alter cellular homing irrespective of their antigen driven responsiveness. Donor K^b-SIINFEKL-$tetramer^{+ve}CD8^+$ T cells ($CD45.2^{+ve}$) were indeed recruited to a lesser extent in the peripheral blood (18% in sham T_x group vs 12% in dexa T_x group; reduced by 1.5 fold), bronchoalveolar lavage (BAL) (23% in sham T_x group vs 11% in dexa T_x group; reduced by more than 2 fold) and spleens (14% in sham T_x group vs 6.7% in dexa T_x group; reduced by more than 2 fold) (Fig 2.8B and C). The total numbers of K^b-SIINFEKL-$tetramer^{+ve}CD8^+$ T cells were reduced by three fold in the peripheral circulation and two fold lower in the spleens and mediastinal LNs of dexamethasone treated animals as compared to controls (Fig 2.8D and E). Not only the magnitudes but also IFN-$\gamma^+CD45.2^+$ cells were lower in the spleens (up to 1.5 fold) of dexamethasone

group as compared to the sham treated mice (Fig 2.8F-H). No significant differences were observed in the frequencies of TNF-α producing $CD8^+$ donor T cells in the sham and dexa treated animals (Fig 2.8F - lower panel, 2.8I and 2.8J).

Thus, our results show that dexamethasone induces a preferential elimination of naïve cells, critical for controlling the subsequent infection and in doing so hosts' ability to mount an efficient anti-viral $CD8^+$ T cell immunity is compromised.

5. Virus-specific $CD8^+$ T cells modulate the expression of glucocorticoid receptor, Nr3c1 during their differentiation.

Dexamethasone acts primarily through receptor Nr3c1[4,5]. We, therefore measured whether herpesvirus expanded $CD8^+$ T cells modulate their Nr3c1 expression levels to account for their observed characteristics such as differential susceptibility to dexamethasone induced apoptosis or their preferential migration pattern. We analyzed naive and activated TCR transgenic OT-I cells, TCR transnuclear (TN) MHV68-ORF8 specific cells as well as endogenous $CD8^+$ T cells that were expanded in the course of infections by γ-(MHV68-M2-SIINFEKL) and α-(HSV1) herpesviruses to establish a causal association of Nr3c1 expression to dexamethasone induced effects. We considered the possibilities that $CD8^+$ T could respond differently depending on the affinity of their antigen receptor, the procedures used for their genesis, pathogen specific elements, the microenvironment in which such cells get activated as well as their functional and phenotypic heterogeneity. In the first set of experiments, OT-I cells were transferred in C57BL/6 mice followed by their infection with MHV68-M2-SIINFEKL. On 10 dpi, different subsets of $CD8^+$ T cells were FACS sorted. Sorted $CD8^+$ T cell population were: $CD44^{hi}K^b$-SIINFEKL-tetramer$^{+ve}CD8^+$ T cells, $CD44^{hi}K^b$-SIINFEKL-tetramer$^{+ve}CD8^+$ T cells and un-activated $CD44^{lo}K^b$-SIINFEKL-tetramer$^{+ve}CD8^+$ T cells (Fig 2.9A). The purity of different subsets of $CD8^+$ T cells were more than 98% (Fig 2.10A). MHV68

expanded cells down regulated Nr3c1 mRNA levels by 1.5 fold as compared to the un-activated cells (Fig 2.9B). MHV68 virus infection expanded transnuclear (TN) $CD8^+$ T cells specific to an epitope of the wild type virus (K^b-ORF8-(KNYIFEKL)-$tetramer^{+ve}CD8^+$ TN T cells) also showed a 2 fold down regulation of Nr3c1 expression as compared to their naïve counterparts when measured by RNAseq (Fig 2.9C)[24]. The expression of Nr3c1 and other molecules associated with $CD8^+$ T cell activation and differentiation were also simultaneously measured for endogenous virus-specific $CD8^+$ T cells isolated from HSV1 infected mice in the acute phase of their response at 7 dpi (Fig 2.9D and E). The expression levels of Bcl2, an anti-apoptotic molecule; PD1, a molecule that was initially found upregulated in cells undergoing apoptosis[25]; the chemokine receptor CXCR3 that facilitates cellular migration to inflammatory tissues[26,27] as well as transcription factors, such as Tbet and Eomes, that control differentiation of $CD8^+$ T cells[28] were measured. Tbet also regulates CXCR3 and IFN-γ expression in virus-specific $CD8^+$ T cells[27,29]. The cross-contamination in sorted populations was less than 0.5% (Fig 2.10). While the expression of Nr3c1 was ~2 fold lower in activated K^b-$gB_{495\text{-}505}$-$tet^+CD44^{hi}CD8^+$ T cells as compared to naïve cells (Fig 2.9E), Bcl2 expression was ~2 fold higher in these cells (Fig 2.9E). A fraction of activated cells differentiate to become long-lived memory cells, therefore an up regulation of Bcl2 was not surprizing. Antigen reactive K^b-$gB_{495\text{-}505}$-$tetramer^{+ve}CD44^{hi}$ $CD8^+$ T cells also upregulated PD1 by 28 fold, CXCR3 by 70 fold, Tbet by 24 fold and the Eomes by two fold (Fig 2.9E). Similar results were reported in earlier studies[24,30–32].

Our earlier data showed that K^b-$gB_{495\text{-}505}$-$tetramer^{-ve}CD44^{hi}CD8^+$ T cells also showed enhanced apoptosis as a result of dexamethasone exposure (Fig 2.7C-F). This population is likely to carry an effector memory population as well. Therefore, we compared the expression levels of Nr3c1 in naïve, activated as well as HSV1-specific

$CD8^+$ T cells in the memory stage at 60 dpi. Antigen reactive K^b-$gB_{495-505}$-$tetramer^{+ve}CD44^{hi}CD8^+$ T cells at 60dpi expressed relatively higher levels of Nr3c1 as compared to those in the acute phase of their response and their expression levels were not significantly different from the naïve cells (Fig 2.9F). The expression pattern of Nr3c1 could also suggest that both naïve and memory cells formed by a resolving infection could similarly respond to an exposure to dexamethasone. This could lead to an attrition of immunological memory generated in response to a previous infection or immunization as a consequence to dexamethasone therapy. We therefore evaluated whether dexamethasone could also cause the apoptosis of memory cells generated during HSV1 infection. Draining LN cells were collected from HSV1 infected mice (30 dpi) and treated with 1 μM conc. of dexamethasone. In some of the wells mifepristone pre-treated cells were added. After 8 hrs of incubation, K^b-$gB_{495-505}$-$tetramer^{+ve}$ and K^b-$gB_{495-505}$-$tetramer^{-ve}CD8^+$ T cells were analysed for the frequencies of annexin V^{+ve} cells (Fig 2.9G and H). Virus specific memory $CD8^+$ T cells (tetramer $^{+ve}CD8^+$ T cells) exhibited enhanced apoptosis (10.5 ± 1.2% in sham vs 35.1 ± 2.5% annexin V^+ in dexa group; 3 fold increase) after 8 hrs (Fig 2.9G upper panel and H). $Tetramer^{-ve}CD8^+$ T cells were also displayed greater apoptosis in similar experiments (40.3 ± 2.7% in sham vs 73.4 ± 3.2% annexin V^{+ve}cells in dexamethasone group; >1.5 fold increase) (Fig 2.9G lower panel and H).

Taken together, our results show that $CD8^+$ T cells differentiating during herpesviruses infection tightly regulate their Nr3c1 expression. While the virus expanded cells downregulate Nr3c1 as compared to naïve cells, memory cells regain the expression. Moreover, the expression pattern of Nr3c1 is directly proportional to their susceptibility to dexamethasone induced apoptosis and hence naïve and memory cells are more prone to their elimination by even a transient dexamethasone therapy.

6. A transient dexamethasone treatment causes bystander activation of $CD8^+$ T cells.

To get further insights into the differentiation of virus-specific $CD8^+$ T cells under the influence of a transient corticosteroid therapy, we measured mRNA levels of different molecules in HSV1 specific (K^b-$gB_{495\text{-}505}$-tetramer^{+ve}$CD44^{hi}$) and HSV1 non-responsive (K^b-$gB_{495\text{-}505}$-tetramer^{-ve}$CD44^{lo}$) $CD8^+$ T cells isolated from infected mice that were either treated with dexamethasone or given a sham treatment (Fig 2.11A). The cross contamination in sorted cells was less than 0.5 % (Fig 2.10C). Although K^b-$gB_{495\text{-}505}$-tetramer^{+ve} $CD44^{hi}CD8^+$ T cells downregulated Nr3c1 expression (Fig 2.9D,F) but dexamethasone did not alter its expression further in either cell types (Fig 2.10C,D). The expression levels of Bcl2 and Eomes also did not change significantly in the two cell populations isolated from dexamethasone treated and control animals (Fig 2.10C, E and F). Naïve $CD8^+$ T cells upregulated PD1 to a staggering 10 fold but its expression remained unaltered in $CD44^{hi}$ K^b-$gB_{495\text{-}505}$-tetramer^{+ve}$CD8^+$ T cells isolated from control and dexamethasone treated mice (Fig 2.11B). PD1 expression is induced in TCR or the co-receptor stimulated cells[33]. Therefore an enhanced expression of PD1 in naïve $CD8^+$ T cells was rather surprizing and could suggest for their alternate activation program induced by dexamethasone. CXCR3 was also further up regulated both in activated K^b-$gB_{495\text{-}505}$-tetramer^{+ve}$CD44^{hi}CD8^+$ T cells (by 2 fold) and naïve cells (by more than 5 folds) isolated from dexamethasone treated group as compared sham treated cells (Fig 2.11C). The transcription factor, Tbet, which governs the differentiation of $CD8^+$ T cells and also plays a role in controlling CXCR3 was upregulated both in $CD44^{hi}K^b$-$gB_{495\text{-}505}$-tetramer^{+ve}$CD8^+$ T cells (1.3 fold) and naïve cells (more than two folds) of dexamethasone treated group as compared control (Fig 2.11D). These results suggest that dexamethasone not only induces a specific transcriptional program in antigen responsive

cells but also activates naïve cells to acquire an alternate transcriptionally regulated phenotype that could suggest for their apparent bystander activation.

We further tested whether or not dexamethasone treatment could activate $CD8^+$ T cells independent of their TCR ligation. We transferred $5x10^6$ OT-I cells (obtained from naïve OT-I x $Rag1^{-/-}$ mice, $CD45.2^{+ve}$) in congenic mice (CD45.1) one-day prior to their administration of dexamethasone. Some animals were given sham treatment only. One dose of dexamethasone was injected, as the aim of these experiments was to investigate the activation profile of $CD8^+$ T cells rather than inducing their apoptosis. Both the donor and the endogenous $CD8^+$ T cells were then analyzed for activation markers such as CD69, PD1, KLRG1 and CXCR3 by flow cytometry (Fig 2.11E-M). The frequencies of OT-I cells ($CD45.2^+$) in control and dexamethasone treated groups were ~2% and 1.2% respectively (Fig 2.11F and G). These observations were in accordance with our data shown in figure 2.7G-I. Both the endogenous (5% in sham T_x vs 11% in dexa T_x) and donor OT-I cells (3.5% in sham T_x vs 17% in dexa T_x) up regulated CD69 in response to dexamethasone treatment as compared to those from control group (Fig 2.11H and I). The expression of KLRG1, an activation marker for $CD8^+$ T cells, was also upregulated by approximately two fold in donor OT-I cells (10% in sham T_x vs 20% in dexa T_x) and 1.5 fold (4% in sham T_x vs 6 % in dexa T_x) in endogenous cells isolated from the drug treated group as compared to those from sham treated (Fig 2.11J and K). Upto 7 fold more OT-I cells upregulated PD1 (2% in sham T_x vs 15 % in dexa T_x) in response to dexamethasone treatment (Fig 2.11L and M). A large majority of PD1 positive cells also expressed CXCR3 (Fig 2.11N and O).

The results described in this section demonstrate that dexamethasone could potentially activate naïve $CD8^+$ T cells in the absence of overt antigen stimulation. However the physiological relevance of such processes is yet to be discovered.

7. A brief exposure of activated $CD8^+$ T cells to dexamethasone alters their proliferating potential and conversion into effector memory cells.

We investigated whether or not dexamethasone exposure of activated $CD8^+$ T cells influences their potential to form memory cells. Treatment of mice with dexamethasone causes the apoptosis of precursor naïve cells, some of which are also likely to get recruited during the course of viral infection and make a transition to become memory cells. Therefore, the overall magnitude of memory cells might not be different in control and dexamethasone treated groups. Our results indeed confirmed this notion as we did not find significantly different numbers of memory cells in the two groups (Fig 2.12). However, a significantly higher proportion of $CD8^+$ T cells (both K^b-$gB_{495\text{-}505}$-$tetramer^{+ve}$ and K^b-$gB_{495\text{-}505}$-$tetramer^{-ve}$) isolated from HSV1 infected mice expressed Ki67, a marker for dividing cells, in the peripheral blood samples of dexamethasone treated animals as compared to those in controls (Fig 2.13 A-D). Thus ~1.5 fold more $tetramer^{+ve}$ (60% in sham T_x vs 78% in dexamethasone T_x gp) and 2 fold more $tetramer^{-ve}$ (21% in sham T_x vs 41% in dexamethasone T_x gp) cells expressed Ki67 in the blood samples of dexamethasone treated gp as compared to control (Fig 2.13B-D). Similarly, a greater proportion of $tetramer^{+ve}$ $CD8^+$ T cells acquired a phenotype of $CD127^{+ve}KLRG1^-$ (35% in sham vs 50% in dexamethasone gp) (Fig 2.13E,F). This phenotype of $CD8^+$ T cells has been shown to predominantly give rise to memory cell populations[30,34]. The analysis of draining mediastinal LNs cells also showed that a significantly higher proportions of $tetramer^{+ve}CD8^+$ T cells expressed Ki67 in dexamethasone treated animals as compared to controls (Fig 2.13G-I). But the expression levels of Ki67 by $tetramer^-$ $CD8^+$ T cells and CD127 or KLRG1 by $tetramer^{+ve}$ $CD8^+$ T cells were similar in the two groups (Fig 2.13G-K). The possible reason for this anomaly could be attributed to the exit of cells from lymphoid tissues due to their enhanced CD103 and CXCR3 expression

(Fig 2.4). Therefore, dexamethasone-induced greater proliferative potential and acquisition of a phenotype associated with memory precursor cells led us to believe that dexamethasone treatment could promote memory generation.

We used an adoptive transfer approach to test this possibility. *In vitro* stimulated $CD8^+$ T cells (OT-I cells) were either exposed for one hour to dexamethasone or to diluent. Equal numbers of these cells were then separately transferred in gender-matched mice and their fates were tracked in the recipient animals subsequently (Fig 2.14 and Fig 2.15). More than 90% of the *in vitro* stimulated cells were $CD69^{+ve}$, suggesting for their activation (Fig 2.14H). More than two fold higher frequencies as well as numbers were obtained for dexamethasone treated cells in comparison the control cells (Fig 2.14B-D). Furthermore, the dexamethasone-exposed cells expressed more Ki67 on a per cell basis (Fig 2.14E-G). We then investigated their recall potential by infecting animals with MHV68-SIINFEKL (Fig 2.15A). The frequencies of transferred cells were similar in the circulation for control and dexamethasone treated cells (Fig 2.15B-D). After 30 days of transfer, all the animals were infected with MHV68-SIINFEKL to induce a recall response of the surviving OT-I cells. Expanded cells were analyzed in different lymphoid organs and BAL samples eight days later (Fig 2.15E-I). Significantly greater frequencies and numbers of dexamethasone pre-treated K^b-SIINFEKL-$tetramer^{+ve}$ $CD8^+$ T cells were found in the BAL and spleens as compared to the cells only treated with diluent (Fig 2.15E-I). Slight but significantly increased frequencies and numbers of K^b-SIINFEKL-$tetramer^{+ve}$ cells were also found in the mediastinal LNs of animals that received dexamethasone treated cells (Fig 2.15F and I). We did not find the increase in either the frequencies or their numbers in cervical LNs (Fig 2.15L-N). Greater numbers of IFN-γ producing $CD8^+$ T cells in response to SIINFEKL stimulation were recovered from the group that received dexamethasone treated cells as compared to diluent treated cells (Fig

2.15O-R). The greater magnitudes and effector cytokine producing $CD8^+$ T cells also led to a better viral control in the animals receiving dexamethasone treated cells as compared to those administered with only diluent treated OT-I cells. Thus more than 20 fold more replicating viral particles were present in animals receiving only diluent treated cells as compared to those that received dexamethasone treated cells (Fig 2.15J). We also analyzed the lung tissue sections histologically. Animals receiving dexamethasone treated OT-I cells displayed lesser disruption in the integrity of lung parenchyma, lesser cellular infiltrates and more alveolar spaces as compared to those receiving diluent treated OT-I cells (Fig 2.15K).

Taken together, our results suggest that stimulated $CD8^+$ T cells that were briefly exposed to dexamethasone have a greater propensity to populate and survive in the host that can be recalled to a greater extent upon secondary infection. A greater proportion of these cells were able to migrate to infection sites, controlled viral infection better and help maintain tissue integrity.

Discussion

Immunosuppressive glucocorticoids are commonly used to control immunoinflammatory reactions caused by infections, autoimmune diseases and some cancers. The long lasting bioactive synthetic analogs of glucocorticoids act through Nr3c1 receptors that are ubiquitously expressed by most immune cells. The receptor ligation induces its translocation to nucleus to alter gene expression pattern in the responding cells to execute various anti-inflammatory functions. We explored the influence of a transient treatment of dexamethasone on differentiating virus-specific $CD8^+$ T cells in herpesvirus-infected mice. The virus-expanded $CD8^+$ T cells resisted dexamethasone induced apoptosis. A greater propensity of naïve and memory $CD8^+$ T cells to undergo dexamethasone-induced apoptosis as compared to virus-specific

activated cells directly correlated with their higher nr3c1expression levels. More of the persisting virus-specific $CD8^+$ T cells produced effector molecules and preferentially homed to inflammatory tissue sites owing to their expression of CD103 and CXCR3. The CXCR3 expression induced by dexamethasone promoted their migration to inflammatory tissue sites was shown by anti-CXCR3 neutralizing antibody that greatly reduced their migration to periphery. Surprisingly, virus unresponsive $CD8^+$ T cells exposed to dexamethasone also up regulated molecules such as CD69, KLRG1, CXCR3, PD1 and the transcription factor (Tbet), which are commonly associated with TCR stimulation of $CD8^+$ T cells. Therefore, dexamethasone could potentially contribute to bystander activation of $CD8^+$ T cells. Interestingly, a brief exposure of dexamethasone to activated cells enhanced their proliferation and transition into functionally protective memory cell populations that could be efficiently recalled by a subsequent infection.

The animals receiving dexamethasone therapy only for a short duration mounted a subdued virus-specific $CD8^+$ T cell response later on. A reduction in the precursor frequencies of naïve cells could be the likely reason. This scenario could have considerable implication for patients with hematopoietic deficiencies where the output of specific $CD8^+$ T is limited. Therefore the available pool of naïve $CD8^+$ T cells could be greatly reduced as a consequence of corticosteroid therapy. Similarly immunosuppressive corticosteroids are likely to make organ transplant patients or those with autoimmune conditions more susceptible to infections encountered subsequently. Of note in many of these situations corticosteroids are usually prescribed[2,35]. Therefore, a therapeutic regimen involving the use of corticosteroids has to be carefully evaluated in the backdrop of their ability to induce a less efficient immune response in the host later on. Another situation where these observations would be of relevance and worth a revisit is in aged individuals, who invariably have a compromised hematopoiesis and thymopoiesis. Our

findings that dexamethasone causes the depletion of a pre-existing virus-specific memory $CD8^+$ T cells could also be of major interest to vaccinologists. Thus, memory cells reside in the host for longer duration and provide a pool of cells to effect a quick protection against re-exposure with the same pathogen[36–38]. If such a pool is eliminated, the host could become greatly susceptible to re-emerging infections to which one would otherwise give little importance.

We demonstrate a pronounced activity of viral reactive $CD8^+$ T cells during an ongoing infection from animals receiving a transient dexamethasone treatment. This was evident both in terms of their enhanced ability to produce secretory effector molecules such as IFN-γ and CD107a, in addition to their up regulation of molecules such as CXCR3 and CD103 that facilitate cellular migration to inflammatory sites (Fig 2.1, 2.4 and 2.6)[26]. While both of these properties of $CD8^+$ T cells are considered favorable in providing a better anti-viral defense but the purpose for which corticosteroid therapy is prescribed would be defeated. Thus, inflammatory cell migration to inflamed tissue sites may not achieve the intended anti-inflammatory effects. $CD8^+$ T cells exposed to dexamethasone in the absence of an overt TCR stimulation up regulated activation markers such as CD69, KLRG1, PD1 and CXCR3 in addition to the transcription factor, Tbet. Therefore it could be speculated that corticosteroids or the endogenous glucocorticoids might induce a bystander T cell activation of $CD8^+$ T cells independent of their specific TCR ligation. Not only the chemokine receptor, CXCR3 triggers $CD8^+$ T cells to migrate to inflamed tissue site but is also responsible for the generation of short-lived effector cells as is also suggested by their high expression of KLRG1[26–28]. It is likely that a simultaneous engagement of TCR expressed by $CD8^+$ T cells and nr3c1 ligation mediates a speciation program to facilitate their better functionality at inflammatory tissue sites, while $CD8^+$ T cells not able to receive signals through TCR

undergo a preferential glucocorticoid induced apoptosis (Fig 2.7). The expression of both CXCR3 and PD1 would suggest that to be the likely scenario as both of these molecules are associated with short-lived effector cells[28]. Alternatively, while the antigen-driven activation of $CD8^+$ T cells predominantly provide a protective role and help remove the infection, a bystander activation of cells could contribute significantly to a tissue damaging response before the demise of such cells. Whether such activated cells could have either protective or pathological roles is not evident yet and constitutes part of our ongoing studies. However, it points to a larger question, whether or not endogenous glucocorticoids, which are commonly produced during many virus infections, tumorigenesis and autoimmune diseases could play a yet unexplored but potentially critical role in dictating the fate and function of antigen-specific $CD8^+$ T cells or those activated independent of their TCRs. This issue has been well documented for $CD4^+$ T cell activation during herpesvirus infections[13,39,40]. A recent study provided evidence that in tumor bearing patients, $CD8^+$ T cells that are not specific to tumor antigen but to many unrelated antigens infiltrate to tumor tissues and many such cells also produced effector molecules[41]. Furthermore, it is well known now that subsequent to a virus infection, the host becomes more susceptible to secondary infections and the potential reduction of granulocytes could account for such a susceptibility phenotype[42]. Whether or not elimination of naïve cells by the activity of endogenous glucocorticoids could contribute to the enhanced susceptibility of host to subsequent infections remains less explored and could indeed be one of the key factors.

The levels of glucocorticoids in the microenvironment could also affect the magnitude of effector cells and memory precursor cells and could impart them with a distinct phenotype (Fig 2.13 and 2.15). We did not find significantly more virus-specific memory cells in dexamethasone treated as compared to controls in HSV1 infected mice

(Fig 2.12). This could either be explained by large animal to animal variations or it can be attributed to the pleotropic effects of dexamethasone such as an induction of apoptosis of naïve $CD8^+$ T cells. Apoptosis would reduce the availability of overall antigen-reactive cells thereby giving rise to a limited pool of effector cells some of which make memory. However, the magnitudes of virus-specific memory $CD8^+$ T cells in two groups were similar suggesting that in fact more cells might differentiate into memory cells under the influence of dexamethasone. Alternatively, the overall variation of available antigen in the two groups could stimulate newly generated cells to become activated and eventually some also contributing to the memory pool. In order to account for all these possibilities, we contrived a system where only activated cells were briefly exposed to dexamethasone and then adoptively transferred into mice. In these experiments we did find that dexamethasone treated activated cells gave rise to memory cells that were protective when recalled by a subsequent infection. A phenotype that is likely to give rise to tissue resident memory cells was also evident among virus-specific $CD8^+$ T cells in dexamethasone treated mice (Fig 2.4G-J). For many infections this population serves as the initial responder and eventually help resolve the infection quickly[13,21,43].

Glucocorticoids levels in the microenvironment could serve as a potentially important factor to help dictate a specific differentiation program of $CD8^+$ T cells and possibly other cell types as well. The relative expression levels of transcription factors, Tbet and Eomes, regulates differentiating effector and memory cells populations during some infections[29]. Naïve or the activated $CD8^+$ T cells isolated from dexamethasone treated animals did not show alteration in Eomes mRNA levels but that of Tbet was induced greatly. This could suggest for the critical contribution of endogenous glucocorticoids present in the microenvironment during infection in deciding the speciation program of T cells[44,45]. Clearly a thorough investigation is essential to better

understand such issues that influence disease outcome during infections. Many of these issues are currently under investigation. A very recent study implicated the role of endogenous glucocorticoids in NK cells activation during some herpesvirus infections[46,47]. Not only during pathological but also during physiological situations the levels of corticosteroids change and whether this could serve as one potential variable in T cells speciation program to subsequent infection could also be a topical issue for investigation.

Our study could have many implications i.e., i) dexamethasone induced differentiation program in $CD8^+$ T cells that limits intended acute anti-inflammatory effects ii) dexamethasone could enhance the host susceptibility to subsequent infections as it depletes innocuous naïve cells iii) dexamethasone could potentially cause an attrition of pre-existing immunological memory generated either as a result of a natural infection or vaccination iv) optimized exposure of recently activated $CD8^+$ T cells to immunosuppressive corticosteroids could enhance their proliferative capacity and transition into memory cells that efficiently home to infected tissue sites to control intracellular infections (Fig 2.16). Therefore, unharnessed potential of immunosuppressive corticosteroids or their synthetic analogs could be tapped into improved antigen-specific memory $CD8^+$ T cells generation.

List of References

1. Cain, D. W. & Cidlowski, J. A. Immune regulation by glucocorticoids. *Nat. Rev. Immunol.* **17**, 233–247 (2017).
2. Coutinho, A. E. & Chapman, K. E. The anti-inflammatory and immunosuppressive effects of glucocorticoids, recent developments and mechanistic insights. *Mol. Cell. Endocrinol.* **335**, 2–13 (2011).
3. Tuckermann, J. P. *et al.* Macrophages and neutrophils are the targets for immune suppression by glucocorticoids in contact allergy. *J. Clin. Invest.* **117**, 1381–1390 (2007).
4. Weikum, E. R., Knuesel, M. T., Ortlund, E. A. & Yamamoto, K. R. Glucocorticoid receptor control of transcription: precision and plasticity via allostery. *Nat. Rev. Mol. Cell Biol.* **18**, 159–174 (2017).
5. Evans, R. M. The steroid and thyroid hormone receptor superfamily. *Science* **240**, 889–95 (1988).
6. Jamieson, A. M., Yu, S., Annicelli, C. H. & Medzhitov, R. Influenza Virus-Induced Glucocorticoids Compromise Innate Host Defense against a Secondary Bacterial Infection. *Cell Host Microbe* **7**, 103–114 (2010).
7. Ruzek, M. C., Pearce, B. D., Miller, A. H. & Biron, C. A. Endogenous glucocorticoids protect against cytokine-mediated lethality during viral infection. *J. Immunol.* **162**, 3527–33 (1999).
8. Ruzek, M. C., Miller, A. H., Opal, S. M., Pearce, B. D. & Biron, C. A. Characterization of early cytokine responses and an interleukin (IL)-6-dependent pathway of endogenous glucocorticoid induction during murine cytomegalovirus infection. *J. Exp. Med.* **185**, 1185–92 (1997).
9. Webster, J. I., Tonelli, L. & Sternberg, E. M. N EUROENDOCRINE R EGULATION OF I MMUNITY. *Annu. Rev. Immunol.* **20**, 125–163 (2002).

10. Van Laethem, F. *et al.* Glucocorticoids attenuate T cell receptor signaling. *J. Exp. Med.* **193**, 803–14 (2001).

11. Liu, T., Khanna, K. M., Chen, X., Fink, D. J. & Hendricks, R. L. CD8(+) T cells can block herpes simplex virus type 1 (HSV-1) reactivation from latency in sensory neurons. *J. Exp. Med.* **191**, 1459–66 (2000).

12. Goldsmith, K., Chen, W., Johnson, D. C. & Hendricks, R. L. Infected cell protein (ICP)47 enhances herpes simplex virus neurovirulence by blocking the CD8+ T cell response. *J. Exp. Med.* **187**, 341–8 (1998).

13. Rouse, B. T. & Sehrawat, S. Immunity and immunopathology to viruses: what decides the outcome? *Nat. Rev. Immunol.* **10**, 514–26 (2010).

14. Sehrawat, S., Kumar, D. & Rouse, B. T. Herpesviruses: Harmonious Pathogens but Relevant Cofactors in Other Diseases? *Front. Cell. Infect. Microbiol.* **8**, 177 (2018).

15. Sehrawat, S. *et al.* A catalytically inactive mutant of the deubiquitylase YOD-1 enhances antigen cross-presentation. *Blood* **121**, 1145–1156 (2013).

16. Altman, J. D. *et al.* Phenotypic analysis of antigen-specific T lymphocytes. *Science* **274**, 94–6 (1996).

17. Sehrawat, S. *et al.* CD8(+) T cells from mice transnuclear for a TCR that recognizes a single H-2K(b)-restricted MHV68 epitope derived from gB-ORF8 help control infection. *Cell Rep.* **1**, 461–71 (2012).

18. Barber, D. L. *et al.* Restoring function in exhausted CD8 T cells during chronic viral infection. *Nature* **439**, 682–687 (2006).

19. Caulfield, J., Fernandez, M., Snetkov, V., Lee, T. & Hawrylowicz, C. CXCR4 expression on monocytes is up-regulated by dexamethasone and is modulated by autologous CD3+ T cells. *Immunology* **105**, 155–62 (2002).

20. Ghosh, M. C. *et al.* Dexamethasone augments CXCR4-mediated signaling in resting human T cells via the activation of the Src kinase Lck. *Blood* **113**, 575–84 (2009).

21. Schenkel, J. M. & Masopust, D. Tissue-resident memory T cells. *Immunity* **41**, 886–97 (2014).

22. Jacquelot, N. *et al.* Chemokine receptor patterns in lymphocytes mirror metastatic spreading in melanoma. *J. Clin. Invest.* **126**, 921–937 (2016).

23. Baulieu, E. E. Contragestion and other clinical applications of RU 486, an antiprogesterone at the receptor. *Science* **245**, 1351–7 (1989).

24. Kaur, M. *et al.* Galectin-3 Regulates γ-Herpesvirus Specific CD8 T Cell Immunity. *iScience* **9**, 101–119 (2018).

25. Ishida, Y., Agata, Y., Shibahara, K. & Honjo, T. Induced expression of PD-1, a novel member of the immunoglobulin gene superfamily, upon programmed cell death. *EMBO J.* **11**, 3887–95 (1992).

26. Hickman, H. D. *et al.* CXCR3 Chemokine Receptor Enables Local CD8+ T Cell Migration for the Destruction of Virus-Infected Cells. *Immunity* **42**, 524–537 (2015).

27. Kurachi, M. *et al.* Chemokine receptor CXCR3 facilitates CD8 $^{+}$ T cell differentiation into short-lived effector cells leading to memory degeneration. *J. Exp. Med.* **208**, 1605–1620 (2011).

28. Serre, K. *et al.* CD8 T cells induce T-bet-dependent migration toward CXCR3 ligands by differentiated B cells produced during responses to alum-protein vaccines. *Blood* **120**, 4552–4559 (2012).

29. Intlekofer, A. M. *et al.* Effector and memory CD8+ T cell fate coupled by T-bet and eomesodermin. *Nat. Immunol.* **6**, 1236–1244 (2005).

30. Sarkar, S. *et al.* Functional and genomic profiling of effector CD8 T cell subsets with distinct memory fates. *J. Exp. Med.* **205**, 625–40 (2008).

31. Kaech, S. M. & Cui, W. Transcriptional control of effector and memory CD8+ T cell differentiation. *Nat. Rev. Immunol.* **12**, 749–761 (2012).

32. Best, J. A. *et al.* Transcriptional insights into the CD8(+) T cell response to infection and memory T cell formation. *Nat. Immunol.* **14**, 404–12 (2013).

33. Agata, Y. *et al.* Expression of the PD-1 antigen on the surface of stimulated mouse T and B lymphocytes. *Int. Immunol.* **8**, 765–72 (1996).

34. Joshi, N. S. *et al.* Inflammation directs memory precursor and short-lived effector CD8(+) T cell fates via the graded expression of T-bet transcription factor. *Immunity* **27**, 281–95 (2007).

35. Tanaka, S. *et al.* Corticosteroid-responsive diabetes mellitus associated with autoimmune pancreatitis. *Lancet* **356**, 910–911 (2000).

36. Amanna, I. J., Slifka, M. K. & Crotty, S. Immunity and immunological memory following smallpox vaccination. *Immunol. Rev.* **211**, 320–337 (2006).

37. Wherry, E. J. & Ahmed, R. Memory CD8 T-Cell Differentiation during Viral Infection. *J. Virol.* **78**, 5535–5545 (2004).

38. Harty, J. T. & Badovinac, V. P. Shaping and reshaping CD8+ T-cell memory. *Nat. Rev. Immunol.* **8**, 107–119 (2008).

39. Deshpande, S. *et al.* Bystander activation involving T lymphocytes in herpetic stromal keratitis. *J. Immunol.* **167**, 2902–10 (2001).

40. Sehrawat, S., Kumar, D. & Rouse, B. T. Herpesviruses: Harmonious Pathogens but Relevant Cofactors in Other Diseases? *Front. Cell. Infect. Microbiol.* **8**, 177 (2018).

41. Simoni, Y. *et al.* Bystander CD8+ T cells are abundant and phenotypically distinct in human tumour infiltrates. *Nature* **557**, 575–579 (2018).

42. Navarini, A. A. *et al.* Increased susceptibility to bacterial superinfection as a consequence of innate antiviral responses. *Proc. Natl. Acad. Sci. U. S. A.* **103**, 15535–9 (2006).

43. Mackay, L. K. *et al.* Long-lived epithelial immunity by tissue-resident memory T (TRM) cells in the absence of persisting local antigen presentation. *Proc. Natl. Acad. Sci. U. S. A.* **109**, 7037–42 (2012).

44. Miller, A. H. *et al.* Effects of viral infection on corticosterone secretion and glucocorticoid receptor binding in immune tissues. *Psychoneuroendocrinology* **22**, 455–474 (1997).

45. Ng, S. S. M., Li, A., Pavlakis, G. N., Ozato, K. & Kino, T. Viral Infection Increases Glucocorticoid-Induced Interleukin-10 Production through ERK-Mediated Phosphorylation of the Glucocorticoid Receptor in Dendritic Cells: Potential Clinical Implications. *PLoS One* **8**, e63587 (2013).

46. Quatrini, L. *et al.* Endogenous glucocorticoids control host resistance to viral infection through the tissue-specific regulation of PD-1 expression on NK cells. *Nat. Immunol.* **19**, 954–962 (2018).

47. Biron, C. A. Glucocorticoids and NK cell PD-1. *Nat. Immunol.* **19**, 908–910 (2018).

APPENDIX

Fig. 2.1 Dexamethasone therapy induces altered response in HSV1 infected animals. C57BL/6 mice were infected with HSV1-KOS ($5x10^5$ pfu/foot pad) and were then injected with the diluent or dexamethasone (10 mg/Kg Bwt) intraperitoneally from 4 to 6 dpi. Distribution and phenotype of immune cells were analyzed in the peripheral blood circulation at 6 dpi (A-C) and draining popliteal lymph node (PLN) at 7 dpi (D-M). A. Representative FACS plots from two groups show the frequency and phenotype of HSV-1 specific (H-$2K^b$-$gB_{498-505}$-Tet^+) $CD8^+$ T cells in the peripheral circulation. B. Bar diagrams show the frequencies of total $CD8^+$ T cells out of $CD45^+$ leukocytes and HSV1 specific (H-$2K^b$-$gB_{498-505}$-Tet^+) $CD8^+$ T cells in peripheral blood. C. Bar diagrams show the numbers of $CD8^+$ T cells and HSV1-specific (H-$2K^b$-$gB_{498-505}$-Tet^+) $CD8^+$ T cells per ml of blood. D. Representative FACS plots from two groups show the frequencies of HSV1 specific (H-$2K^b$-$gB_{498-505}$-Tet^+) $CD8^+$ T cells among $CD45^+$ leukocytes present in draining popliteal LNs. E. Percentage of total $CD8^+$ T cells and HSV1 specific (H-$2K^b$-$gB_{498-505}$-Tet^+) $CD8^+$ T cells among $CD45^+$ leukocytes present in draining popliteal LNs are shown by bar diagrams. F. Total numbers of $CD8^+$ T cells and HSV1 specific (H-$2K^b$-$gB_{498-505}$-Tet^+) $CD8^+$ T cells among $CD45^+$ leukocytes present in draining popliteal LNs are shown by bar diagrams. G-I & M. ICCS assays were performed by stimulating PLN cells with SSIFERAL peptide to measure cytokine producing $CD8^+$ T cells in the PLNs of HSV1 infected and dexamethasone treated animals. The percentages and numbers of cytokine producing $CD8^+$ T cells in PLN are shown by representative FACS plots (G) and bar diagrams (H). I. Total numbers of $CD8^+$ T cells that produced indicated cytokines are shown by bar diagrams. M. The mean fluorescence intensities (MFI) for IFN-γ production by peptide stimulated $CD8^+$ T cells from control and dexamethasone group are shown by bar diagrams. Representative FACS plots (J) and bar diagrams (K) show the frequencies of de-granulating ($CD107a^+$) $CD8^+$ T cells isolated from dexamethasone and control groups of animals. L. The mean fluorescence intensities (MFI) for CD107a by $CD8^+$ T cells from control and dexamethasone group are shown by bar diagrams. N. Viral loads measured from the extracted footpads of sham and dexamethasone treated mice are shown by bar diagram. Mean values and ± SD are shown. In each experimental group 5-6 animals were included. The

experiments were repeated with similar results. **P < 0.005; *P < 0.05 and NS (P > 0.05)- not significant (Mann-Whitney U test- two tailed).

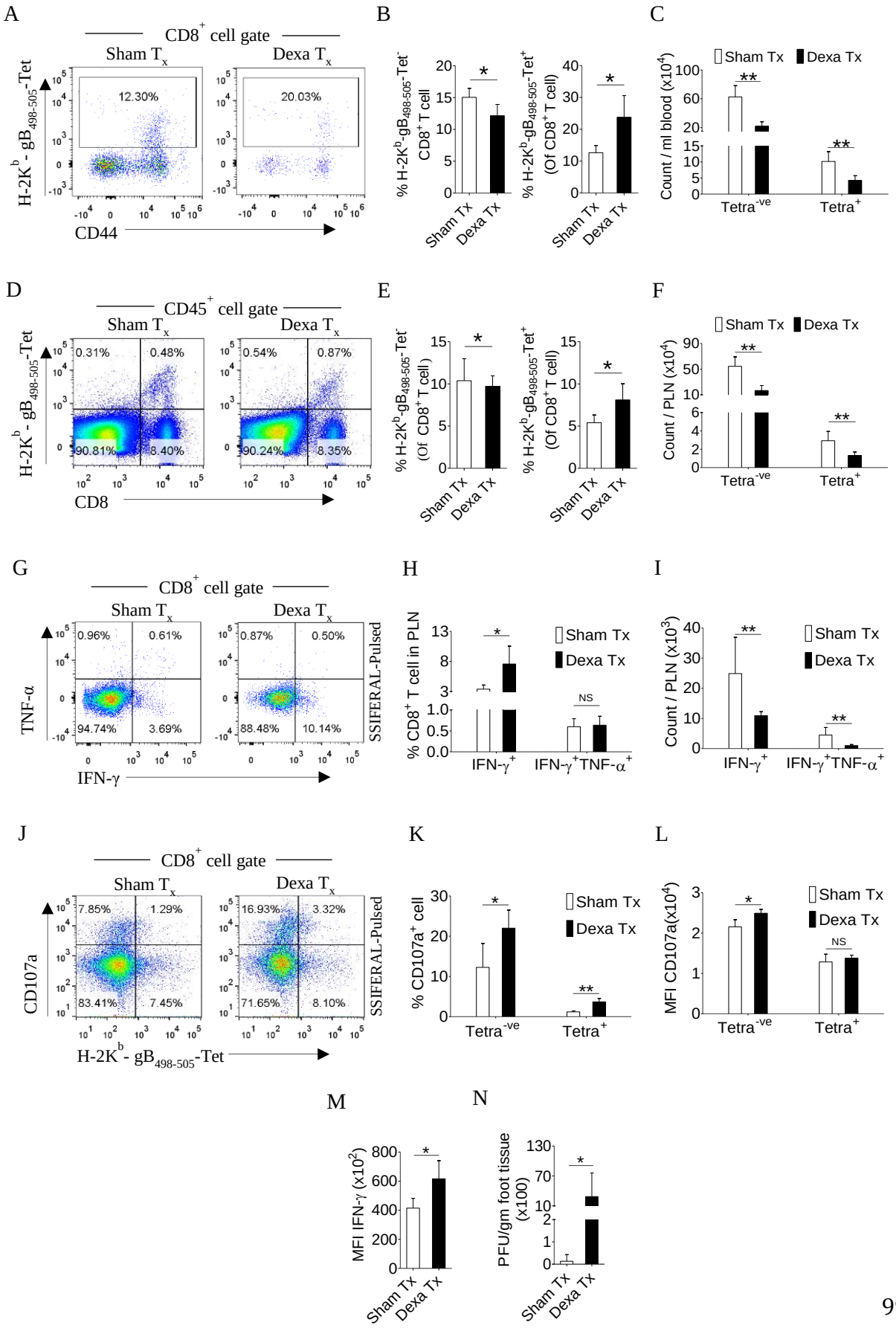

Fig. 2.2 Effect of glucocorticoid on immune cells.

Level of leukocytes and myeloid cells was measured in blood circulation of sham and dexa treated mice. (Experimental plan discussed in Fig 2.1). $CD45^+$ leukocytes frequency (A,B) and their numbers are shown (C). Similarly $CD11b^+$ myeloid cells frequency (A,D) and their numbers in blood are shown (E) at 6 dpi of acute stage of infection setup as discussed in Fig 2.1 legend. Each symbol shows an individual animal, where error bars indicate ± SD. **P < 0.005 and NS (P > 0.05)- not significant (Mann-Whitney U test- two tailed).

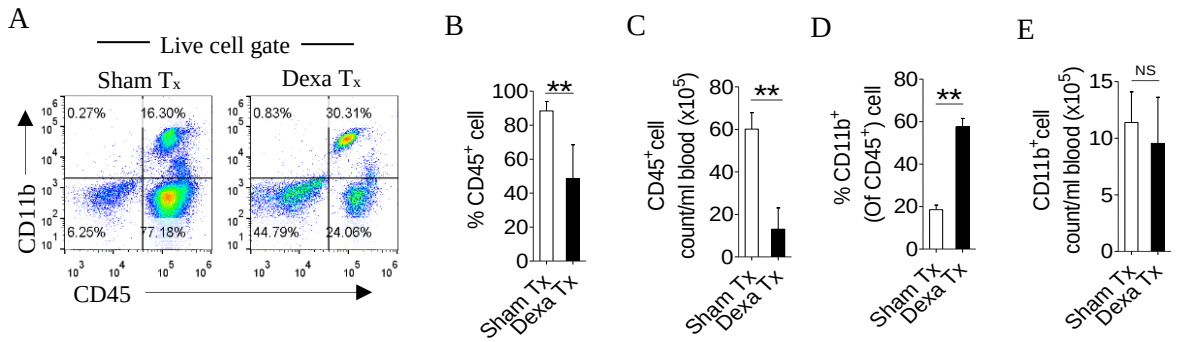

Fig. 2.3 Effect of different dose of dexamethasone on virus specific $CD8^+$ T cells.

C57BL/6 mice (n=15) were infected with HSV1. At 4-6 dpi these animals were treated with sham (3 mice), and graded dose of dexamethasone (10, 0.1 and 0.01 mg/kg – 4 mice in each group) through intraperitoneally route. On 6 dpi the cell types in blood circulation were counted. Frequency (A and B) and count/ml (C) of $CD8^+$ T cells are shown by graphs. Similarly the percentage (D and E) and count/ml (F) of $tetramer^{+ve}$ $CD8^+$ T cells are shown. Frequency (G) of $CXCR3^+tetramer^{+ve}CD8^+$ T cells are shown. Levels of HSV reactive cells at memory stage and recall infection were measured. Frequency and count (H-J) of $CD8^+$ T cells in blood circulation at memory stage (30 dpi) are shown. At 4 dpi of recall infection the frequency and count of $tetramer^{+ve}$ $CD8^+$ T cells (K-M), and count of $CD8^+$ T cells (N) are shown. For recall response these mice were infected with $2x10^6$ PFU/foot pad of HSV1-KOS on 31 dpi and analyzed for $CD8^+$ T cell subsets on 4 dpi in draining PLN. Each symbol shows an individual animal, where error bars indicate ± SD. *$P < 0.05$ and NS ($P > 0.05$)- not significant (Mann-Whitney U test- two tailed).

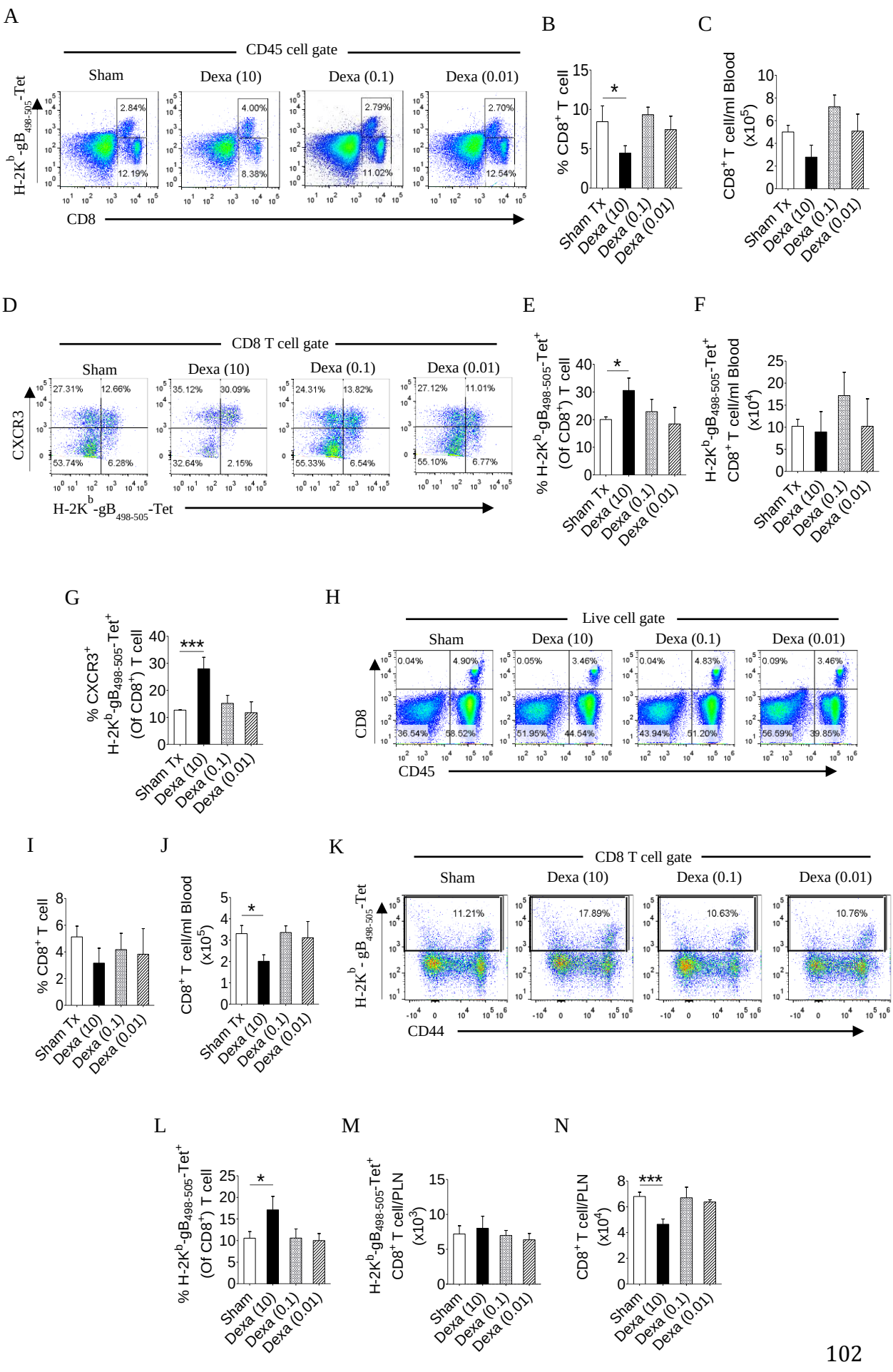
A
CD45 cell gate
Sham
Dexa (10)
Dexa (0.1)
Dexa (0.01)
H-2K^b-gB$_{498-505}$-Tet
CD8
2.84%
12.19%
4.00%
8.38%
2.79%
11.02%
2.70%
12.54%
B
% CD8$^+$ T cell
C
CD8$^+$ T cell/ml Blood (x10^5)
D
CD8 T cell gate
CXCR3
H-2K^b-gB$_{498-505}$-Tet
27.31%
12.66%
53.74%
6.28%
35.12%
30.09%
32.64%
2.15%
24.31%
13.82%
55.33%
6.54%
27.12%
11.01%
55.10%
6.77%
E
% H-2K^b-gB$_{498-505}$-Tet$^+$ (Of CD8$^+$) T cell
F
H-2K^b-gB$_{498-505}$-Tet$^+$ CD8$^+$ T cell/ml Blood (x10^4)
G
% CXCR3$^+$ H-2K^b-gB$_{498-505}$-Tet$^+$ (Of CD8$^+$) T cell
H
Live cell gate
CD8
CD45
0.04%
4.90%
36.54%
58.52%
0.05%
3.46%
51.95%
44.54%
0.04%
4.83%
43.94%
51.20%
0.09%
3.46%
56.59%
39.85%
I
% CD8$^+$ T cell
J
CD8$^+$ T cell/ml Blood (x10^5)
K
CD8 T cell gate
H-2K^b - gB$_{498-505}$ -Tet
CD44
11.21%
17.89%
10.63%
10.76%
L
% H-2K^b-gB$_{498-505}$-Tet$^+$ (Of CD8$^+$) T cell
M
H-2K^b-gB$_{498-505}$-Tet$^+$ CD8$^+$ T cell/PLN (x10^3)
N
CD8$^+$ T cell/PLN (x10^4)
Sham Tx
Sham
Dexa (10)
Dexa (0.1)
Dexa (0.01)

Fig. 2.4 Dexamethasone modulates tissue homing molecules in $CD8^+$ T cells during HSV1 infection. C57BL/6 mice were infected with HSV1-KOS ($5x10^5$ pfu/foot pad) and were then injected with the diluent or dexamethasone (10 mg/Kg Bwt) intraperitoneally from 4 to 6 dpi. Expression levels of CXCR3 on $CD8^+$ T cell subsets in blood (6 dpi) and draining popliteal LNs (7 dpi) isolated from diluent and dexamethasone treated mice were measured by flow cytometry. Representative FACS plots shows CXCR3 expression on K^b-$gB_{498-505}$-tet^{+ve} and K^b-$gB_{498-505}$-$tet^{-ve}CD8^+$ T cells in blood circulation (A) and draining PLN (D). B. The percentage of $CXCR3^+K^b$- $gB_{498-505}$-tet^{+ve} and $CXCR3^+K^b$-$gB_{498-505}$-tet^{-ve}cells is shown by bar diagrams. C. Mean fluorescence intensities (MFI) for CXCR3 expression by K^b- $gB_{498-505}$-tet^{+ve} and K^b-$gB_{498-505}$-$tet^{-ve}CD8^+$ T cells are shown by bar diagrams. E. The percentage of $CXCR3^+K^b$-$gB_{498-505}$-tet^{+ve} and $CXCR3^+K^b$- $gB_{498-505}$-tet^{-ve} cells is shown by bar diagrams. F. MFI for CXCR3 on K^b-$gB_{498-505}$-tet^{+ve} and K^b-$gB_{498-505}$-$tet^{-ve}CD8^+$ T cells are shown by bar diagrams. G-J. The frequencies $CD103^+$ $KLRG1^-$ T cells out of K^b-$gB_{498-505}$-$tet^{+ve}CD8^+$ T cells in sham and dexamethasone treated mice infected with HSV1 are shown by representative FACS plots (G and H) and bar graphs (I) in the draining popliteal LNs cells. J. MFI for the expression of CD103 and KLRG1 in HSV1 specific (K^b-$gB_{498-505}$-tet^{+ve}) $CD8^+$ T cells at 7 dpi are shown by bar diagrams. Mean ± SD are represented. The experiments were repeated two times with similar results. In each experimental group 4-6 animals were included. ***P < 0.001; **P<0.005; *P < 0.05 and NS (P > 0.05)- not significant (Unpaired t test).

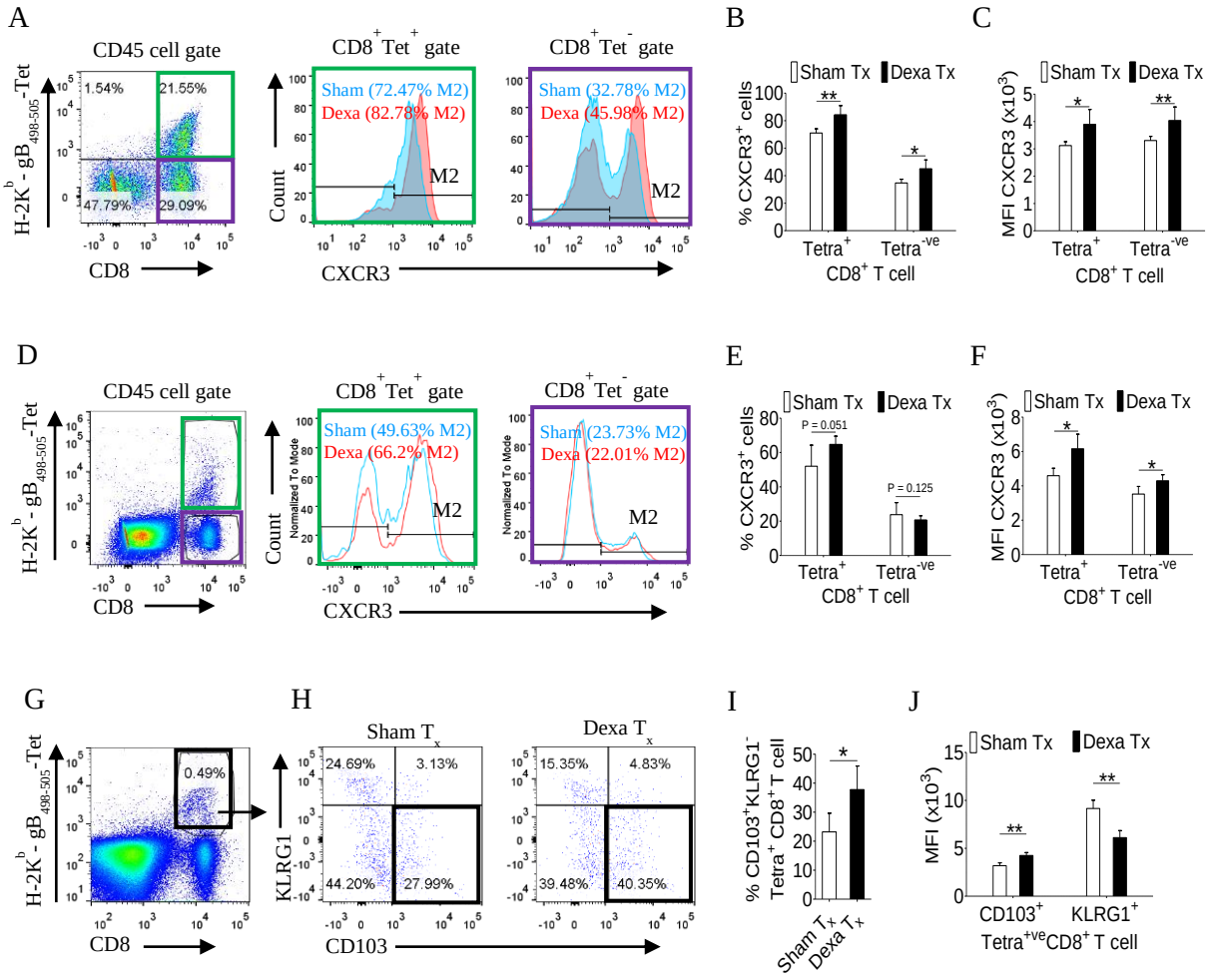
A
CD45 cell gate
H-2K^b - gB498-505-Tet
1.54%
21.55%
47.79%
29.09%
CD8
CD8+Tet+ gate
CD8+Tet- gate
Sham (72.47% M2)
Dexa (82.78% M2)
Sham (32.78% M2)
Dexa (45.98% M2)
M2
Count
CXCR3
B
Sham Tx
Dexa Tx
% CXCR3+ cells
Tetra+
Tetra-ve
CD8+ T cell
C
MFI CXCR3 (x10^3)
D
Sham (49.63% M2)
Dexa (66.2% M2)
Sham (23.73% M2)
Dexa (22.01% M2)
Normalized To Mode
E
P = 0.051
P = 0.125
F
G
0.49%
H
Sham Tx
Dexa Tx
24.69%
3.13%
44.20%
27.99%
15.35%
4.83%
39.48%
40.35%
KLRG1
CD103
I
% CD103+KLRG1- Tetra+CD8+T cell
Sham Tx
Dexa Tx
J
MFI (x10^3)
CD103+
KLRG1+
Tetra+veCD8+ T cell

Fig. 2.5 Measuring chemokine receptors in $CD8^+$ T cells HSV1 infected mice that received either the diluent or dexamethasone

At acute stage of HSV1 infection CXCR4 and CCR7 expression on $tetramer^{+ve}$ and $tetramer^{-ve}$ $CD8^+$ T cells in blood circulation (A-E) and draining popliteal LN (F-J) are shown. A Representative FACS plots and overlaid histograms for CXCR4 and CCR7 in $tetramer^{+ve}$ and $tetramer^{-ve}$ $CD8^+$ T cells are shown from peripheral blood of sham and dexamethasone treated animals. The frequencies (B and D) and MFI values (C and E) for CXCR4 and CCR7 expression on $tetramer^{+ve}$ or $tetramer^{-ve}$ $CD8^+$ T cells in peripheral blood are shown. F. Representative FACS plots and overlaid histograms for CXCR4 and CCR7 in $tetramer^{+ve}$ and $tetramer^{-ve}$ $CD8^+$ T cells are shown from draining popliteal LNs of sham and dexamethasone treated animals. The frequencies (G and I) and MFI values (H and J) for CXCR4 and CCR7 expression on $tetramer^{+ve}$ or $tetramer^{-ve}$ $CD8^+$ T cells in draining popliteal LNs are shown. Data is represented as mean ± SD. $**P < 0.005$; $*P < 0.05$ and NS ($P > 0.05$)- not significant (Mann-Whitney U test- two tailed).

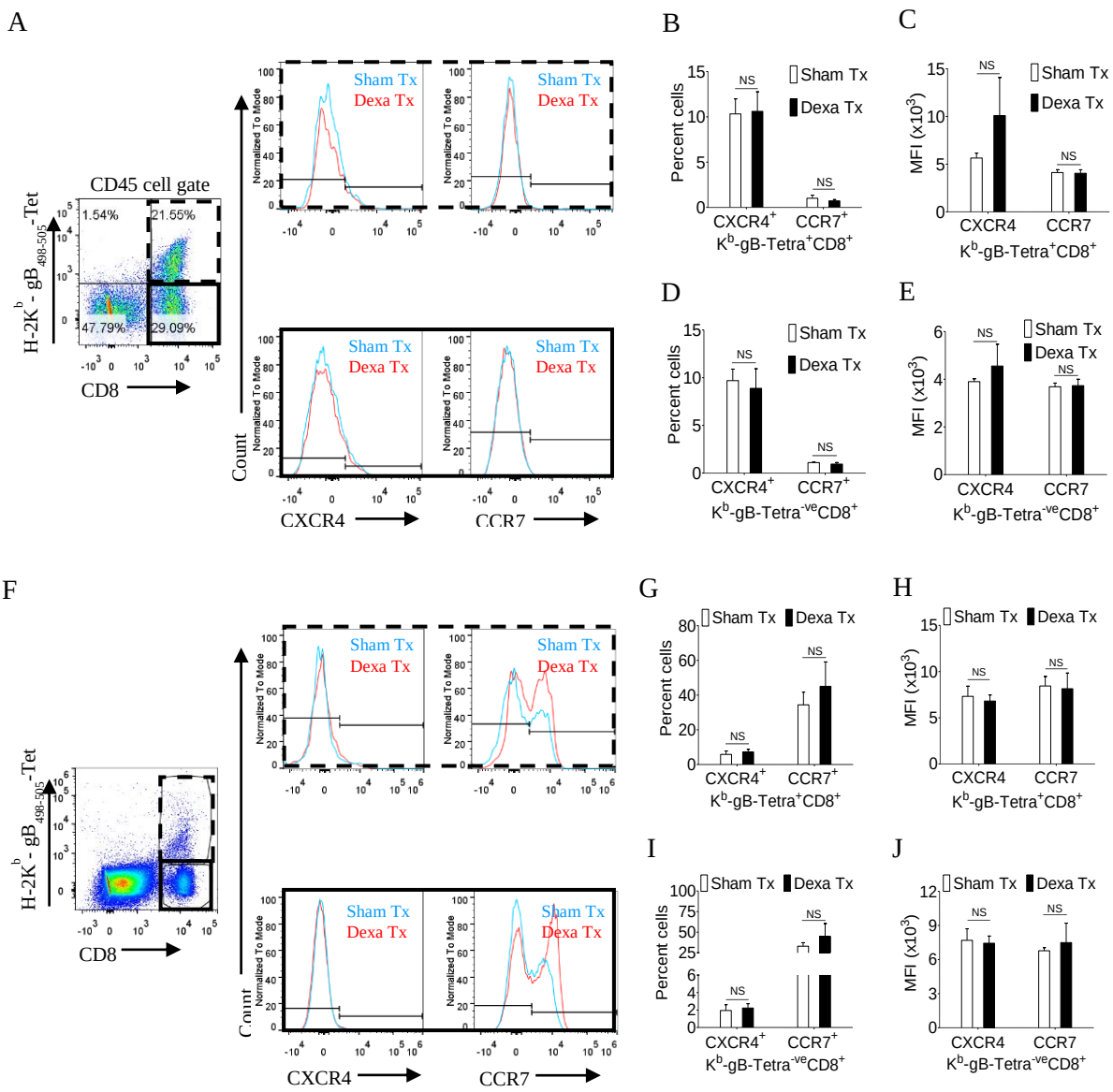
A
CD45 cell gate
1.54%
21.55%
47.79%
29.09%
H-2K - gB -Tet
CD8
Sham Tx
Dexa Tx
Normalized To Mode
Count
CXCR4
CCR7
B
Percent cells
NS
CXCR4+ CCR7+
Kb-gB-Tetra+CD8+
C
MFI (x10³)
CXCR4 CCR7
Kb-gB-Tetra+CD8+
D
Kb-gB-Tetra-veCD8+
E
F
G
H
I
J

Fig. 2.6 A transient dexamethasone therapy induces CXCR3 mediated $CD8^+$ T cells migration to tissue sites. A. A schematic of the experiments is shown. $10x10^3$ OT-I cells were transferred in C57BL/6 mice. Recipient animals were infected with MHV68 M2-SIINFEKL virus the following day. Infected animals were then divided into three groups. One group received diluent. The second group received dexamethasone (10 mg/kg B Wt) and the third group received both dexamethasone and anti-CXCR3 antibody at day 6 and 7 post infection. The response of $CD8^+$ T cells and viral load were analyzed at 8 dpi. B and C. The frequencies and phenotype of K^b-SIINFEKL-$tet^{+ve}CD8^+$ T cells are shown by representative FACS plots (B) and bar diagrams (C) in the peripheral blood of animals in different groups. D and E. The frequencies of K^b-SIINFEKL-$tet^{+ve}CD8^+$ T cells are shown by representative FACS plots (D) and bar diagrams (E) in bronchoalveolar tissue lavage samples of animals from different groups. F and G. The frequencies and phenotype of K^b-SIINFEKL-$tet^{+ve}CD8^+$ T cells are shown by representative FACS plots (F) and bar diagrams (G) in the draining mediastinal LNs of animals in different groups. H and I. The frequencies and phenotype of K^b-SIINFEKL-$tet^{+ve}CD8^+$ T cells are shown by representative FACS plots (H) and bar diagrams (I) in the spleens of animals in different groups. J. Viral load was measured from lung homogenates of different groups of animals by plaque forming assays. The replicating virus load is shown by bar diagrams in different groups. In each experimental group >3 animals were included. ***$P < 0.001$; **$P<0.005$; *$P < 0.05$ and NS ($P > 0.05$)- not significant (Unpaired t test).

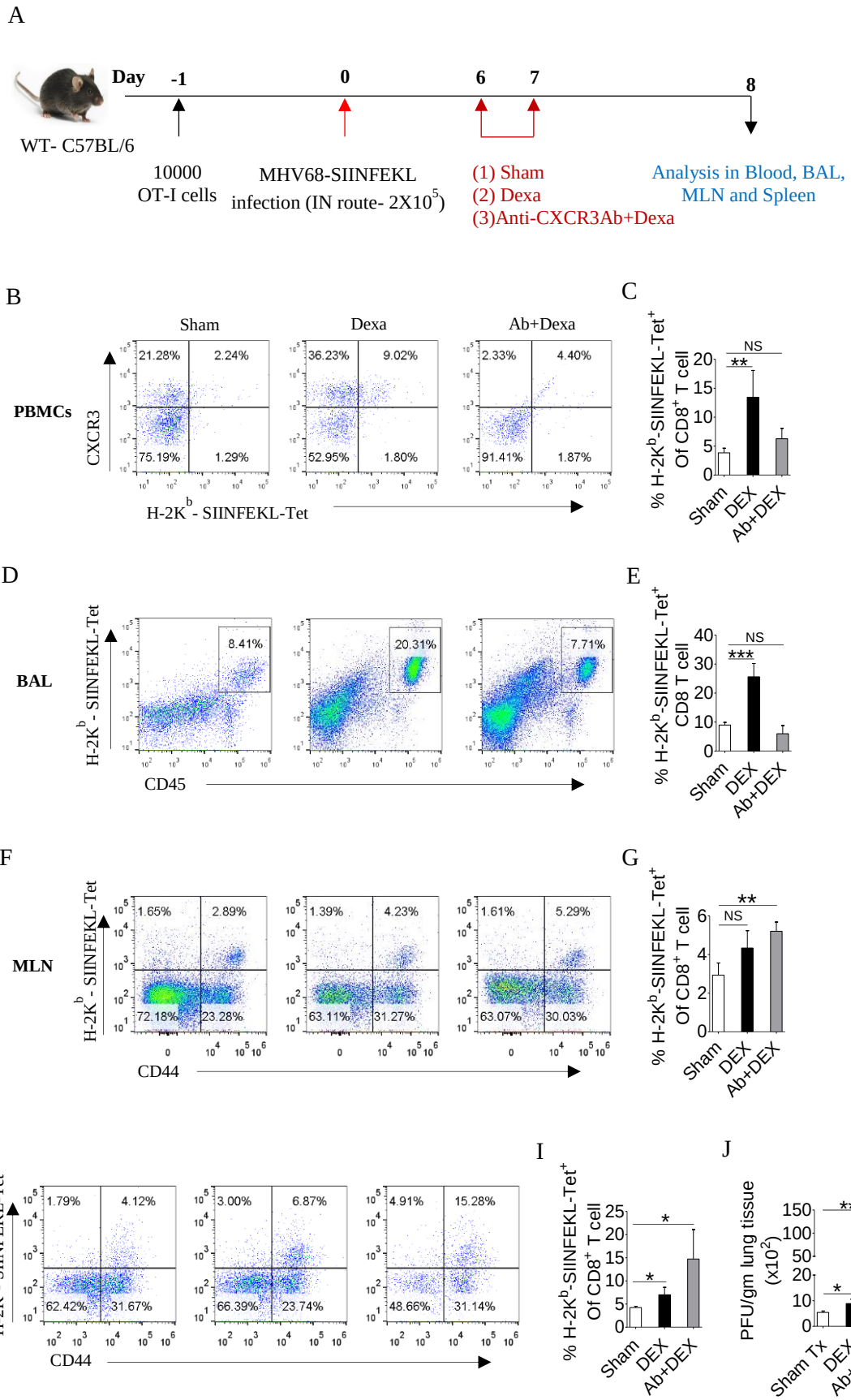
A
Day -1 0 6 7 8
WT- C57BL/6
10000 OT-I cells
MHV68-SIINFEKL infection (IN route- 2X10^5)
(1) Sham
(2) Dexa
(3)Anti-CXCR3Ab+Dexa
Analysis in Blood, BAL, MLN and Spleen
B
Sham
Dexa
Ab+Dexa
PBMCs
CXCR3
H-2K^b - SIINFEKL-Tet
21.28%
2.24%
75.19%
1.29%
36.23%
9.02%
52.95%
1.80%
2.33%
4.40%
91.41%
1.87%
C
% H-2K^b-SIINFEKL-Tet+ Of CD8+ T cell
NS
**
Sham
DEX
Ab+DEX
D
BAL
H-2K^b - SIINFEKL-Tet
CD45
8.41%
20.31%
7.71%
E
% H-2K^b-SIINFEKL-Tet+ CD8 T cell
NS
***
F
MLN
CD44
1.65%
2.89%
72.18%
23.28%
1.39%
4.23%
63.11%
31.27%
1.61%
5.29%
63.07%
30.03%
G
**
NS
H
Spleen
1.79%
4.12%
62.42%
31.67%
3.00%
6.87%
66.39%
23.74%
4.91%
15.28%
48.66%
31.14%
I
*
*
J
PFU/gm lung tissue (x10^2)
***
*
Sham Tx
DEX
Ab+DEX

Fig. 2.7 Naive $CD8^+$ T cell are more susceptible to glucocorticoid-induced cell death. Single cells suspension prepared from the draining popliteal LN cells of HSV1 infected mice were incubated with diluent and dexamethasone for the indicated time points. Some cells were pretreated with 5 µM mifepristone. The frequencies of apoptotic cells were measured by annexin V staining after incubation period was over. A. Representative overlaid histograms show annexin V^{+ve} cells from dexamethasone and dexamethasone combined with mifepristone treated samples B. Bar diagrams show the percentage of annexin V^{+ve} cells in different groups. C, Annexin V^{+ve} cells in boxed $CD8^+$ T cells (naïve, $CD44^+Tet^{-ve}$ and $CD44^+$-Tet^{+ve}) that were incubated with diluent, dexamethasone (1 µM) and dexamethasone (1 µM) + mifepristone (5 µM) are shown. D-F. Kinetics of annexin V^{+ve} cells in different $CD8^+$ T cell subsets is shown. Mean and ± SD are shown. ***$P \leq 0.001$, **$P \leq 0.005$, *$P \leq 0.05$ (Bonferroni test-Two-way ANOVA). G-I. *in vivo* killing of different subsets of CD8 T cells was measured. G. Schematic of the experiments to measure *in vivo* killing of identifiable cells is shown. H. Population of naive ($CFSE^{hi}$) and activated ($CFSE^{lo}$) $CD45.1^+CD8^+$ T cells in different tissues (BM, Spleen and PBMCs) of sham (upper panel) and dexamethasone (lower panel) treated CD45.2 mice are shown by histograms. I. % Specific elimination of naive $CD8^+$ T cells in different tissue sites of dexamethasone treated mice as compared to diluent treatment group is shown by bar diagrams. The percent specific elimination was calculated as described in material and methods section. In each experimental group 6 animals were included.

A

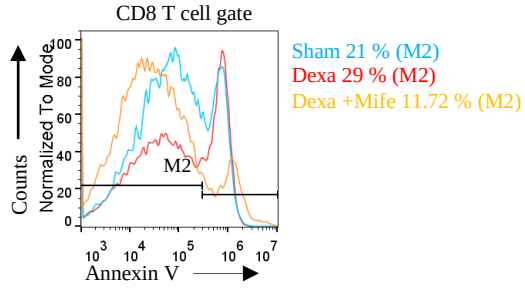
CD8 T cell gate
Sham 21 % (M2)
Dexa 29 % (M2)
Dexa +Mife 11.72 % (M2)
Counts
Normalized To Mode
M2
Annexin V

B

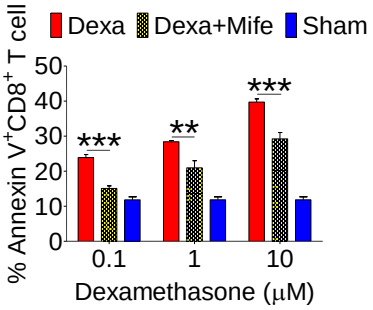
Dexa
Dexa+Mife
Sham
% Annexin V+CD8+ T cell
***
**
***
0.1
1
10
Dexamethasone (μM)

C

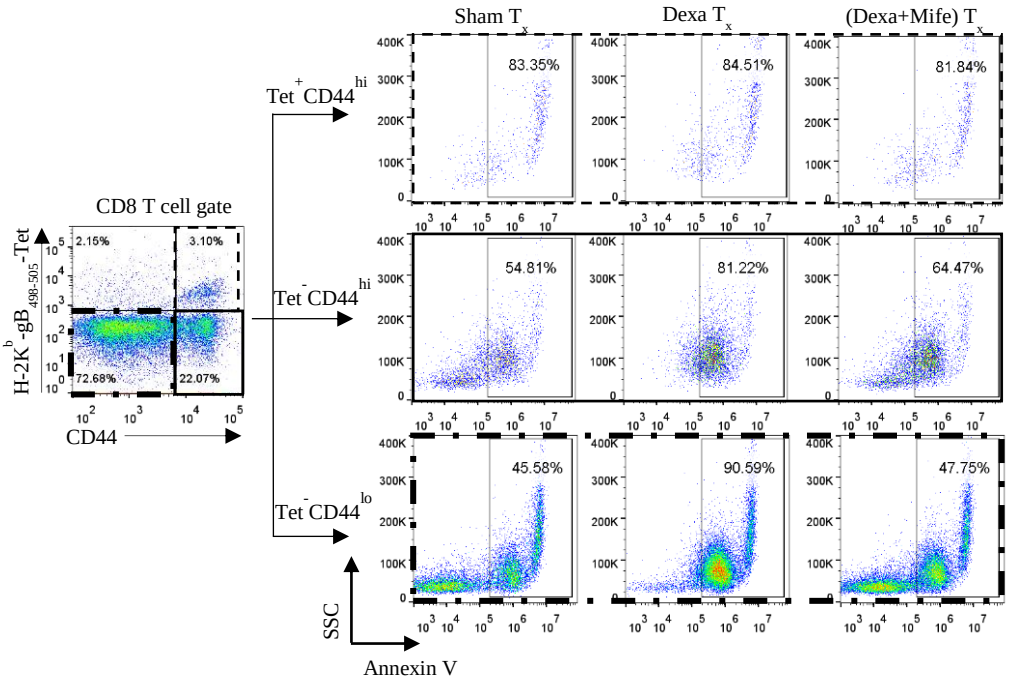
Sham Tx
Dexa Tx
(Dexa+Mife) Tx
CD8 T cell gate
H-2Kb-gB 498-505-Tet
CD44
2.15%
3.10%
72.68%
22.07%
Tet+ CD44hi
Tet- CD44hi
Tet- CD44lo
83.35%
84.51%
81.84%
54.81%
81.22%
64.47%
45.58%
90.59%
47.75%
SSC
Annexin V

D

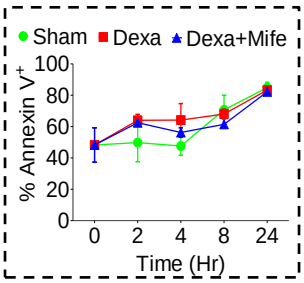
Sham
Dexa
Dexa+Mife
% Annexin V+
Time (Hr)

E

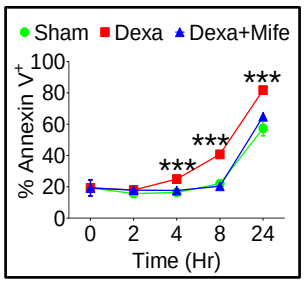
Sham
Dexa
Dexa+Mife
% Annexin V+
***
***
***
Time (Hr)

F

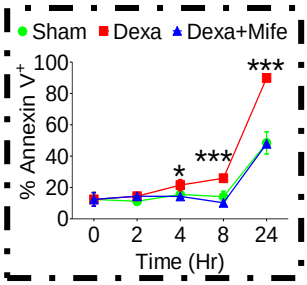
Sham
Dexa
Dexa+Mife
% Annexin V+
*
***
***
Time (Hr)

G

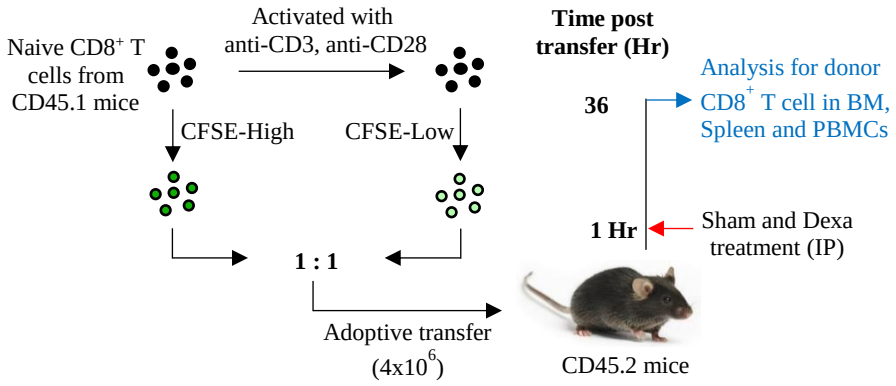
Naive CD8+ T cells from CD45.1 mice
Activated with anti-CD3, anti-CD28
CFSE-High
CFSE-Low
1 : 1
Adoptive transfer (4x10^6)
Time post transfer (Hr)
36
Analysis for donor CD8+ T cell in BM, Spleen and PBMCs
1 Hr
Sham and Dexa treatment (IP)
CD45.2 mice

H

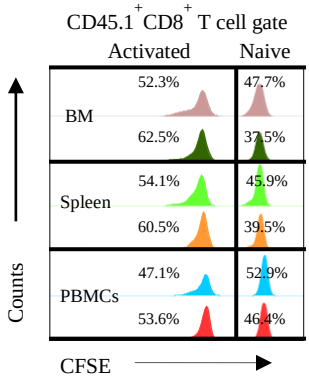
CD45.1+CD8+ T cell gate
Activated
Naive
BM
52.3%
47.7%
62.5%
37.5%
Spleen
54.1%
45.9%
60.5%
39.5%
PBMCs
47.1%
52.9%
53.6%
46.4%
Counts
CFSE

I

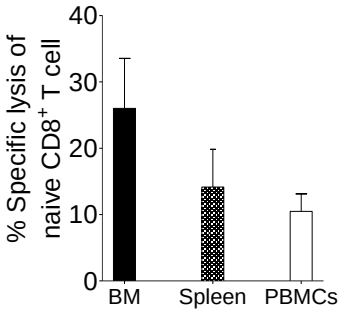
% Specific lysis of naive CD8+ T cell
40
30
20
10
0
BM
Spleen
PBMCs

Fig. 2.8 Glucocorticoid treatment compromises the host's ability to mount an efficient $CD8^+$ T cells response to a subsequent infection. A. Schematic of the experiments is shown. Congenic CD45.1 mice were injected $10x10^3$ OT-I cells one day prior to injecting complete Freund's adjuvant (CFA) to induce a non-specific inflammation in footpads. The animals were subsequently treated on day 4-6 either with dexamethasone or sham. One 30 days, mice were infected with MHV68-M2 SIINFEKL via intranasal route and simultaneously CFA was injected in the footpad to neutralize the influence of any inflammation induced cellular migration. The response of remaining OT-I cells was measured at 10 and 11 dpi in the peripheral circulation (at 10 dpi) and different lymphoid organs and tissue sites (at 11 dpi). B and C. The frequencies and numbers of SIINFEKL specific $CD45.2^+CD8^+$ T cells in blood circulation, Bronchoalveolar lavage, spleen and mediastinal LNs are shown by representative FACS plots and bar diagrams. D. The numbers of H-$2K^b$-SIINFEKL-Tet^+ cells /ml of blood are shown by bar diagrams. E. The numbers of H-$2K^b$-SIINFEKL-Tet^+ cells in spleen and mediastinal LNs are shown by bar diagrams. F-J. Single cell suspensions prepared from spleens and mediastinal LNs were subjected to ICCS assays to measure SIINFEKL-specific $CD8^+$ T cells that produced IFN-γ and TNF-α. The frequencies and numbers of IFN-γ^+CD8^+ T cells or TNF-α^+CD8^+ T cells in spleen and mediastinal LNs are shown by representative FACS plots (F) and bar diagrams (G-J). Bar diagrams shown the frequencies (G) and numbers (H) of IFN-γ^+CD8^+ T cells in spleen and MLN samples. Bar diagrams shown the frequencies (I) and numbers (J) of TNF-α^+CD8^+ T cells in spleen and MLN samples. Mean ± SD for each bars are depicted. In each experimental group 5 animals were included and the experiments were repeated two times.**$P < 0.005$, *$P < 0.05$ and ns ($P > 0.05$)- not significant (Mann-Whitney U test- two tailed).

A

CD45.1 mice

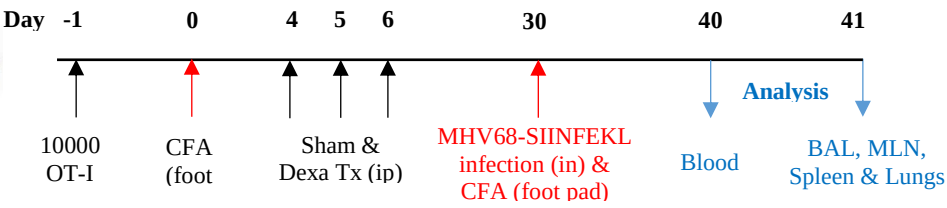

B

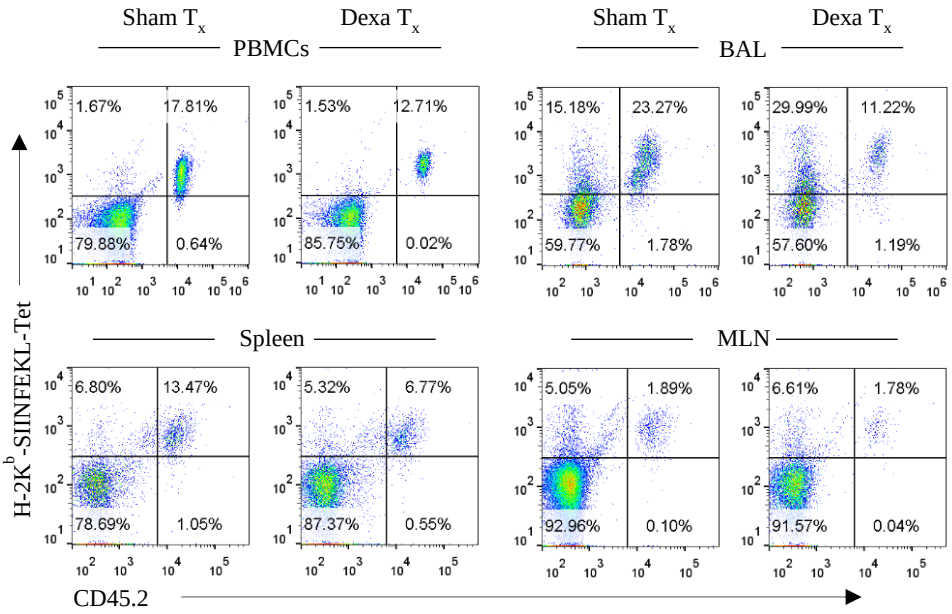

C

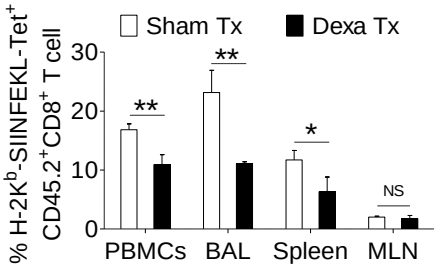

D

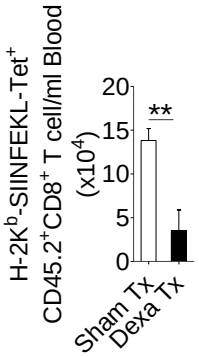

E

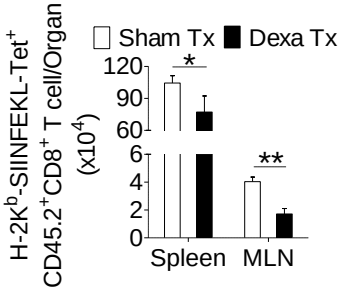

F

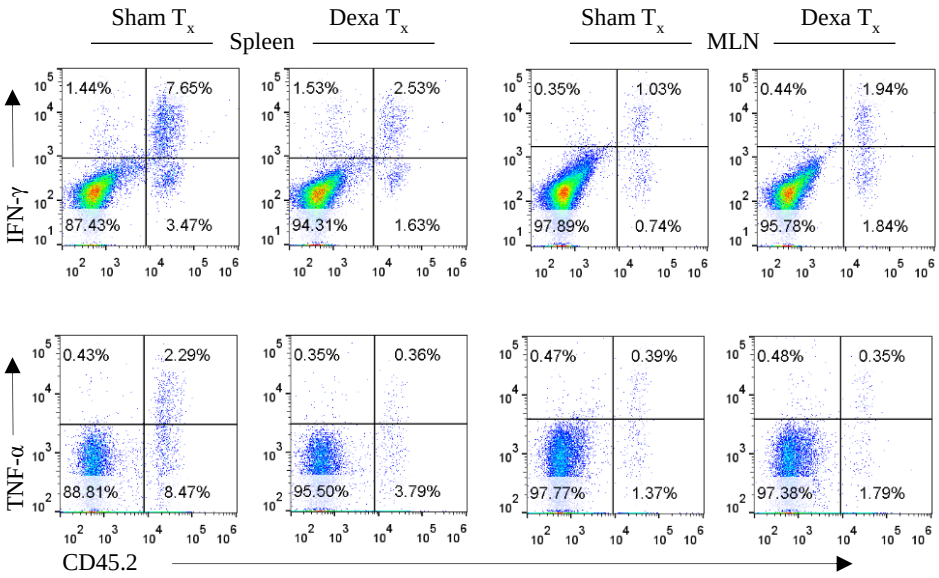
Sham T$_x$
Spleen
Dexa T$_x$
Sham T$_x$
MLN
Dexa T$_x$
IFN-γ
1.44%
7.65%
87.43%
3.47%
1.53%
2.53%
94.31%
1.63%
0.35%
1.03%
97.89%
0.74%
0.44%
1.94%
95.78%
1.84%
TNF-α
0.43%
2.29%
88.81%
8.47%
0.35%
0.36%
95.50%
3.79%
0.47%
0.39%
97.77%
1.37%
0.48%
0.35%
97.38%
1.79%
CD45.2

G

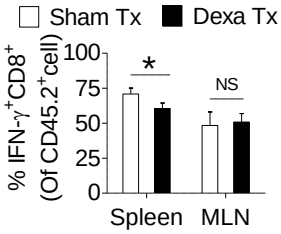
Sham Tx
Dexa Tx
% IFN-γ$^+$CD8$^+$ (Of CD45.2$^+$cell)
100
75
50
25
0
*
NS
Spleen
MLN

H

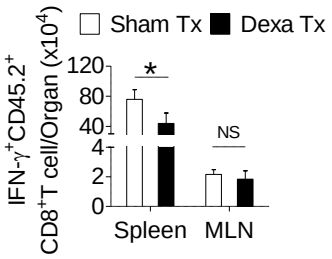
Sham Tx
Dexa Tx
IFN-γ$^+$CD45.2$^+$ CD8$^+$T cell/Organ (x10^4)
120
80
40
4
2
0
*
NS
Spleen
MLN

I

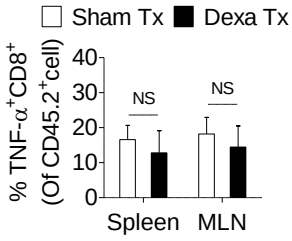
Sham Tx
Dexa Tx
% TNF-α$^+$CD8$^+$ (Of CD45.2$^+$cell)
40
30
20
10
0
NS
NS
Spleen
MLN

J

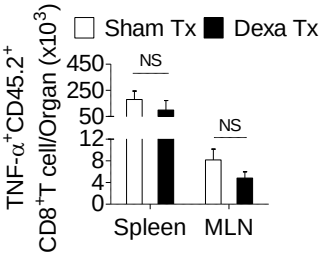
Sham Tx
Dexa Tx
TNF-α$^+$CD45.2$^+$ CD8$^+$T cell/Organ (x10^3)
450
250
50
12
8
4
0
NS
NS
Spleen
MLN

Fig. 2.9 Transcriptional profile of virus expanded CD8$^+$ T cells and susceptibility of memory CD8$^+$ T cells to dexamethasone. Different subsets of CD8$^+$ T cells were FACS sorted from C57BL/6 mice that were transferred with 1x10^5 of OT-I cells and infected with MHV68-M2-SIINFEKL. Indicated cell populations were FACS sorted. A. Sorted CD8$^+$ T cell subsets (naive - CD44^{lo}; K^b-SIINFEKL tet^{-ve}CD44^{hi} and K^b-SIINFEKL-tet$^+$CD44$^+$) from spleens of MHV68-M2-SIINFEKL infected mice. B. Quantitative RT-PCR data for glucocorticoid receptor (Nr3c1) expression in sorted CD8$^+$ T cell subsets as shown as fold change of naïve K^b-SIINFEKL tetramer^{+ve}. C. RPKM values of Nr3c1 in naïve and activated MHV68 specific TCR transnuclear (TN) CD8$^+$ T cells as measured by RNAseq are shown. D and E. HSV1 expanded endogenous CD8$^+$ T cells of indicated phenotype were FACS-sorted from the draining popliteal LNs at 7 dpi of HSV1 infected mice. D. A representative FACS plot show the sorted cell population. E. RT-PCR was performed for measuring mRNA of indicated gene expression in naive and virus specific (K^b-gB$_{498\text{-}505}$-tet^{+ve}) CD8$^+$ T cell subsets activated and expanded by HSV1 infection. Relative expression as fold change for different gene is shown. F. RT-PCR was performed for measuring the mRNA of nr3c1 gene expression in naïve, HSV1 specific (K^b- gB$_{498\text{-}505}$-tet^{+ve}) CD8$^+$ T cells in the acute (7 dpi) and memory stage (60 dpi) of the response in HSV1 infected mice. Relative fold change is shown by bar diagram. G-H. Single cells suspension prepared from the draining popliteal LN cells of HSV1 infected mice (30 dpi) were incubated with diluent and dexamethasone (1 µM) for eight hours. Some cells were pretreated with 5 µM mifepristone then dexamethasone was added and apoptosis was measured by annexin V staining after incubation period was over. G. Annexin V^{+ve} cells in boxed CD8$^+$ T cells populations (tetramer^{-ve} and tetramer^{+ve}) that were incubated with diluent, dexamethasone (1 µM) and dexamethasone (1 µM) + mifepristone (5 µM) are shown by representative FACS plots. H. Annexin V^{+ve} cells in different CD8$^+$ T cell subsets are shown by bar diagrams. Mean and ± SD are shown. ***P≤0.001, **P≤0.005, *P≤0.05 (Bonferroni test-Two-way ANOVA).

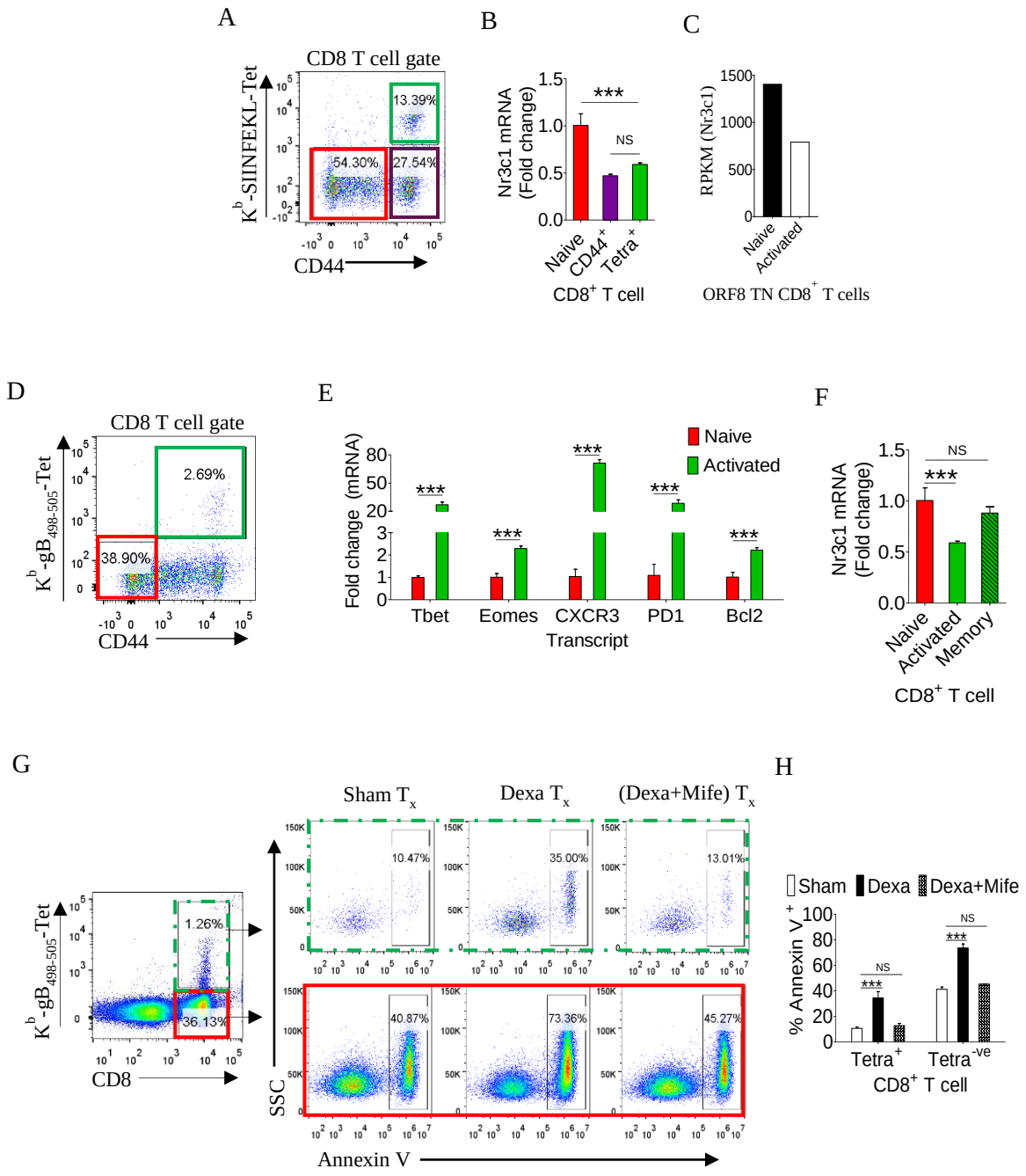
A
CD8 T cell gate
K^b-SIINFEKL-Tet
CD44
13.39%
54.30%
27.54%
B
Nr3c1 mRNA (Fold change)
***
NS
Naive
CD44+
Tetra+
CD8+ T cell
C
RPKM (Nr3c1)
Naive
Activated
ORF8 TN CD8+ T cells
D
CD8 T cell gate
K^b-gB498-505-Tet
CD44
2.69%
38.90%
E
Naive
Activated
Fold change (mRNA)
Tbet
Eomes
CXCR3
PD1
Bcl2
Transcript
F
Nr3c1 mRNA (Fold change)
NS
***
Naive
Activated
Memory
CD8+ T cell
G
Sham Tx
Dexa Tx
(Dexa+Mife) Tx
K^b-gB498-505-Tet
CD8
1.26%
36.13%
SSC
Annexin V
10.47%
35.00%
13.01%
40.87%
73.36%
45.27%
H
Sham
Dexa
Dexa+Mife
% Annexin V+
NS
***
Tetra+
Tetra-ve
CD8+ T cell

Fig. 2.10 mRNA expression on naive and activated CD8^{+} T cells.

A. FACS plots show sorted populations and the post sort purity in sorted cells for different subsets of cells used in Fig. 2.9(A,B). B. Post sort purity of naive and tetramer^{+ve} cells sorted from sham and dexa treated group mice is shown. Impact of dexamethasone treatment on mRNA level in naive and tetramer^{+ve} cells for Nr3c1 (D), Bcl2 (E) and Eomes (F) isolated from HSV1 infected mice. The qPCR was performed in triplicates. **P < 0.005; *P < 0.05 and NS (P > 0.05)- not significant (Unpaired Student's t-test two tailed).

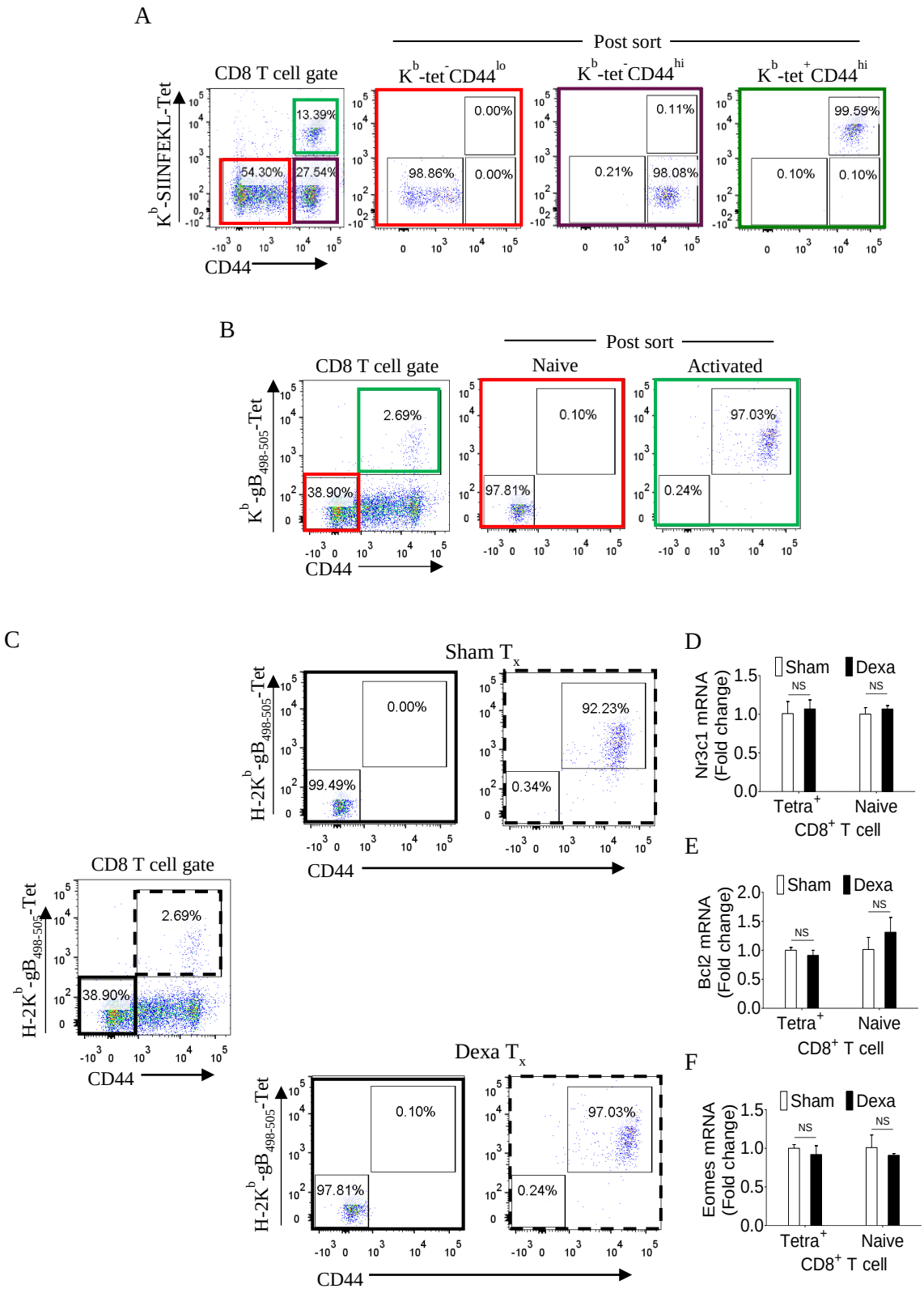
A
Post sort
CD8 T cell gate
K^b-tet^-CD44^lo
K^b-tet^-CD44^hi
K^b-tet^+CD44^hi
K^b-SIINFEKL-Tet
CD44
13.39%
54.30%
27.54%
0.00%
98.86%
0.00%
0.11%
0.21%
98.08%
99.59%
0.10%
0.10%
B
Post sort
CD8 T cell gate
Naive
Activated
K^b-gB498-505-Tet
CD44
2.69%
38.90%
0.10%
97.81%
97.03%
0.24%
C
Sham Tx
Dexa Tx
CD8 T cell gate
H-2K^b-gB498-505-Tet
CD44
0.00%
99.49%
92.23%
0.34%
2.69%
38.90%
0.10%
97.81%
97.03%
0.24%
D
Sham
Dexa
Nr3c1 mRNA (Fold change)
NS
Tetra+
Naive
CD8+ T cell
E
Bcl2 mRNA (Fold change)
F
Eomes mRNA (Fold change)

Fig. 2.11 Dexamethasone therapy causes bystander activation of CD8$^+$ T cells. A. A schematic of the experiments is shown. B-D. Naïve and activated HSV1 specific (K^b-SSIFERAL-tet^{+ve}) CD8$^+$ T cells were isolated from control and dexamethasone HSV1 infected animals (7 dpi). The expression levels PD1 (B), CXCR3 (C) and T-bet (D) were measured by quantitative RT-PCR. Bar diagrams show the relative fold change in the expression for different genes. Mean ± SD are shown. ***P < 0.001; **P<0.005; *P < 0.05 and NS (P > 0.05)- not significant (Unpaired t test). E. A schematic of the experiments to measure the influence of dexamethasone treatment on naïve identifiable C8$^+$ T cells (OT1 cells) is shown. Congenic CD45.1 mice were injected with 5x10^6 OT-I cells (CD45.2^{+ve}). Next day recipient animals were administered with dexamethasone (10 mg/kg B Wt) or the diluent and the following day CD8$^+$ T cell responses were analyzed for the expression of activation markers such as CD69, KLRG1, PD1 and CXCR3 in peripheral blood, LNs and spleens. F-G. The representation of donor cells is shown in the spleens of sham and dexamethasone treated animals. F. Representative overlaid histograms show for the frequencies of donor (OT-I) cells in two groups. G. The percentage of donor cells is shown in the spleen samples of sham and dexamethasone treated mice. H-O. Endogenous (CD45.2^{-ve}) and donor (CD45.2^{+ve}) cells were analyzed for the expression of different molecules. Representative FACS plots show the frequencies of endogenous (left panels) and donor (right panels) CD8$^+$ T cells that express CD69 (H), KLRG1 (J), PD1 (L) and CXCR3 (N) in sham and dexamethasone treated animals. Bar diagrams show the frequencies of CD69 (I), KLRG1 (K), PD1 (M) and CXCR3 (O) in both the endogenous and donor cells of sham and dexamethasone treated animals. Mean ± SD are shown. ***P < 0.001; **P<0.005; *P < 0.05 and NS (P > 0.05) not significant (n > 4 in each group, Unpaired t test).

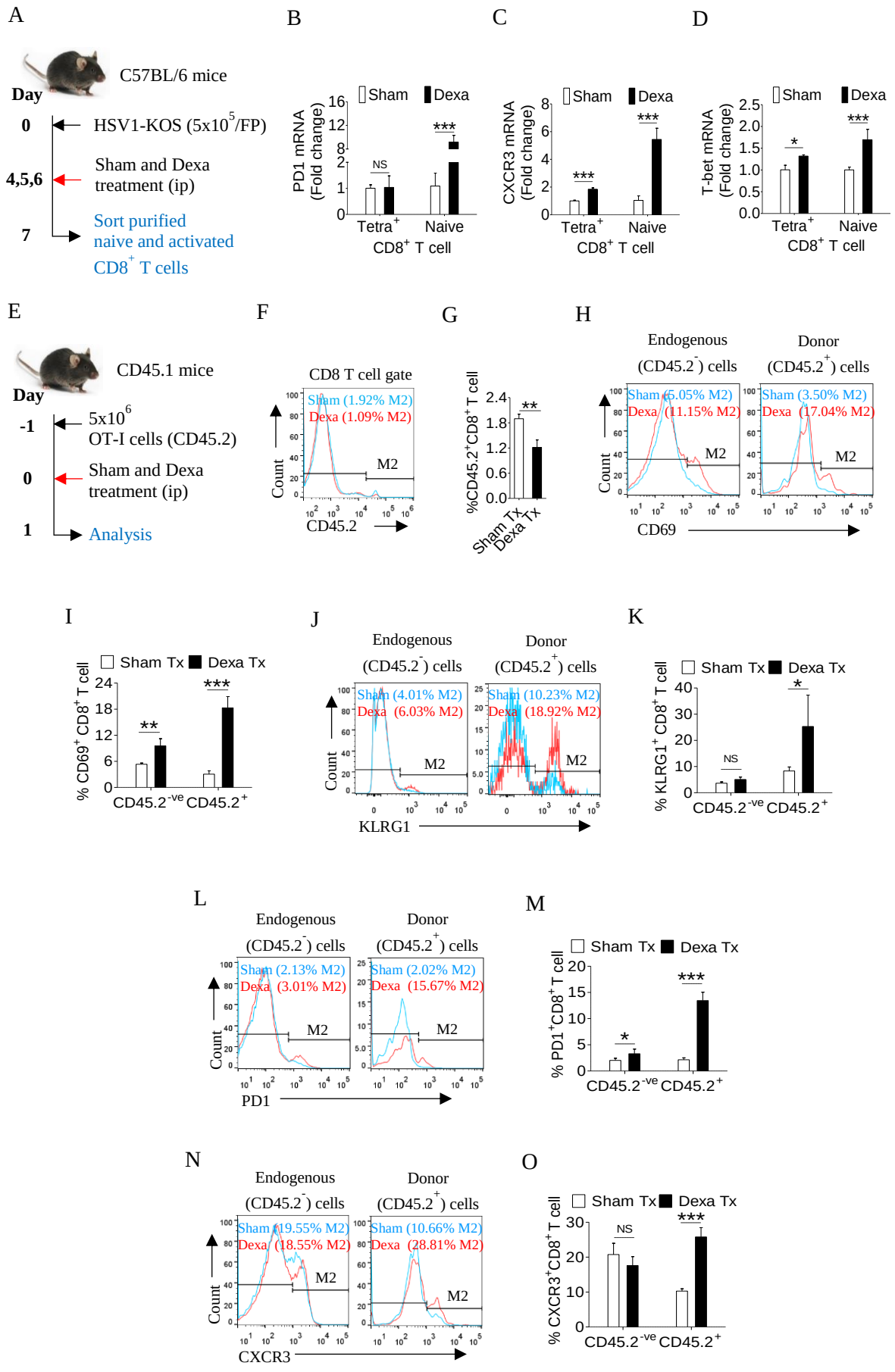
A
Day
C57BL/6 mice
0
HSV1-KOS (5x10^5/FP)
4,5,6
Sham and Dexa treatment (ip)
7
Sort purified naive and activated CD8+ T cells
B
PD1 mRNA (Fold change)
Sham
Dexa
NS
***
Tetra+
Naive
CD8+ T cell
C
CXCR3 mRNA (Fold change)
***
***
Tetra+
Naive
CD8+ T cell
D
T-bet mRNA (Fold change)
Sham
Dexa
*
***
Tetra+
Naive
CD8+ T cell
E
Day
CD45.1 mice
-1
5x10^6 OT-I cells (CD45.2)
0
Sham and Dexa treatment (ip)
1
Analysis
F
CD8 T cell gate
Sham (1.92% M2)
Dexa (1.09% M2)
M2
Count
CD45.2
G
%CD45.2+CD8+ T cell
**
Sham Tx
Dexa Tx
H
Endogenous (CD45.2-) cells
Donor (CD45.2+) cells
Sham (5.05% M2)
Dexa (11.15% M2)
Sham (3.50% M2)
Dexa (17.04% M2)
M2
M2
Count
CD69
I
Sham Tx
Dexa Tx
% CD69+ CD8+ T cell
**
***
CD45.2-ve
CD45.2+
J
Endogenous (CD45.2-) cells
Donor (CD45.2+) cells
Sham (4.01% M2)
Dexa (6.03% M2)
Sham (10.23% M2)
Dexa (18.92% M2)
M2
M2
Count
KLRG1
K
Sham Tx
Dexa Tx
% KLRG1+ CD8+ T cell
NS
*
CD45.2-ve
CD45.2+
L
Endogenous (CD45.2-) cells
Donor (CD45.2+) cells
Sham (2.13% M2)
Dexa (3.01% M2)
Sham (2.02% M2)
Dexa (15.67% M2)
M2
M2
Count
PD1
M
Sham Tx
Dexa Tx
% PD1+CD8+ T cell
*
***
CD45.2-ve
CD45.2+
N
Endogenous (CD45.2-) cells
Donor (CD45.2+) cells
Sham (19.55% M2)
Dexa (18.55% M2)
Sham (10.66% M2)
Dexa (28.81% M2)
M2
M2
Count
CXCR3
O
Sham Tx
Dexa Tx
% CXCR3+CD8+ T cell
NS
***
CD45.2-ve
CD45.2+

Fig 2.12 Treatment of HSV1 infected mice with dexamethasone does not alter $CD8^+$ T cell memory generation.

$CD8^+$ T cells frequencies (A, B) and count/PLN (C) HSV1-$gB_{498\text{-}505}{}^{+ve}$ $CD8^+$ T cells frequency (A,D) and count/PLN (E) at 4 dpi of recall infection are shown. The frequencies (F, G, I), and count/PLN (H, J) of cytokines producing $CD8^+$ T cell after pulsing with SSIEFARL peptide and 1x-brefeldin A for 4 hrs at 37^{o}C are shown. Each symbol shows an individual animal, where error bars indicate ± SD, NS ($P > 0.05$)- not significant (Mann-Whitney U test- two tailed). K and L. *In vivo* CTL assay, where CFSE labelled cells transferred in HSV1 infected animals to recall the response were determined in peripheral circulation for target (CFSE-high) and non-target (CFSE-low) cells in uninfected and HSV1 recall (4 dpi) infected (sham and dexa treated at 4-6 dpi of acute stage of infection) mice. The frequencies (K) of peptide (SSIEFARL) pulsed (High CFSE) target cells in uninfected (naive) and recall infected (sham and dexa treated) mice are shown. Percent specific lysis (L) of target cells in sham and dexa treated group animals are shown. Error bars indicate ± SD, NS ($P > 0.05$)- not significant (Unpaired Student's t-tests, n = 4 in each group).

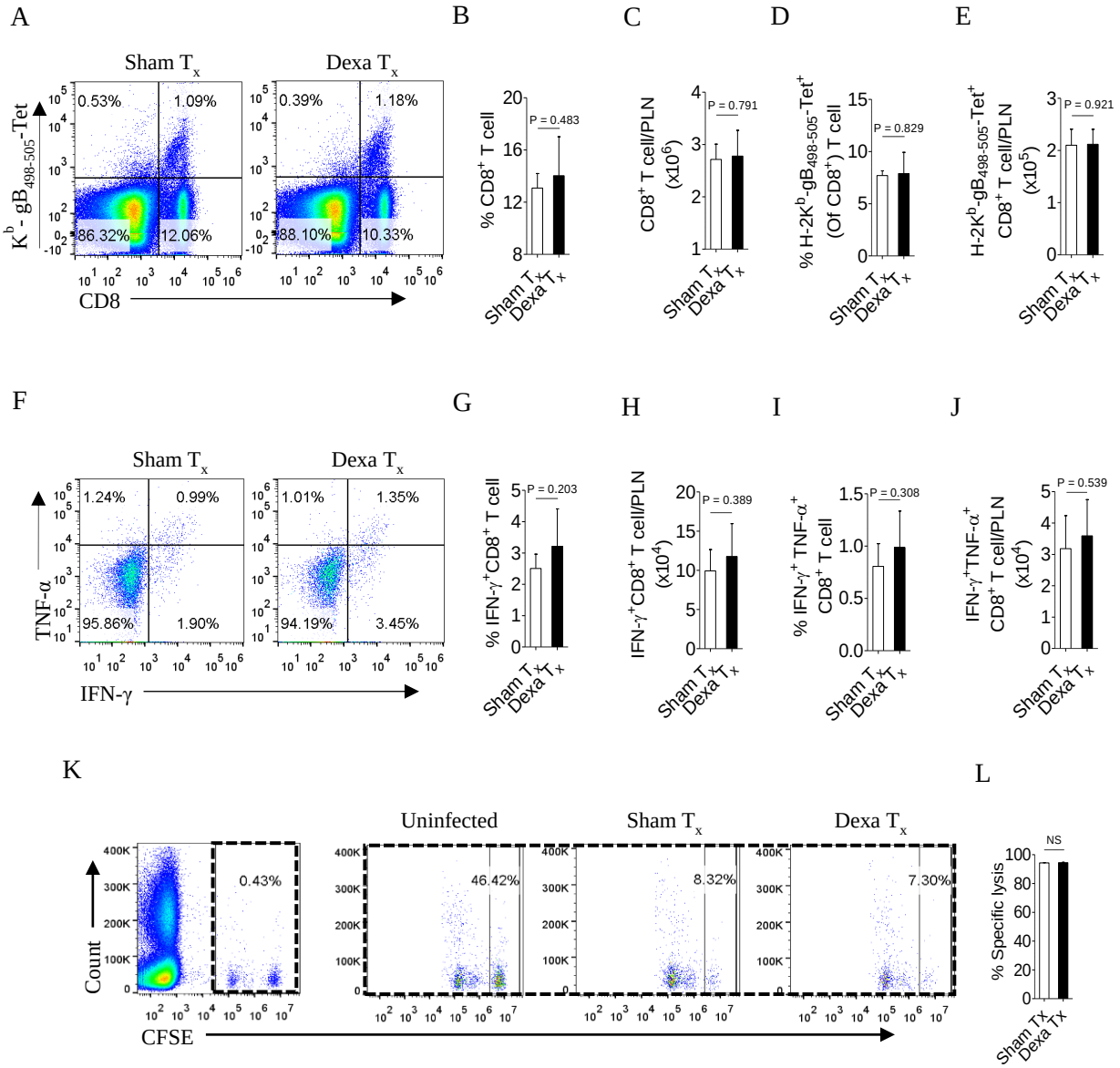
A
Sham Tx
Dexa Tx
0.53%
1.09%
86.32%
12.06%
0.39%
1.18%
88.10%
10.33%
Kb - gB498-505-Tet
CD8
B
% CD8+ T cell
P = 0.483
C
CD8+ T cell/PLN (x10^6)
P = 0.791
D
% H-2Kb-gB498-505-Tet+ (Of CD8+) T cell
P = 0.829
E
H-2Kb-gB498-505-Tet+ CD8+ T cell/PLN (x10^5)
P = 0.921
F
Sham Tx
Dexa Tx
1.24%
0.99%
95.86%
1.90%
1.01%
1.35%
94.19%
3.45%
TNF-α
IFN-γ
G
% IFN-γ+CD8+ T cell
P = 0.203
H
IFN-γ+CD8+ T cell/PLN (x10^4)
P = 0.389
I
% IFN-γ+ TNF-α+ CD8+ T cell
P = 0.308
J
IFN-γ+TNF-α+ CD8+ T cell/PLN (x10^4)
P = 0.539
K
Uninfected
Sham Tx
Dexa Tx
0.43%
46.42%
8.32%
7.30%
Count
CFSE
L
% Specific lysis
NS
Sham Tx
Dexa Tx

Fig 2.13 A transient dexamethasone therapy induces enhanced proliferation and memory precursor phenotype in CD8$^+$ T cells. A. Schematic of the experiments is shown. C57BL/6 mice were infected with HSV1-KOS ($5x10^5$ pfu/foot pad) and were then injected with the diluent or dexamethasone (10 mg/Kg Bwt) intraperitoneally from 4 to 6 dpi. Expression levels of Ki67, CD127 and KLRG1 in CD8$^+$ T cell subsets in the peripheral blood (7 dpi) and draining popliteal LNs (8 dpi) isolated from diluent and dexamethasone treated mice were measured by flow cytometry. Representative overlaid histograms (B and C) and bar diagrams (D) show Ki67 expression in K^b-$gB_{498-505}$-Tet^{+ve} and K^b-$gB_{498-505}$-Tet^{-ve}CD8$^+$ T cells obtained from PBMCs. Representative FACS plots (E) and bar diagrams (F) show CD127 and KLRG1 expression in K^b-$gB_{498-505}$-Tet^{+ve}CD8$^+$ T cells obtained from PBMCs. Representative overlaid histograms (G and H) and bar diagrams (I) show Ki67 expression in K^b-$gB_{498-505}$-Tet^{+ve} and K^b-$gB_{498-505}$-Tet^{-ve}CD8$^+$ T cells obtained from draining popliteal LNs. Representative FACS plots (J) and bar diagrams (K) show CD127 and KLRG1 expression in K^b-$gB_{498-505}$-Tet^{+ve}CD8$^+$ T cells obtained from draining popliteal LNs. Mean ± SD are represented. The experiments were repeated two times with similar results. In each experimental group 6 animals were included. ***P < 0.001; **P<0.005; *P < 0.05 and NS (P > 0.05)- not significant (Unpaired t test).

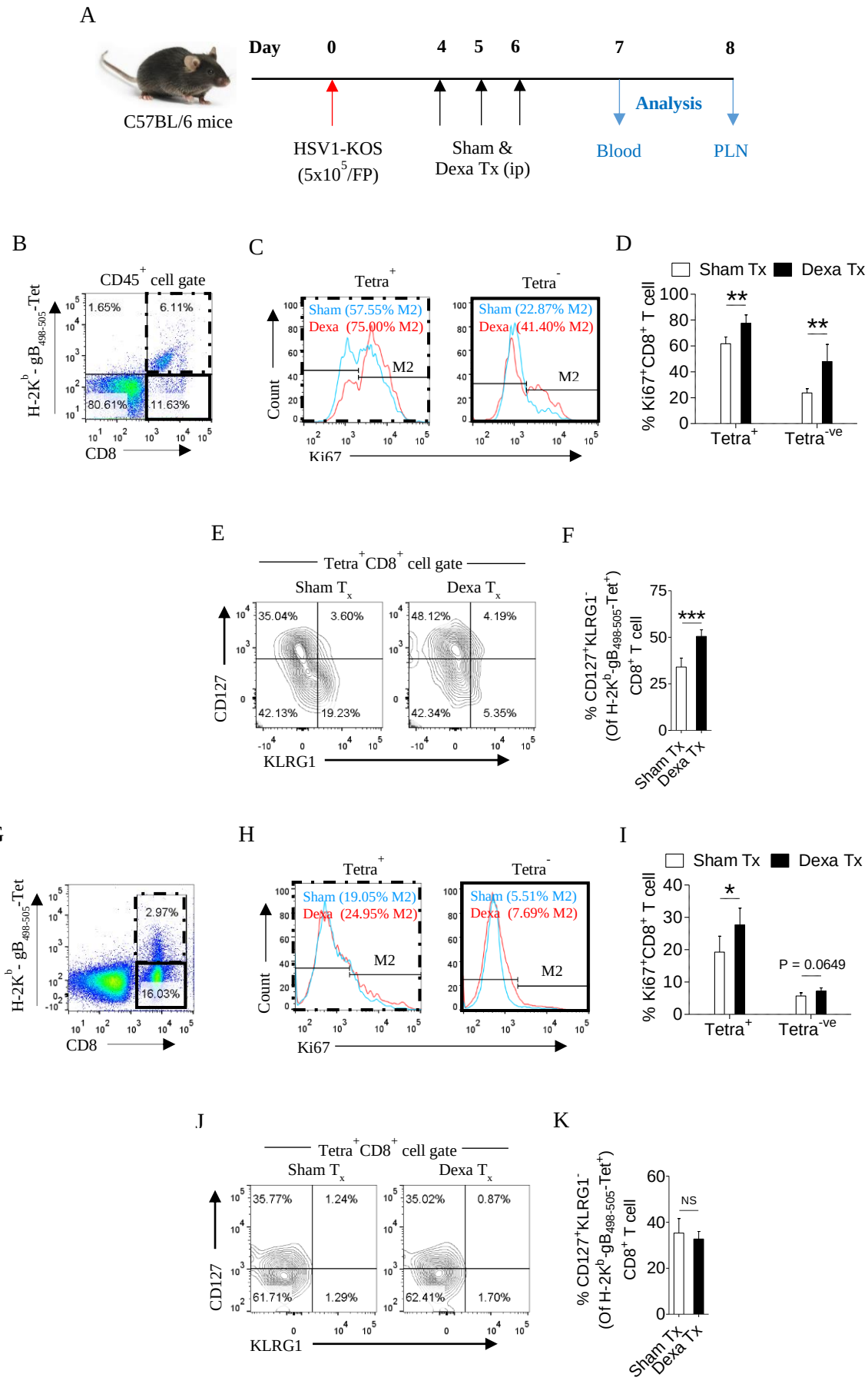
A
C57BL/6 mice
Day 0 4 5 6 7 8
Analysis
HSV1-KOS (5x10^5/FP)
Sham & Dexa Tx (ip)
Blood
PLN
B
CD45+ cell gate
H-2K^b - gB498-505-Tet
CD8
1.65%
6.11%
80.61%
11.63%
C
Tetra+
Tetra-
Sham (57.55% M2)
Dexa (75.00% M2)
Sham (22.87% M2)
Dexa (41.40% M2)
M2
Count
Ki67
D
Sham Tx
Dexa Tx
% Ki67+CD8+ T cell
Tetra+
Tetra-ve
E
Tetra+CD8+ cell gate
Sham Tx
Dexa Tx
35.04%
3.60%
42.13%
19.23%
48.12%
4.19%
42.34%
5.35%
CD127
KLRG1
F
% CD127+KLRG1- (Of H-2K^b-gB498-505-Tet+) CD8+ T cell
Sham Tx
Dexa Tx
G
2.97%
16.03%
H
Sham (19.05% M2)
Dexa (24.95% M2)
Sham (5.51% M2)
Dexa (7.69% M2)
I
P = 0.0649
J
35.77%
1.24%
61.71%
1.29%
35.02%
0.87%
62.41%
1.70%
K
NS

Fig 2.14 A demonstration that brief exposure of in vitro stimulated $CD8^+$ T cells enhances their proliferation potential. A. Schematic of the experiments is shown. OT-I cells were stimulated *in vitro* with anti-CD3 and CD28 antibodies for 16 hours. These cells were then exposed for one hour either to dexamethasone (1 µM) or to the diluent only. $2x10^6$ cells per mouse were adoptively transferred separately in gender-matched mice and The K^b-SIINFEKL-$Tet^{+ve}CD8^+$ T cells were measured for their frequencies and phenotype in the peripheral blood of recipient animals on 6 days post transfer. Representative FACS plots (B) and bar diagrams (C and D) show the frequencies and numbers of transferred cells 6 day later in the peripheral circulation. Overlaid histograms (E) and bar diagrams (F) show the frequencies of $Ki67^{+ve}$ K^b-SIINFEKL-$Tet^{+ve}CD8^+$ T cells in PBMCs. (G). Bar diagrams show the MFI values for Ki67 expression in control and dexamethasone treated transferred cells at 6 days post transfer in the circulation. (H) Activation profile of OT-I cells post stimulation (CD3 and CD28 as discussed in experiment schematics). The experiments were repeated two times with similar results. In each experimental group 6 animals were included. ***$P < 0.001$; **$P<0.005$; *$P < 0.05$ and NS ($P > 0.05$) - not significant (Unpaired Student t test).

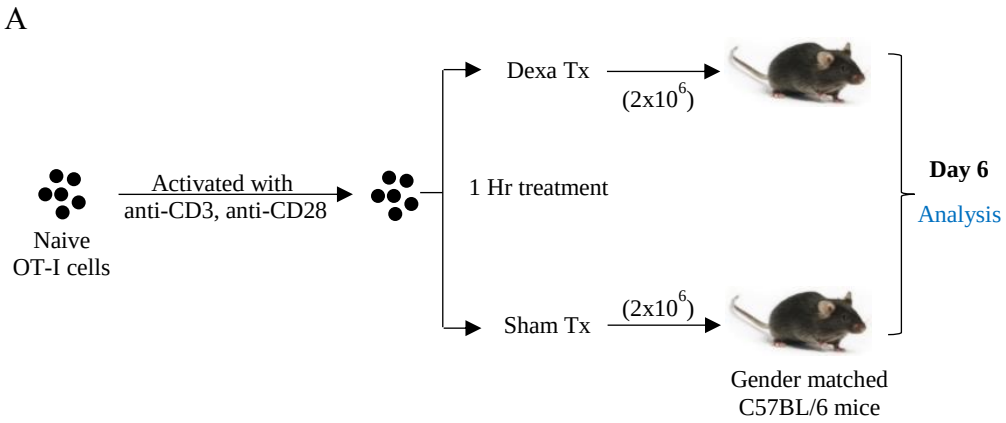
A
Dexa Tx
(2x10^6)
Activated with
anti-CD3, anti-CD28
Naive
OT-I cells
1 Hr treatment
Day 6
Analysis
Sham Tx
(2x10^6)
Gender matched
C57BL/6 mice

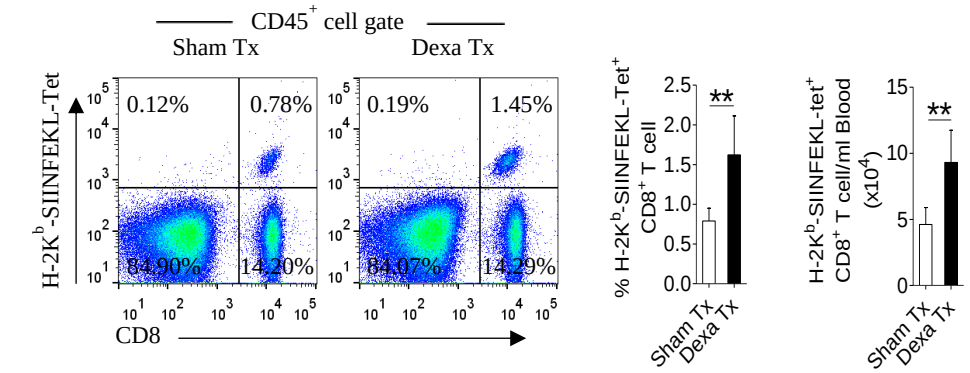
B
CD45+ cell gate
Sham Tx
Dexa Tx
H-2K^b -SIINFEKL-Tet
0.12%
0.78%
0.19%
1.45%
84.90%
14.20%
84.07%
14.29%
CD8
C
% H-2K^b-SIINFEKL-Tet+ CD8+ T cell
**
Sham Tx
Dexa Tx
D
H-2K^b-SIINFEKL-tet+ CD8+ T cell/ml Blood (x10^4)
**
Sham Tx
Dexa Tx

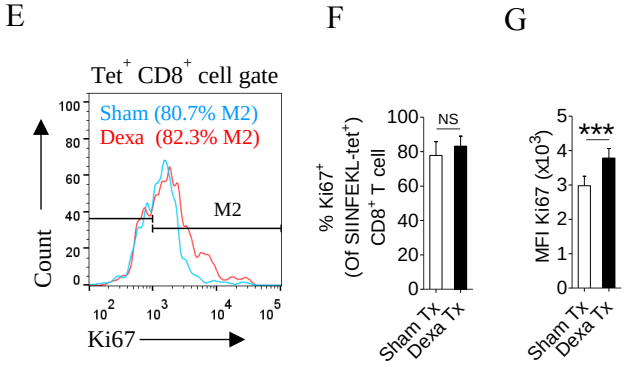
E
Tet+ CD8+ cell gate
Sham (80.7% M2)
Dexa (82.3% M2)
M2
Count
Ki67
F
% Ki67+ (Of SIINFEKL-tet+ CD8+ T cell
NS
Sham Tx
Dexa Tx
G
MFI Ki67 (x10^3)
***
Sham Tx
Dexa Tx

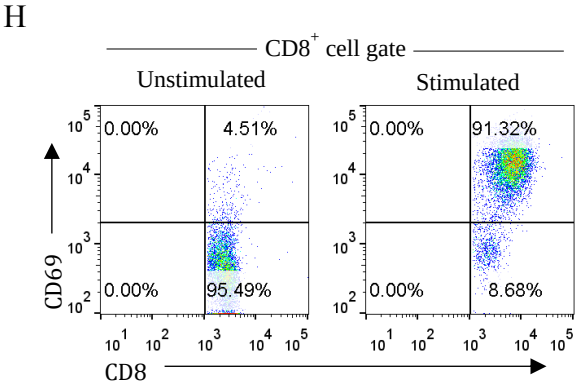
H
CD8+ cell gate
Unstimulated
Stimulated
0.00%
4.51%
0.00%
95.49%
0.00%
91.32%
0.00%
8.68%
CD69
CD8

Fig 2.15 A brief exposure of activated CD8$^+$ T cells with dexamethasone enhance their survival and conversion into protective effector memory cells. A. Schematic of the experiments is shown. OT-I cells were stimulated *in vitro* with anti-CD3 and CD28 antibodies for 16 hours (cells activation profile shown in Fig 2.14H). These cells were then exposed for one hour either to dexamethasone (1 μM) or to the diluent only. 2x10^6 cells per mouse were adoptively transferred separately in gender-matched mice and their fates were tracked in the recipient animals subsequently. Representative FACS plots (B) and bar diagrams (C and D) show the status of transferred cells one day later in the peripheral circulation. One-month post transfer all the animals were infected intranasally with MHV68-SIINFEKL virus to recall surviving cells and the phenotypic analysis for the recalled cells (E-I) and lung tissues for viral load measurement (J) as well as the histology of lung tissues (K) were performed. Representative FACS plots from two groups of mice show the frequencies of expanded K^b-SIINFEKL-Tet^{+ve} cells obtained from bronchoalveolar lavage samples (E), draining mediastinal LNs (F), spleens (G) and cervical LNs (L). The cumulative data is shown for the frequencies (H and M) and total numbers (I and N) of expanded K^b-SIINFEKL-Tet^{+ve} cells for two groups of animals. J. Lung tissues were quantified for the viral loads from two groups and pfu/g of lung tissues are shown by bar diagrams. K. Representative sections of lung tissues stained by H&E are shown as histological micrographs from different groups of animals. The cytokines (IFN-γ and TNF-α) production by CD8$^+$ T cells in draining mediastinal LNs and Spleen samples (O-R). Representative FACS plots from two groups of mice show the frequencies of IFN-γ and TNF-α producing CD8$^+$ T cells after pulsing with SIINFEKL peptide for 4 hrs in draining mediastinal LNs (O) and spleens (P). The cumulative data is shown for the frequencies (Q) and total numbers (R) of cytokines producing CD8$^+$ T cells for two groups of animals. The experiments were repeated two times with similar results. In each experimental group 6 animals were included. ***P < 0.001; **P<0.005; *P < 0.05 and NS (P > 0.05)- not significant (Unpaired t test).

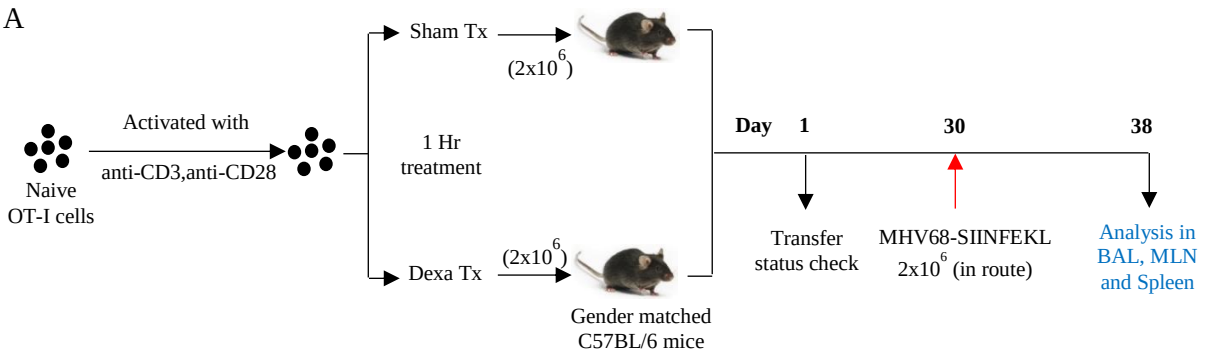
A
Naive
OT-I cells
Activated with
anti-CD3,anti-CD28
1 Hr
treatment
Sham Tx
(2x10^6)
Dexa Tx
(2x10^6)
Gender matched
C57BL/6 mice
Day 1
30
38
Transfer
status check
MHV68-SIINFEKL
2x10^6 (in route)
Analysis in
BAL, MLN
and Spleen

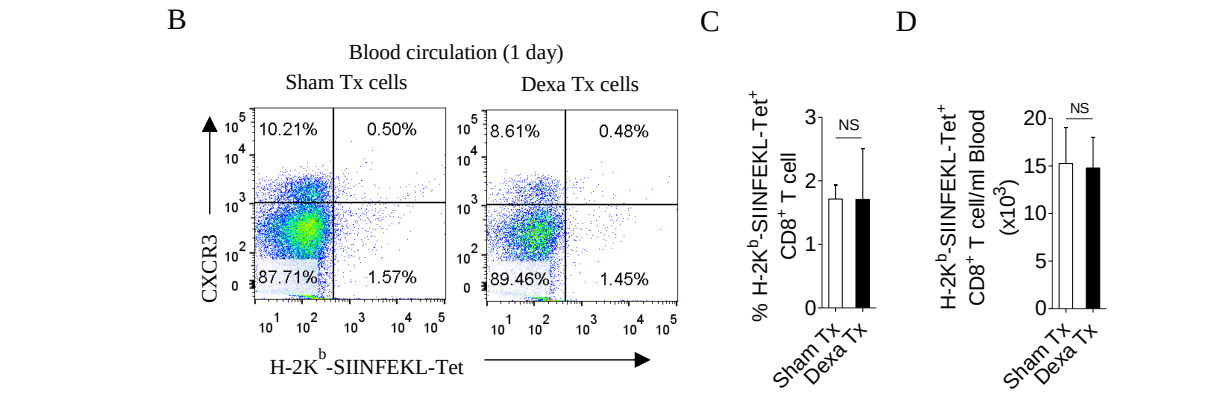
B
Blood circulation (1 day)
Sham Tx cells
Dexa Tx cells
10.21%
0.50%
87.71%
1.57%
8.61%
0.48%
89.46%
1.45%
CXCR3
H-2K^b-SIINFEKL-Tet
C
% H-2K^b-SIINFEKL-Tet^+ CD8^+ T cell
NS
Sham Tx
Dexa Tx
D
H-2K^b-SIINFEKL-Tet^+ CD8^+ T cell/ml Blood (x10^3)
NS
Sham Tx
Dexa Tx

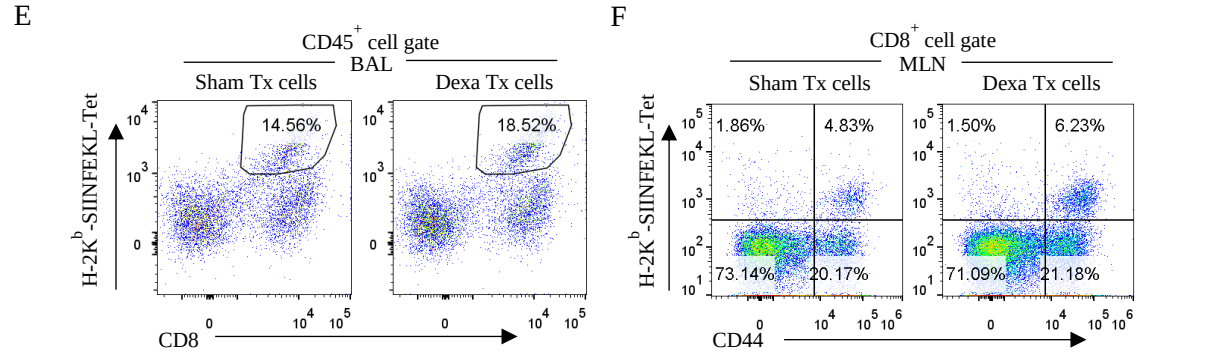
E
CD45^+ cell gate
BAL
Sham Tx cells
Dexa Tx cells
14.56%
18.52%
H-2K^b-SIINFEKL-Tet
CD8
F
CD8^+ cell gate
MLN
Sham Tx cells
Dexa Tx cells
1.86%
4.83%
73.14%
20.17%
1.50%
6.23%
71.09%
21.18%
H-2K^b-SIINFEKL-Tet
CD44

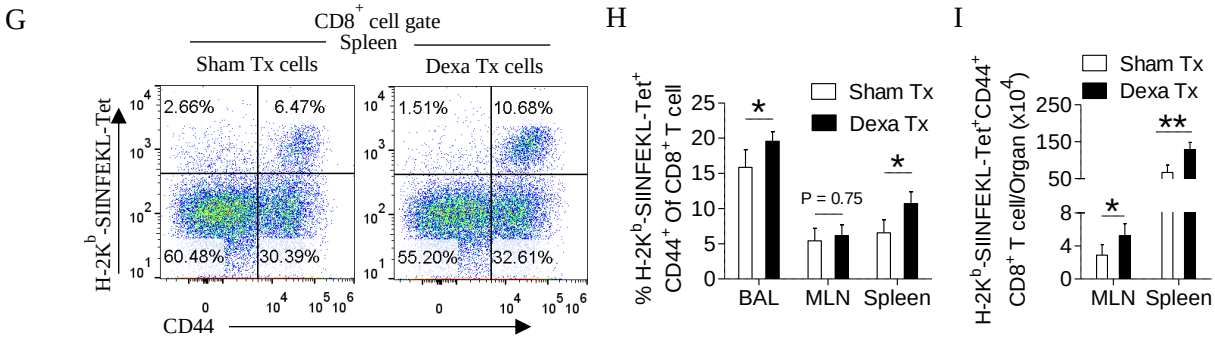
G
CD8^+ cell gate
Spleen
Sham Tx cells
Dexa Tx cells
2.66%
6.47%
60.48%
30.39%
1.51%
10.68%
55.20%
32.61%
H-2K^b-SIINFEKL-Tet
CD44
H
% H-2K^b-SIINFEKL-Tet^+ CD44^+ Of CD8^+ T cell
Sham Tx
Dexa Tx
*
P = 0.75
*
BAL
MLN
Spleen
I
H-2K^b-SIINFEKL-Tet^+CD44^+ CD8^+ T cell/Organ (x10^4)
Sham Tx
Dexa Tx
*
**
MLN
Spleen

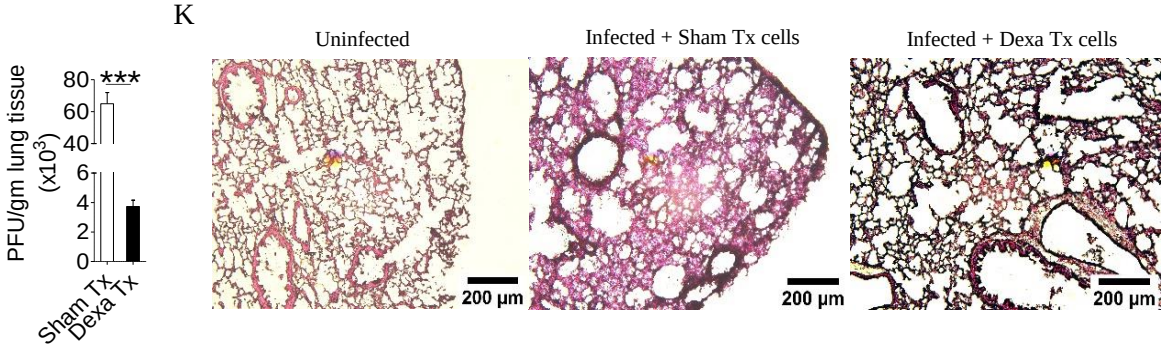
J
PFU/gm lung tissue (x10^3)
***
Sham Tx
Dexa Tx
K
Uninfected
Infected + Sham Tx cells
Infected + Dexa Tx cells
200 µm
200 µm
200 µm

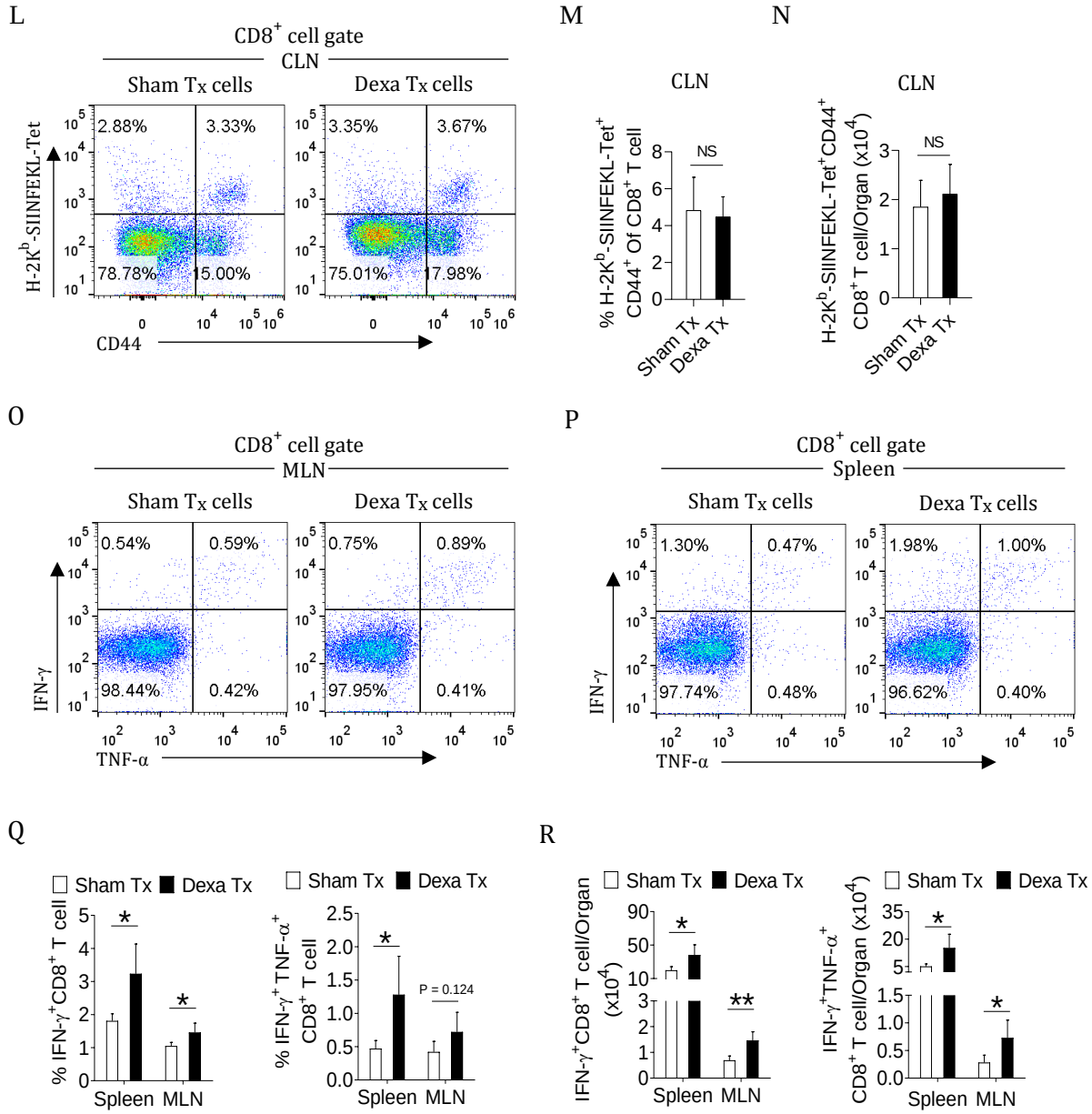
L
CD8+ cell gate
CLN
Sham Tx cells
Dexa Tx cells
H-2Kb-SIINFEKL-Tet
2.88%
3.33%
78.78%
15.00%
3.35%
3.67%
75.01%
17.98%
CD44
M
CLN
% H-2Kb-SIINFEKL-Tet+ CD44+ Of CD8+ T cell
NS
Sham Tx
Dexa Tx
N
CLN
H-2Kb-SIINFEKL-Tet+CD44+ CD8+ T cell/Organ (x10^4)
NS
Sham Tx
Dexa Tx
O
CD8+ cell gate
MLN
Sham Tx cells
Dexa Tx cells
IFN-γ
0.54%
0.59%
98.44%
0.42%
0.75%
0.89%
97.95%
0.41%
TNF-α
P
CD8+ cell gate
Spleen
Sham Tx cells
Dexa Tx cells
IFN-γ
1.30%
0.47%
97.74%
0.48%
1.98%
1.00%
96.62%
0.40%
TNF-α
Q
Sham Tx
Dexa Tx
% IFN-γ+CD8+ T cell
Spleen
MLN
Sham Tx
Dexa Tx
% IFN-γ+TNF-α+ CD8+ T cell
P = 0.124
Spleen
MLN
R
Sham Tx
Dexa Tx
IFN-γ+CD8+ T cell/Organ (x10^4)
Spleen
MLN
Sham Tx
Dexa Tx
IFN-γ+TNF-α+ CD8+ T cell/Organ (x10^4)
Spleen
MLN

Fig 2.16 A proposed model to elucidate the role of glucocorticoids during differentiation of CD8$^+$ T cells. Naïve CD8$^+$ T cells upon their activation downregulate the Nr3c1 receptor. However as the effector cells further differentiate to become memory cells, Nr3c1 receptor is up regulated. Naïve and memory cells owing to their enhanced expression for glucocorticoids undergo dexamethasone induced apoptosis while the effector cells only have limited pool of Nr3c1 available for ligating to dexamethasone. The receptor ligation induces translocation of complexed Nr3c1 to nucleus where the relative abundance of such complexes dictates the cell function and fate by transcriptional regulation.

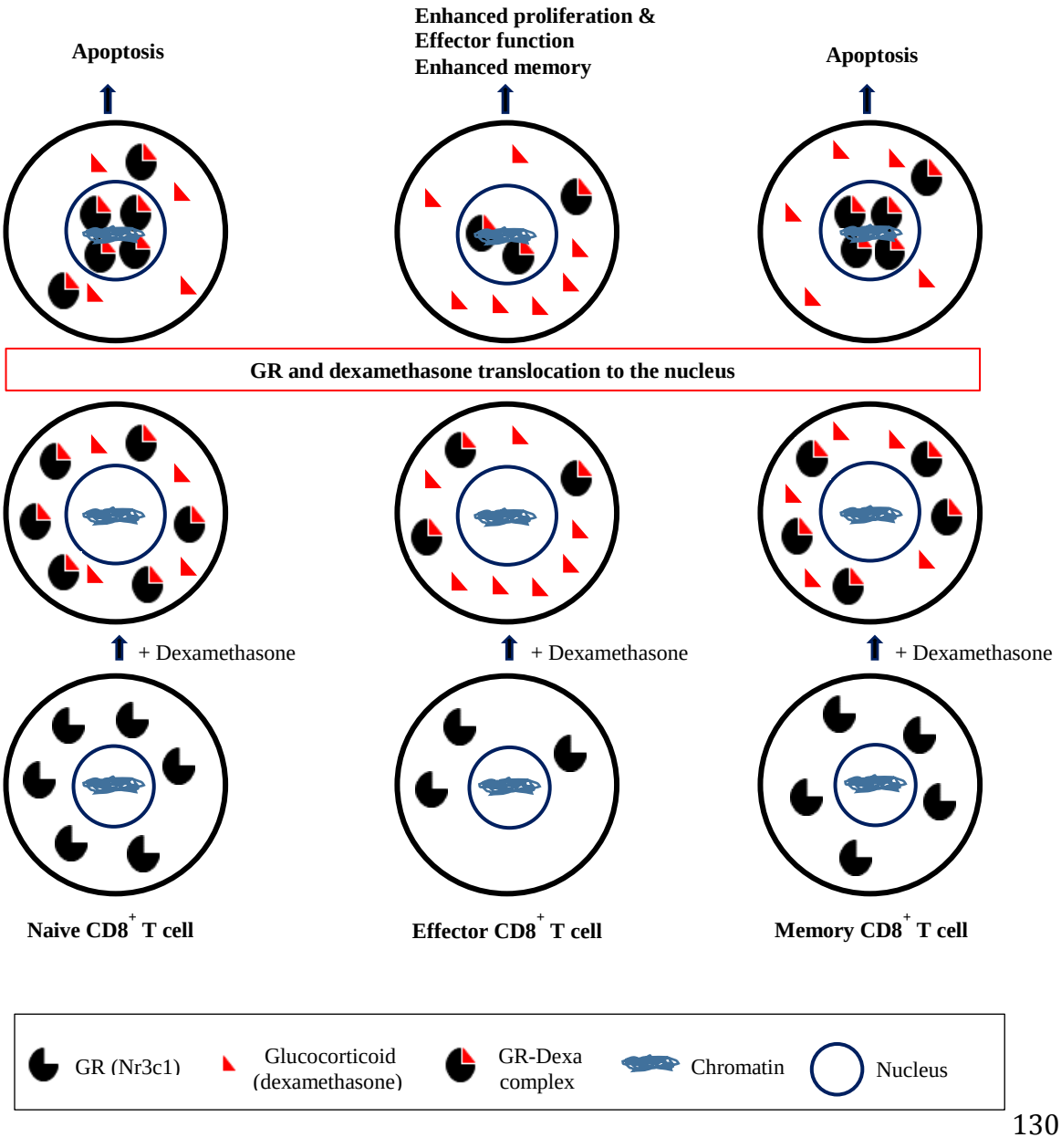

PART III

Identifying and characterizing virus-specific $CD8^+$ T cells in herpes simplex virus 1 infected zebrafish

The research work described in this part is a slight modification of a paper in preparation for publication. Identifying and characterizing virus-specific $CD8^+$ T cells in herpes simplex virus 1 infected zebrafish.

In this chapter the words "our" and "we" allude to me and co-authors. My contribution in the project includes (1) Selection of the topic (2) Designing and performing the experiments (3) Preparation of figures and graphs (4) Results interpretation (5) Compiling and elucidation of the literature (6) Writing and editing of the manuscript (7) Bestowing comprehensive structure to the paper

Abstract

We sought to identify and characterize the HSV1 specific $CD8^+$ T cells in experimentally infected zebrafish, a model system that offers a real time tracking of cellular dynamics *in vivo*. We generated class I MHC tetramer (Uda-tet) for zebrafish and used this technology to measure the kinetics of viral epitope specific $CD8^+$ T cells during HSV1 infection. We demonstrate that infected animals rapidly expanded virus-specific $CD8^+$ T cells in the spleens and such cells were abundantly recovered from non-lymphoid organs such as liver. Lymphocytes isolated from spleen and liver of infected animals in the acute and memory phase of the infection expanded enormously in response to the virus re-stimulation. The memory cells generated during primary infection could be efficiently recalled. The expanded cells upregulated effector molecules such as IFN-γ and TNF-α and effectively controlled viral growth. Therefore, zebrafish could serve as a model organism to decipher antigen-specific $CD8^+$ T cell differentiation and cellular dynamics in live animals. Furthermore, the dynamics of virus-specific $CD8^+$ T cells in zebrafish suggests for an evolutionary conserved yet functional adaptive immune cell homeostatic mechanisms in response to viral infection across vertebrates.

Introduction

Zebrafish (*Danio rerio*) has been extensively used as a model system to study development, regeneration, haematopoiesis and to elucidate immunological phenomena in small vertebrates[1–5]. Kidney marrow is the major site of haematopoiesis in zebrafish and most lineages of hematopoietic cells such as erythroid, myeloid and lymphoid cells have been demonstrated using genetically tractable fluorescent markers[6–9]. T cells develop in kidney marrow while B cells were shown to develop in pancreas of developing zebrafish[10–13]. Not only the cellular components of immune system but the complement system components, other inflammatory proteins, antibodies and different types of MHC molecules have been described in zebrafish[3,4,14,15]. Despite the availability of some data to demonstrate the presence of immune cells by transgenesis approaches, the immunophenotyping, functionality and differentiation of helper and cytotoxic T cells have not been elucidated in zebrafish. Furthermore, the data on T cell activation, differentiation and migration during infectious diseases particularly those caused by viral infections are altogether lacking.

Visual transparency of developing zebrafish provides unmatched advantages for cellular tracking in real-time, efficient visualization of cellular interactions and migratory potential of cells from the immune inductive sites to infection sites. Thus, up to one month post fertilization (pf), larvae of zebrafish survive with only the innate immune responses and adaptive immune system matures both morphologically and functionally after 4-6 weeks pf[3,15]. This temporal distinction in innate and adaptive immune parameters can also help decipher the relative contribution of two branches of immunity during the pathogenesis of infectious diseases. The other attributes which make adult zebrafish a better biological model system include its smaller size, relatively short life cycle, ease of handling, the requirement of smaller doses of inoculum as well as the

availability and employability of a growing list of molecular tools used for genome editing. Zebrafish has been used as a valuable model for elucidating events involved in innate immune responses and inflammation[16]. Recent scattered studies demonstrated the presence of dendritic cells (DCs) as the antigen presenting cells (APCs), γδ T cells and Treg-like cells in zebrafish[17-19].

The unavailability of reagents to detect antigen-specific $CD8^+$ and $CD4^+$ T cells in zebrafish however still remain a major hurdle in utilizing its optimal potential as a model system to study the differentiation and function of T cells during inflammatory and infectious diseases. Therefore, we focused our investigation to elucidate antigen-specific $CD8^+$ T cell responses during a herpesvirus infection. Understanding events involved in the activation and differentiation of cytotoxic $CD8^+$ T cells leading to the control of pathogens and capturing such events in live animals is a topical issue for investigation. We generated class I MHC tetramers as fluorescent probes for zebrafish to detect and characterize antigen-specific $CD8^+$ T cell responses against viral infection. Using these tetramers we then measured the kinetics of HSV1 specific $CD8^+$ T cells in experimentally infected zebrafishes. We further determined the differentiation of such cells into memory cells and established their effector functions during HSV1 infection. These studies pave the way for extensive utility of zebrafish as a model system for elucidating differentiation and dynamics of antigen-specific $CD8^+$ T cells responses during different diseases.

Materials and methods

Zebrafish husbandry and their infection with HSV1

Zebrafish were obtained from local vendors and were bred at 25 ± 2 ^{o}C in house in clean rooms for multiple generations and were then used for experiments. HSV1 was cultivated and titrated using Vero cells as described earlier[20]. Zebrafish was infected intraperitoneally (IP) by injecting 2x10^{6} pfu of HSV1 in 10 µl volumes. At different days post infection (dpi), spleens and liver samples were isolated and single cell suspensions were prepared for further analysis.

In vitro proliferation assays

Single cells suspensions were prepared from isolated spleen and liver samples of HSV1 infected zebrafishes. The single cell suspensions thus obtained were labelled with 1 µM CFSE as described earlier. The labelled cells were then stimulated in U bottomed well of tissue culture plates for different durations in the presence or the absence of UV inactivated HSV1. The gated lymphocytes were then analyzed by flow cytometry.

Sequence analysis of class I MHC molecules and their comparison with mouse H-2K^{b}

The amino acid sequence of mouse MHC class I HC, H-2K^{b} was aligned with U and Z lineages (classical MHC I molecules) of MHC class I HC of zebrafish. The sequence used for the alignment were as follows: H-2K^{b} **(**U_47328.1), Ula (NP_001304679.1), Uma (XP_005161940.1), Uaa (CAA86731.1), Uba (AAH74095.1), Uda (AAI28863.1, Uka (AGL92230.1), Uia (AGL92229.1), Uea (NP_571780.1), Ufa (CAD58763.1), Uga (NP_956879.1; formerly known as Uxa 2), Uca (XP_005159526.1), Uha (NP_001070109.1), Uja (NP_956700.1); Zaa (NM_194425.1), Zba (NM_001110118.1), Zca (NM_001083545.1), Zda (NM_001287097.1), Zea (NM_001089550.2), Zfa (XM_003197994.1), Zga (AJ420975.1), Zha (XM_001919256.3), Zia (AJ420977.1), Zja

(NM_001109718.1), Zka (AJ420976.1) and Zla (AJ420954.1). The accession number used for Z lineage of heavy chains were described earlier[21]. The α1 and α2 sequences of all the HCs were aligned with mouse H-2K^b α1 and α2 regions by Clustal Omega program and the phylogenetic tree was constructed from FigTree v1.4.4 software. The top five genes showing closer similarity with H-2K^b HC were further aligned with H-2K^b HC (using T-Coffee and BoxShade) to identify the HSV1-gB-SSIEFARL peptide interacting amino acid residues. The tertiary structure of Uda heavy chain was predicted using I-TASSER and the best model of tertiary structure that had a confidence score of 1.07, expected TM-score of 0.86 ± 0.7, expected RMSD of 3.9 ± 2.6 was selected. For determining the SSIEFARL binding pocket present on Uda HC, the tertiary structure obtained from I-TASSER was overlaid on crystal structure of H-2K^b-SSIEFARL (PDB id – 1T0M) molecule, using VMD software.

Cloning, expression and purification of zebrafish class I MHC molecule

Total RNA from zebrafish liver was isolated using trizol method and cDNA was synthesized using oligo d(T) and random hexamer primers. The Uda genes (heavy chain (HC) of class I MHC molecule) and β_2 microglobulin (β_2m) were PCR amplified. The sequences for the forward and reverse primers used were as follows: Uda HC, FP; 5'GGAATTCCATATGGGTACACACTCTCTGAGATACTTCTACACTGCTG3' and RP;5'ATGGGATCCTA**ATCGCGCAGCTCCATCTTCATAGCCTCGAAGATACC ACCCAG**GGGAACAGAAACTTCGTTTGTCC3'. The primers used for amplifying β_2m,FP; 5'GGAATTCCATATGAAAGTCTCCACTCCGAAAGTTCATGTGTACAG3' and RP; 5'ACGCGGATCCTTACATGTTGGGCTCCCA3'. The nucleotide sequence for biotin acceptor peptide was incorporated (bold) at the C' terminal end of Uda HC. The PCR product for both the heavy chain and β_2m were truncated to remove signal sequences. The cytoplasmic and transmembrane domains for Uda HC were also removed

for generating the monomer. In addition to cloning and expressing truncated product, full length sequence for the Uda HC was also amplified and cloned separately. The PCR products were cloned into pET22b vector. The plasmid encoding for Uda HC and β_2m were then transformed into BL21 strain of *E. coli*. Both the Uda HC and β_2m proteins were expressed in *E. coli* and purified from the inclusion bodies.

Generation of class I MHC tetramers

The class I MHC monomers were generated using rapid dilution method as per the protocol described elsewhere[22–25]. Briefly, the Uda HC and β_2m were rapidly diluted with separate peptides that include SSIFERAL of HSV1 gB protein, a conditional ligand, FAPG(Anp)YPAL the peptide is a derivative of sendi virus gp having a UV photocleavable artificial amino acid, amononitrophenyl and SIINFEKL. The composition of refolding solution was 100mM Tris, 400mM L-Arginine-HCl, 2mM EDTA, 0.5mM oxidized glutathione, 5mM reduced glutathione and 1mM phenylmethylsulphonyl fluoride (PMSF). The sequence in which different components were injected in the refolding buffer includes PMSF, respective peptides, β_2m and Uda HC. The same sequence was followed three times after an interval of 12 hours each time. After 48 hrs of refolding reaction, the whole content was filtered and concentrated using 10 kDa cutoff centriprep filters in the final volume of up to 1 ml. The concentrated solution was then subjected to size exclusion chromatography using S200 sephadex columns and fractions of 0.5 ml (of different peaks) were collected using AKTA pure™ apparatus. The desired fractions of class I MHC monomers were collected, concentrated and biotinylated at room temperature for overnight. After biotinylation, the monomers were again subjected to size exclusion chromatography. The purified biotinylated class I MHC monomers were collected, concentrated and stored at -80 °C until use. The biotinylation was confirmed by western blotting using streptavidin HRP conjugate. For the generation of class I MHC

tetramer 1nM of PE conjugated streptavidin was incubated with 4nM of class I MHC monomers at 4°C in dark in ten different aliquots separated by 30 minutes each.

Analysis of single cell suspension using flow cytometry

Spleens and liver were collected from the control and HSV1 infected zebrafishes. The single cell suspensions from these organs were prepared in FACS buffer containing 2% FBS. The cells were prepared and surface stained cells were analyzed using flow cytometry.

Detection and characterization of antigen-specific T cell using flow cytometry

Isolated spleens from HSV1 infected zebrafishes at different time intervals were processed to prepare single cell suspension. The single cell suspensions were incubated with PE conjugated tetramer at 4°C for 30min. After three washes the cell suspensions were analyzed using a flow cytometer.

Quantitative PCR for effector molecules and viral load determination

Total lymphocytes and Uda-tetramer^{+ve} cells were FACS sorted using FACS Aria on different time points post HSV1 infection. The total RNA was isolated using trizol method as per the manufacturer protocol and treated with DNAse to remove any DNA contamination. cDNA was synthesized by using 25 ng of total RNA using SuperScript IV cDNA synthesis kit (Cat. No. 18091050; Invitrogen). The qPCR reactions were performed using thermofisher SYBR Green qPCR kit (Cat. F416L) in QuantStudio Real-Time PCR system from Thermofisher. The primers for genes analysed and the product sizes for the amplification were as follows; β-Actin (FP: 5' CGAGCAGGAGATGGGAACC 3' & RP: 5' CAACGGAAACGCTCATTGC 3') = 102bp, CD3e (FP: 5' ACAGCGTTTCCATCCTTTCG 3' & RP: 5' GCTCATCTCCATCACCCACA 3') = 116 bp, CD8α (FP: 5' GGAGCAAAGCCCATGTTG 3' & RP: 5' GTGGGGACATCGTCTTGT 3') = 132 bp,

IFN-γ1 (FP: 5' TATGGGCGATCAAGGAAAAC 3' & RP: 5' GCCGTCTCTTGCGTTCTTTA 3') = 120bp, TNF-α (FP: 5' AGGCTGCCATCCATTTAACA 3' & RP: 5' CAAGCCACCTGAAGAAAAGG 3') = 95 bp, IL-15 (FP: 5' TGTGCTTTGAGAATCACATGG 3' & RP: 5' TGTTCTGGATGTCCTGCTTG 3') = 121bp and HSV1 DNA polymerase (UL30) catalytic subunit (gene id 2703462) (FP: 5′-CATCACCGACCCGGAGAGGGAC & RP: 5′-GGGCCAGGCGCTTGTTGGTGTA-3′) = 92bp. The relative mRNA expression for different molecules was calculated as per $2^{-\Delta\Delta}$ CT values. The reaction conditions used for qPCR were as follows: initial denaturation (95°C for 7 min), denaturation (95°C for 10 sec) then annealing and extension (60°C for 30 sec) for total 40 cycles, followed by a melt curve analysis. For viral load determination, the total RNA was isolated from spleen samples of uninfected and at different time intervals after infection i.e. 1, 24, 48 and 72 hrs post infection (hpi) from HSV1 infected zebrafishes. All the steps for measuring viral mRNA were as described above.

Viral load determination using plaque assays

Spleen and the whole body from HSV1 infected and control zebrafishes were collected, dipped in 70% ethanol and extensively washed with sterile PBS and homogenized using a tissue ruptor at 4°C. Spleens and remaining body of zebrafishes were homogenized in one and two ml serum free cold DMEM, respectively. The lysates were centrifuged at 5000 rpm 4°C for 15 min and the supernatants were collected. After preparing different dilutions in serum free DMEM, 300 µl of homogenates were plated on to Vero cells monolayer. The viral load in these organs calculated as per the mentioned formula:

Pfu/ml = Number of plaque/amount plated (0.3 ml) x dilution of supernatant used

Pfu/spleen or pfu/ml

Pfu/whole fish = (pfu/ml) x 2

Statistics analysis

To determine the levels of significance between samples obtained from different groups, student t test and ANOVA were used. The results shown represent mean ± SD. The level of significance are represented as NS>0.05, *, P<0.05, **, P<0.01 and ***P<0.001.

Results and Discussion

1. HSV1 infection of zebrafishes

Zebrafish is an established model for studying pathogenesis during some infections but its susceptibility to HSV1 infection is ill explored[26–28]. We first determined whether or not zebrafish is infectable by HSV1 and the replicating virus could be recovered from infected animals. We infected zebrafishes with $2x10^6$ pfu of HSV1 through intraperitoneal (IP) route. This is because a lower dose of virus resulted in a rapid clearance and replicating virus was not recovered beyond 24 hours. In HSV1 infected zebrafishes, we measured the replicating virus particles in spleen as well as the remaining body parts by preparing the homogenates at different time points post infection (Fig 3.1A). We recovered increasing concentration of replicating virus in spleens until 48 hrs post infection (hpi) (Fig 3.1B, upper panel). As early as 1hpi, the splenic tissues demonstrated replicating HSV1 and the level increased until 24 hpi (Fig 3.1B, upper panel). Thereafter, the virus titers were reduced and by 72 hours no detectable replicating viral particles were present in the splenic tissues (Fig 3.1B,C). The replicating viral particles in the homogenates of sacrificed zebrafishes after the removal of spleens were in fact recovered at a greater level as compared to those obtained from spleens. Upto 72 hpi the viral load were detectable to a very low level and no replicating HSV1 was recovered by 96 hpi (Fig 3.1B lower panel and Fig 3.1C).

We then observed the mRNA for viral DNA polymerase gene (UL30), a crucial molecule for the viral replication in the host[29] and its presence after 24 and 48 hrs of infection suggested that the virus was able to infect and replicate in the host. The presence of HSV1 mRNA at 24 and 48 hrs post infection (Fig 3.1D) and the detection of measurable replicating virus subsequent to infection support the notion that HSV1 replicated in experimentally infected zebrafish. In some of the earlier studies HSV1 infection was reported in zebrafish[26,27]. The presence of HSV1 DNA was quantified by PCR and viral antigens derived from a tegument protein (VP16) were detectable by immunofluorescence[25]. The maximum viral genomic load was measured at 48 and 72 hpi in encephalon of infected animals. Therefore our finding are in concordance with the published results but we additionally demonstrated replicating viral particles in spleens and elsewhere in zebrafish for upto 72 hpi. The susceptibility for HSV1 infection was also supported by a recent study where liposome encapsulation of HSV1 enhanced the ocular infectivity in 3 day old zebrafish[30].

Our data therefore show that HSV1 infection of zebrafish allows for the virus replication in the infected animals.

2. Measuring anti-HSV1 immunity in infected zebrafishes

We sought to first measure the *in vitro* responsiveness of immune cells isolated from uninfected and HSV1 infected animals. We measured the proliferation of splenocytes obtained from uninfected and infected fishes at 4 and 28 dpi. The single cell suspension prepared from splenic tissues were labelled with CFSE and incubated in the presence or absence of UV inactivated HSV1. After 72 hrs of incubation, the cells were analysed flow cytometrically. We observed a significant alteration in the morphology as well as scattering characteristics of HSV1 antigen pulsed cells as compared to those cultured without viral antigens (Fig 3.1E). The frequencies of live cells that were

predominantly present in the lymphocyte region were increased by seven fold (12% in control vs 84% in virus pulsed splenocytes) in the HSV1 antigen pulsed splenocytes as compared to no virus control (Fig 3.1E). Furthermore a greater proportion of HSV1 pulsed splenocytes (were collected at 4 dpi in the acute phase of response and at 28 dpi in the memory stage of the infection) diluted CFSE content suggesting for their extensive proliferation (Fig 3.1F). We also measured the proliferation of liver infiltrating immune cells obtained from the HSV1 infected fishes at 4 dpi in the acute phase of response (Fig 3.1H). The splenocytes and liver infiltrating lymphocytes (LILs) were CFSE labelled and pulsed with inactivated HSV1. Similar to what was observed for splenocytes collected in the acute phase of response at 4 dpi, the splenocytes extensively diluted CFSE on 28 dpi (Fig 3.1F and G). Lymphocytes of spleen and liver samples were pulsed with inactivated virus undergone activation and might have started IL-2 expression, whereas those cells kept without any pulsing were not able to produce it for their survival-expansion, henceforth we got a lower number of cells (as shown in forward and side scatter plot) from unpulsed samples. The LILs also divided in response to HSV1 antigens when analyzed by *in vitro* assays in the acute stage (4 dpi) (Fig 3.1H) of HSV1 infection as an extensive dilution of their CFSE content was observed.

Our results therefore demonstrate that HSV1 expanded immune cells could be recovered from splenic as well as liver tissues. Furthermore, the immune cells extensively proliferated *in vitro* upon their re-stimulation with the viral antigens.

3. Generation of Uda-MHCI tetramer for detecting HSV1 specific $CD8^+$ T cell

Having established the infectivity and immune reactivity of zebrafish to HSV1, we sought to measure and quantify the antigen-specific $CD8^+$ T cell responses. We developed class I MHC (Uda)-tetramers that could identify virus-specific cytotoxic T cells in the HSV1 infected zebrafishes. First, we aligned the sequence of MHC class I

heavy chain of zebrafish (U and Z lineages) with H-2K^b (MHC class I heavy chain of C57BL/6 mice), the latter displays one of the major immunodominant viral peptide gB$_{498-505}$(SSIEFARL)[31,32]. The U lineage MHC class I molecules showed closer similarity with H-2K^b (Fig 3.2A). Then, we selected top five MHC class I molecules of zebrafish i.e., Ula, Uma, Uda, Uaa and Uba that exhibited greater sequence homology to H-2K^b and analyzed their peptide binding sites in the α1 and α2 domains for comparing the amino acid sequence with those in mouse H-2K^b. Specifically we searched for similarities in the amino acid residues that could serve as the anchor for the SSIEFARL peptide[33] (Fig 3.2B). The maximum number of H-2K^b amino acids which make contacts with SSIEFARL peptide were also present on zebrafish Uda HC, however all of the five U lineage HC of zebrafish showed some of the similar amino acids that interacts with S1 and L8 residues as well. Additionally, H-2K^b and Uda HC having more of the shared interacting partners for S1, R7 and L8 of SSIEFARL peptide (which serve as a dominant anchor residues for the HC of class I MHC) were present at similar positions. Although S1 of SSIEFARL peptide interacts with Uda Y7, Y157, W165, Y169; yet Y7 also the binding affinity with S2 amino acid as well. An amino acid, W144 showed interaction with R7 and L8 residues of the SSIEFARL peptide. Amino acids such as T140, K143 and W144 displayed strong interaction with L8 residue of the peptide. Along with some of the shared amino acids present in H-2K^b and all the five U lineage HCs, the presence of additional amino acids such as V74 and D75 that interacted with R7 and L8 of the SSIEFARL peptide, were present only in H-2K^b and Uda HC binding pockets. These results suggested that Uda molecule could present gB-SSIEFARL peptide of HSV1, the immunodominant peptide in C57BL/6 mice.

The docking of SSIEFARL peptide on the overlaid H-2K^b and Uda HCs revealed conservation in the majority of the interacting anchor residues (either same amino acid or

those having similar biochemical characteristics present at similar or contiguous positions) for the SSIEFARL peptide (Fig 3.2C). This suggested that Uda HC could yield us a refolded heterotrimeric monomer consisting of SSIEFARL peptide, β_2m and the Uda molecule. If tetramerized using a fluorescent probe, such reagents could be used for detecting HSV1 specific $CD8^+$ T cells in HSV1 infected zebrafishes.

We PCR amplified the extracellular domains of Uda HC and β_2m using synthesized cDNA as template converted from zebrafish liver RNA (Fig. 3.3A). A biotin acceptor peptide sequence was incorporated in the reverse primer to modify the C terminus of Uda HC. This allows for a site specific labelling with biotin using BirA enzyme[24]. We then cloned the Uda amplicon (883 bp) in pET22b plasmid for its bacterial expression (Fig 3.3B). After cloning and sequence verification, we expressed Uda (~35 kDa MW) in *E. coli* and purified it from the inclusion bodies as described in the materials and methods section (Fig 3.3C and D). Similarly we also cloned zebrafish β_2m (353 bp) in pET22b plasmid and expressed it to purify from the inclusion bodies (Fig 3.3E-G). Both the Uda and β_2m were refolded in the presence of SSIEFARL peptide by a rapid dilution method followed by fractionation by size exclusion chromatography[24,25]. We obtained four peaks in the size exclusion chromatogram and observed upon their electrophoretic separation the major portion of the refolded MHC I monomer in peak no 2 that had the polypeptide bands of Uda (~35 kDa) and β_2m (~13 kDa) (Fig 3.3H and I). The peptide being smaller in size could not be detected. In order to ensure the refolding of monomer, we analyzed the pooled and concentrated fraction by circular dichroism (CD) spectra and observed β sheets (47.11%) and α helical structures (3.66%) that further confirmed our results for the refolded monomer (Fig 3.3J). We also tested the possibility of refolding Uda HC and β_2m in the presence of two more H-$2K^b$ restricted epitopes i.e., SIINFEKL and FAPG(Anp)YPAL, a conditional ligand that can be cleaved upon

exposure with the UV rays at 365 nm wavelength. The latter peptide could help generate tetramers for a high throughput screening of immunogenic epitopes[34,35]. We show that indeed both of these peptides resulted in the formation of refolded monomeric products albeit with varying degrees (Fig 3.6). We then biotinylated the refolded Uda-SSIEFARL-monomers using BirA ligase as per the manufacturer (Avidity, LLC) protocol and removed the excess of biotin and other reaction components from the biotinylated-monomer using size exclusion chromatography. Thereafter, the biotinylated monomers were incubated with PE conjugated streptavidin in 4:1 ratio at 4°C for tetramerization and the biotinylation efficiency of monomers and the tetramerization levels were analyzed by resolving such refolded products on a 12% gel in reducing SDS-PAGE (Fig 3.3K) and native PAGE (Fig 3.3L) followed by probing the electroblotted membranes using streptavidin-HRP conjugate (Fig 3.3K and L). We observed a band corresponding to ~35kDa in reducing (Fig 3.3K) and ~48kDa in native PAGE corresponding to the biotinylated Uda HC and the tetramers having a MW of ~200kDa (Fig 3.3L). Our results therefore show the generation of Uda-SSIEFARL-tetramer and such reagents could potentially help detect HSV1 specific $CD8^+$ T cells in the infected zebrafishes.

4. Detecting and measuring the kinetics of HSV1 specific $CD8^+$ T cells during virus infection

Till date studies focusing on the development and detection of T cells have used transgenic zebrafish lines[10]. Based on the scattering properties of lymphocytes isolated from transgenic zebrafish expressing GFP under Lck promoter, the presence of T cells was demonstrated[10]. However, approaches involving transgenesis could have limitations when used to measure the homeostasis of T cells during infections. Since we generated Uda-SSIEFARL-tetramers which could potentially identify HSV1 specific $CD8^+$ T cells in zebrafish, we aimed at detecting and measuring the kinetics of HSV1 specific $CD8^+$ T

cell response. We infected zebrafish with $2x10^6$ PFU of HSV1 intraperitoneally, collected spleens at 5 dpi and stained splenocytes with PE conjugated Uda-SSIEFARL-tetramer (Fig 3.4A). The cells were then analyzed by flow cytometry. The total live cell gate from the forward and side scatter plots were analyzed for the presence of tetramer^{+ve} cells. We could detect 6-8% tetramer^{+ve} cells in infected and 1-2% in uninfected fishes (Fig 3.4B,D). We confirmed these cells by backgating to measure the forward and side scattering characteristics to find out the origin of these cells. As expected the backgating showed that ~94% of tetramer^{+ve} cells originated from lymphocyte region. These results showed the functionality of tetramers and their ability to identify HSV1 reactive CD8$^+$ T cells. We then aimed at measuring the kinetics of virus-specific CD8$^+$ T cells in HSV1 infected zebrafishes (Fig 3.4 A,C,D). We collected splenocytes at different days post infection infection (dpi). After HSV1 infection the antigen-specific CD8$^+$ T cells increased until 5-6 dpi (~7% tetramer^{+ve} of total live cells). Thereafter, the frequencies of tetramer^{+ve} cells decreased and stabilized by 45 dpi at ~2.0% tetramer^{+ve}. Once the primary infection with HSV1 is cleared in the vertebrate hosts, the magnitude of expanded CD8$^+$ T cells contracts leaving behind a pool of memory CD8$^+$ T cells that are recruited in the response, should the host is infected subsequently with the same infectious agent to provide a quick protection[36–38]. The observed slightly higher frequency of antigen-reactive CD8$^+$ T cells in this model could be because of the generation of memory CD8$^+$ T cells. We then re-infected zebrafishes on 45 day post primary infection and measured Uda-SSIEFARL-tetramer^{+ve} cells at 7 days of secondary infection. Elevated levels of HSV1 reactive cells were observed at 7 dpi of secondary infection suggesting for the recall of memory CD8$^+$ T cells in this model organism. The lower responsiveness of memory cells could be attributed to the same virus used for the recall response. Thus, the neutralizing antibodies might limit the overall antigen load[39,40].

A similar pattern and magnitude of recall response is observed in the murine model of HSV1 infection under similar experimental conditions[41]. Taken together, our results suggest for a similar kinetics of antigen-specific $CD8^+$ T cell expansion, contraction and memory formation that can be recalled in response to the same infection as is observed for higher vertebrates such as rodents and humans. Our results therefore attest to the fact that zebrafish could serve as an alternative and probably better model system for investigating virus-specific $CD8^+$ T cells responses.

5. HSV1 expanded lymphocytes express effector molecules

Having successfully demonstrated the HSV1 infectivity in zebrafish and the utility of generated Uda-tetramer to identify and measure the kinetics of T cells response, we next aimed to explore the adaptive immune function of such cells by measuring their production of effector molecules that are associated with functional $CD8^+$ T cells post herpesvirus infection. To this end we infected zebrafishes with HSV1 and sort purified the total lymphocytes from the spleens of uninfected and different days post infected fishes (Fig 3.5), the isolated RNA was converted into cDNA from these cells. The mRNA levels for different effector molecules such as IFN-γ1, TNF-α, IL-15, CD3e and CD8α were quantified using quantitative PCR We detected enhanced levels of pro-inflammatory cytokines, such as IFN-γ1 (~4 fold) and TNF-α (~2 fold) at 4 dpi and 2 dpi, respectively post HSV1 infection whereas the expression of IL-15 was reduced (two fold) at 2 dpi but reached at a similar levels as observed in the uninfected animals at 7 dpi (Fig 3.5D). We also determined whether the cytokines produced were indeed contributed by T cells at 4dpi, in the sorted immune cells by measuring the mRNA expression of CD3e, a marker for T cells and CD8α, a predominant marker of cytotoxic T lymphocytes at mRNA levels. This is because the specific monoclonal antibodies for these molecules to detect their surface expression are not available currently for zebrafish. In sorted

lymphocytes as compared to the total splenocytes we observed a higher expression of these molecules (CD3, up by 20 fold and CD8 up by 50 fold) as compared to the total splenocytes (Fig 3.5E). These results further attested to the fact that the sorted cell population were mainly cytotoxic T lymphocytes. Upregulation of pro-inflammatory cytokines post HSV1 infection support the adaptive immune function of T cells in zebrafish. So these molecules might contribute to the protection of the host from HSV1 infection.

Conclusions

We showed here the HSV1 infectivity and a successful recovery of the replicating virus particles from the zebrafishes, a model organism that allows investigating cellular dynamics with ease *in vivo*. The maximum viral load was observed in spleen after 24 hpi as quantified by both the plaque forming assays and qPCR for viral DNA polymerase, a key molecule for the virus replication in the host. Splenocytes and liver infiltrating immune cells collected from HSV1 infected animals when pulsed with the virus antigens proliferated extensively that implies their initial responsiveness to antigens during infection.

$CD8^+$ T cells constitute an important arm of adaptive immune system and are critical for controlling intracellular pathogens. T cell receptor confers the antigen-specificity to $CD8^+$ T cells and it recognizes peptides derived from the pathogen in context of class I MHC products[45–49]. Receiving three signals (TCR-p-MHC, co-stimulatory molecules and cytokines in the milieu) during induction phase of response, $CD8^+$ T cells get activated and proliferate profoundly to lyse target cells. As infected/ target cells are killed, intracellular pathogen is also controlled. Multiple mechanisms then control the magnitude of $CD8^+$ T cells not only to establish homeostasis but also to limit

any possible damage caused by immune cells. Many of these mechanisms are still less well defined. A minor fraction of memory population from the responding cells remains only to be efficiently recalled to confer a quick protection, should the host encounters the same pathogenic exposure at a later time.

For studying cytotoxic T cell response in these animals, we first identified the class I MHC molecule of zebrafish that had most of the interacting residues for the HSV1 derived SSIEFARL peptide, the most immunodominant peptide in C57BL/6 strain of mouse presented by H-2K^{b} HC. This lead us to believe that a probing reagent (the monomer of class I MHC trimeric complex consisting of the SSIEFARL peptide, β_2m and the HC of Uda molecule) for detecting HSV1 specific cytotoxic T cells could be generated for zebrafish. We scanned all of the known classical MHC I HCs of zebrafish and found Uda molecule as the most appropriate candidate. In addition we also explored the feasibility of generating Uda monomer with different peptides including a conditional ligand (FAPG(Anp)YPAL ; UV cleavable peptide) which can be replaced with other peptides and allows for a high-throughput screening of immunogenic peptides eliciting specific T cell response in zebrafish. We obtained a varying degree of refolded Uda monomers depending on the peptides used (Fig 3.6), highlighting the involvement of preferential interacting partners and were able to generate monomers with SSIEFARL, SIINFEKL and conditional ligand (FAPG(Anp)YPAL).

The Uda-SSIEFARL monomers were tetramerized with fluorochrome conjugated streptavidin and such a reagent could successfully identify the HSV1 specific T cells in flow cytometric analysis. Furthermore, the analysis involving the kinetics of tetramer^{+ve} cells post HSV1 injection in zebrafish revealed their previously undocumented close similarity to higher vertebrates such as mice and humans suggesting for the existence of an evolutionary conserved mechanism involving T cells in these organism that diverged

400 million years ago. Thus the very same HSV1 peptide could be displayed by zebrafish Uda molecule that serves as one of the most immunodominant epitope in C57BL/6 mice. Our study also provides a further impetus to the usability of this model system in studying HSV1 infection and its clearance by cytotoxic T cells. We further determined the cytokines production by cytotoxic T cells in HSV1 infected zebrafish and observed an upregulation of message for pro-inflammatory cytokines such as IFN-γ1 and TNF-α in the lymphocytes collected from 2 and 4 dpi. The higher level of CD3e and CD8α mRNA in lymphocytes (sorted from different days post HSV1 infection) as compared to the total splenocytes (of uninfected animals) counterparts, supports the notion that a major portion of such cells constitute cytotoxic T cells. Therefore this study established HSV1 infectivity in zebrafish, and the generation of class I MHC-tetramers that could identify the virus-specific cytotoxic T cells. The detection of mRNA for the effector molecules highlights the cytokine producing ability of T lymphocytes in HSV1 infected zebrafishes. The present study therefore, pave the way for using zebrafish as an *in vivo* tractable animal model system whose potential can be optimally harnessed for visualization of the cellular dynamics during virus infections such as the one caused by HSV1.

The ease of performing experiments, the requirement of smaller doses of inoculum and the availability of biological reagents additionally make zebrafish as a favored vertebrate animal model for investigating host pathogen interactions. For deciphering the pathogenesis and mediators of granulomatous lesion during tuberculosis, zebrafish model has provided greater insights into the contribution of immune cells as compared to other vertebrate animals[42–44]. Therefore, zebrafish as an *in vivo* model system certainly has the potential to change the current thinking how we study host-pathogen interaction in vertebrates.

List of References:

1. Kari, G., Rodeck, U. & Dicker, A. P. Zebrafish: An Emerging Model System for Human Disease and Drug Discovery. *Clin. Pharmacol. Ther.* **82**, 70–80 (2007).
2. Lieschke, G. J. & Currie, P. D. Animal models of human disease: Zebrafish swim into view. *Nat. Rev. Genet.* **8**, 353–367 (2007).
3. Trede, N. S., Langenau, D. M., Traver, D., Look, A. T. & Zon, L. I. The use of zebrafish to understand immunity. *Immunity* **20**, 367–79 (2004).
4. Meeker, N. D. & Trede, N. S. Immunology and zebrafish: Spawning new models of human disease. *Dev. Comp. Immunol.* **32**, 745–757 (2008).
5. Yoder, J. A., Nielsen, M. E., Amemiya, C. T. & Litman, G. W. Zebrafish as an immunological model system. *Microbes Infect.* **4**, 1469–78 (2002).
6. Ma, D., Zhang, J., Lin, H. -f., Italiano, J. & Handin, R. I. The identification and characterization of zebrafish hematopoietic stem cells. *Blood* **118**, 289–297 (2011).
7. Stachura, D. L. *et al.* Zebrafish kidney stromal cell lines support multilineage hematopoiesis. *Blood* **114**, 279–89 (2009).
8. Stachura, D. L. & Traver, D. Cellular dissection of zebrafish hematopoiesis. in *Methods in cell biology* **133**, 11–53 (2016).
9. Traver, D. Cellular Dissection of Zebrafish Hematopoiesis. *Methods Cell Biol.* **76**, 127–149 (2004).
10. Langenau, D. M. *et al.* In vivo tracking of T cell development, ablation, and engraftment in transgenic zebrafish. *Proc. Natl. Acad. Sci.* **101**, 7369–7374 (2004).
11. Danilova, N. & Steiner, L. A. B cells develop in the zebrafish pancreas. *Proc. Natl. Acad. Sci. U. S. A.* **99**, 13711–6 (2002).
12. Page, D. M. *et al.* An evolutionarily conserved program of B-cell development and activation in zebrafish. *Blood* **122**, e1–e11 (2013).

13. Langenau, D. M. & Zon, L. I. The zebrafish: a new model of T-cell and thymic development. *Nat. Rev. Immunol.* **5**, 307–317 (2005).

14. Dirscherl, H., McConnell, S. C., Yoder, J. A. & de Jong, J. L. O. The MHC class I genes of zebrafish. *Dev. Comp. Immunol.* **46**, 11–23 (2014).

15. Renshaw, S. A. *et al.* A model 450 million years in the making: zebrafish and vertebrate immunity. *Dis. Model. Mech.* **5**, 38–47 (2012).

16. Novoa, B. & Figueras, A. Zebrafish: Model for the Study of Inflammation and the Innate Immune Response to Infectious Diseases. in *Advances in experimental medicine and biology* **946**, 253–275 (2012).

17. Lugo-Villarino, G. *et al.* Identification of dendritic antigen-presenting cells in the zebrafish. *Proc. Natl. Acad. Sci. U. S. A.* **107**, 15850–5 (2010).

18. Kasheta, M. *et al.* Identification and characterization of T reg-like cells in zebrafish. *J. Exp. Med.* **214**, 3519–3530 (2017).

19. Wan, F., et al. Characterization of γδ T cells from zebrafish provides insights into their important role in adaptive humoral immunity. *Frontiers in immunology*, **7**, 675, 1-18 (2017).

20. Baer, A. & Kehn-Hall, K. Viral Concentration Determination Through Plaque Assays: Using Traditional and Novel Overlay Systems. *J. Vis. Exp.* e52065 (2014). doi:10.3791/52065

21. Dirscherl, H. & Yoder, J. A. Characterization of the Z lineage Major histocompatability complex class I genes in zebrafish. *Immunogenetics* **66**, 185–98 (2014).

22. Altman, J. D. *et al.* Phenotypic analysis of antigen-specific T lymphocytes. *Science* **274**, 94–6 (1996).

23. Schatz, P. J. Use of Peptide Libraries to Map the Substrate Specificity of a Peptide-Modifying Enzyme: A 13 Residue Consensus Peptide Specifies Biotinylation in Escherichia coli. *Nat. Biotechnol.* **11**, 1138–1143 (1993).

24. Busch, D. H., Pilip, I. M., Vijh, S. & Pamer, E. G. Coordinate regulation of complex T cell populations responding to bacterial infection. *Immunity* **8**, 353–362 (1998).

25. Busch, D. H., Pilip, I. & Pamer, E. G. *Evolution of a Complex T Cell Receptor Repertoire during Primary and Recall Bacterial Infection*. *J. Exp. Med* **188**, (1998).

26. Burgos, J. S., Ripoll-Gomez, J., Alfaro, J. M., Sastre, I. & Valdivieso, F. Zebrafish as a New Model for Herpes Simplex Virus Type 1 Infection. *Zebrafish* **5**, 323–333 (2008).

27. Antoine, T. E., Jones, K. S., Dale, R. M., Shukla, D. & Tiwari, V. Zebrafish: Modeling for Herpes Simplex Virus Infections. *Zebrafish* **11**, 17–25 (2014).

28. Yakoub, A. M. *et al.* Comprehensive Analysis of Herpes Simplex Virus 1 (HSV-1) Entry Mediated by Zebrafish 3-O-Sulfotransferase Isoforms: Implications for the Development of a Zebrafish Model of HSV-1 Infection. *J. Virol.* **88**, 12915–12922 (2014).

29. Weller, S. K. & Coen, D. M. Herpes simplex viruses: Mechanisms of DNA replication. *Cold Spring Harb. Perspect. Biol.* **4**, (2012).

30. Burnham, L. A. *et al.* Liposome-mediated herpes simplex virus uptake is glycoprotein-D receptor-independent but requires heparan sulfate. *Front. Microbiol.* **7**, 973 (2016).

31. Wallace, M. E., Keating, R. & Heath, W. R. The Cytotoxic T-Cell Response to Herpes Simplex Virus Type 1 Infection of C57BL / 6 Mice Is Almost Entirely Directed against a Single Immunodominant Determinant. *J. Virol.* **73**, 7619–7626 (1999).

32. Treat, B. R. *et al.* Influence of an immunodominant herpes simplex virus type 1 CD8 + T cell epitope on the target hierarchy and function of subdominant CD8 + T cells. doi:10.1371/journal.ppat.1006732

33. Webb, A. I. *et al.* The Structure of H-2Kb and Kbm8 Complexed to a Herpes Simplex Virus Determinant: Evidence for a Conformational Switch That Governs T Cell Repertoire Selection and Viral Resistance. *J. Immunol.* **173**, 402–409 (2004).

34. Luimstra, J. J. *et al.* A flexible MHC class I multimer loading system for large-scale detection of antigen-specific T cells. *J. Exp. Med.* **215**, 1493–1504 (2018).

35. Rodenko, B. *et al.* Generation of peptide–MHC class I complexes through UV-mediated ligand exchange. *Nat. Protoc.* **1**, 1120–1132 (2006).

36. Muruganandah, V., Sathkumara, H. D., Navarro, S. & Kupz, A. A Systematic Review: The Role of Resident Memory T Cells in Infectious Diseases and Their Relevance for Vaccine Development. *Front. Immunol.* **9**, 1574 (2018).

37. Barber, D. L., Wherry, E. J. & Ahmed, R. Cutting Edge: Rapid In Vivo Killing by Memory CD8 T Cells. *J. Immunol.* **171**, 27–31 (2003).

38. Wherry, E. J. & Ahmed, R. Memory CD8 T-cell differentiation during viral infection. *J. Virol.* **78**, 5535–45 (2004).

39. Klasse, P. J. Neutralization of Virus Infectivity by Antibodies: Old Problems in New Perspectives. *Adv. Biol.* **2014**, 1–24 (2014).

40. Bootz, A. *et al.* Protective capacity of neutralizing and non-neutralizing antibodies against glycoprotein B of cytomegalovirus. *PLoS Pathog.* **13**, e1006601 (2017).

41. Lang, A. & Nikolich-Zugich, J. Functional CD8 T cell memory responding to persistent latent infection is maintained for life. *J. Immunol.* **187**, 3759–68 (2011).

42. Lesley, R. & Ramakrishnan, L. Insights into early mycobacterial pathogenesis from the zebrafish. *Curr. Opin. Microbiol.* **11**, 277–83 (2008).

43. Prouty, M. G., Correa, N. E., Barker, L. P., Jagadeeswaran, P. & Klose, K. E. Zebrafish- *Mycobacterium marinum* model for mycobacterial pathogenesis. *FEMS Microbiol. Lett.* **225**, 177–182 (2003).

44. Swaim, L. E. *et al.* Mycobacterium marinum infection of adult zebrafish causes caseating granulomatous tuberculosis and is moderated by adaptive immunity. *Infect. Immun.* **74**, 6108–17 (2006).

45. Tallquist, M. D., Yun, T. J. & Pease, L. R. A single T cell receptor recognizes structurally distinct MHC/peptide complexes with high specificity. *J. Exp. Med.* **184**, 1017–26 (1996).

46. Kalergis, A. M. *et al.* Efficient T cell activation requires an optimal dwell-time of interaction between the TCR and the pMHC complex. *Nat. Immunol.* **2**, 229–234 (2001).

47. Stone, J. D., Chervin, A. S. & Kranz, D. M. T-cell receptor binding affinities and kinetics: impact on T-cell activity and specificity. *Immunology* **126**, 165–76 (2009).

48. Chaudhri, G. *et al.* T cell receptor sharing by cytotoxic T lymphocytes facilitates efficient virus control. *Proc. Natl. Acad. Sci. U. S. A.* **106**, 14984–9 (2009).

49. Stone, J. D. & Kranz, D. M. Role of T cell receptor affinity in the efficacy and specificity of adoptive T cell therapies. *Frontiers in Immunology* **4**, 244 (2013).

APPENDIX

Fig. 3.1 HSV1 infection in zebrafish and viral reactivity of immune cells.

Zebrafishes were infected with HSV1-KOS ($2x10^6$ pfu) intraperitoneally and their spleens and remaining body parts were collected at 1, 24, 48 and 72 hpi (hour post infection) for viral load determination and some of the infected animals were sacrificed at 4 and 28 dpi and spleen were collected for *in vitro* cell proliferation experiments (A). B. Representative images for the plaques formed by virus recovered from the spleen and remaining body parts of zebrafishes collected at indicated time points post infection. The images for spleen (upper panel) and whole fish except spleen (lower panel) at indicated different dilution of plated samples are shown. C. The cumulative data for the virus load determination is shown in the spleens and whole zebrafishes (except spleen) at given time point post HSV1 infection. D. Viral mRNA levels were measured by qPCR in the spleen samples of HSV1 infected animals and relative fold changes in the expression of DNA polymerase (UL30) is shown by bar graphs. E. Gating strategy of CFSE labelled splenocytes analysed in proliferation experiment (as shown in Fig 3.1F and G). F. The representative FACS plots show the proliferation of splenocytes isolated from HSV1 infected animals at 4 and 28 dpi, labelled with 1µM CFSE and cultured in the absence (unpulsed) or the presence of UV-inactivated HSV1 at 28°C in CO_2 incubator for 72 hrs. G. The cumulative data for the total number of cells observed in live cell gate (Fig 3.1E) of splenocytes which were obtained from the HSV1 pulsed and unpulsed samples of 4 and 28 dpi animals. H. Representative figure shows the CFSE dilution by liver infiltrating cells collected from 4 dpi and setup for *in vitro* proliferation experiment as setup for the splenocytes. For pulsing CFSE labelled splenocytes and/or liver cells were incubated with 1 MOI of inactivated virus. At each time points N>8 animals, where error bars indicate ± SD. ***P < 0.001, **P<0.01, *P<0.05 and NS (P>0.05)- not significant (Unpaired t test).

A

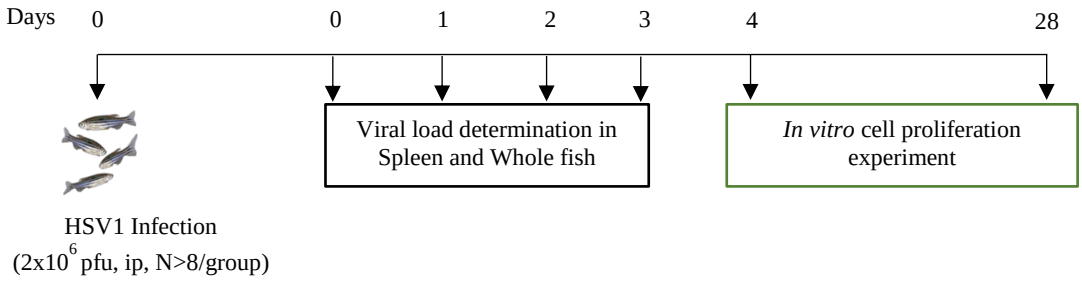
Days
0
0
1
2
3
4
28
Viral load determination in Spleen and Whole fish
In vitro cell proliferation experiment
HSV1 Infection
(2x10^6 pfu, ip, N>8/group)

B

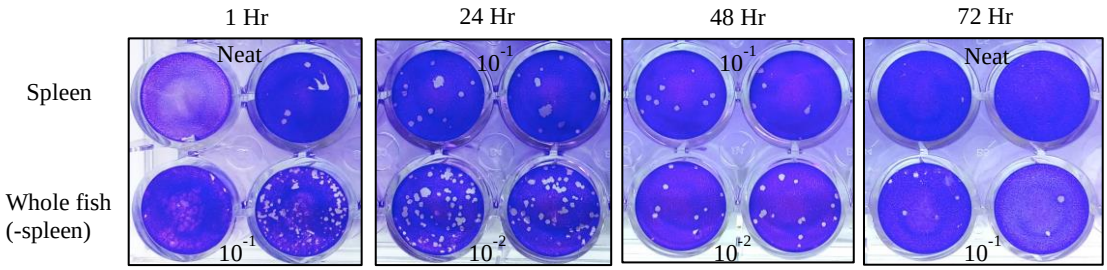
1 Hr
24 Hr
48 Hr
72 Hr
Spleen
Whole fish
(-spleen)
Neat
10^-1
10^-2
10^-1
10^-2
10^-1
10^-2
Neat
10^-1

C

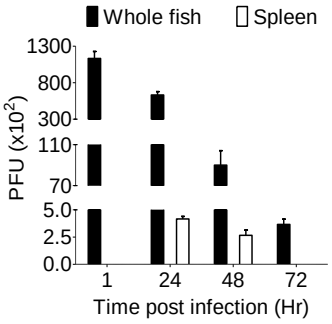
Whole fish
Spleen
PFU (x10^2)
1300
800
300
110
70
5.0
2.5
0.0
1
24
48
72
Time post infection (Hr)

D

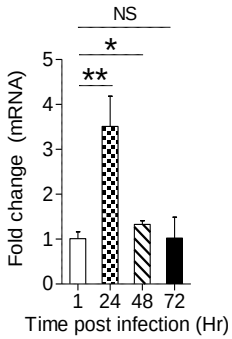
NS
*
**
Fold change (mRNA)
5
4
3
2
1
0
1
24
48
72
Time post infection (Hr)

E

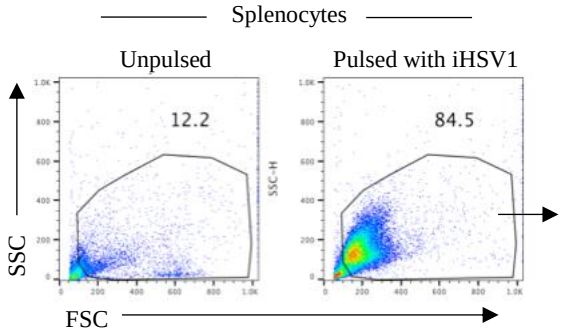
Splenocytes
Unpulsed
Pulsed with iHSV1
12.2
84.5
SSC
FSC

F

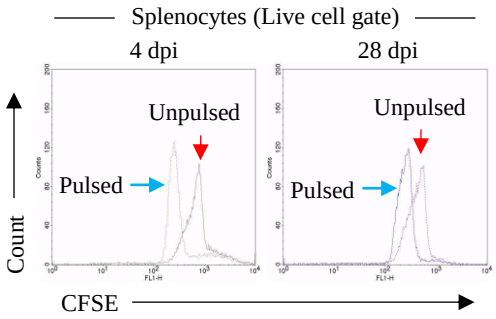
Splenocytes (Live cell gate)
4 dpi
28 dpi
Unpulsed
Pulsed
Unpulsed
Pulsed
Count
CFSE

G

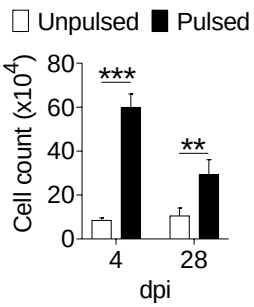
Unpulsed
Pulsed
Cell count (x10^4)
80
60
40
20
0
***
**
4
28
dpi

H

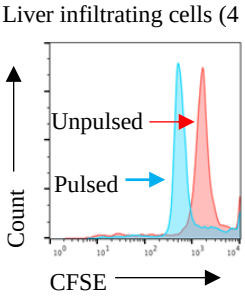
Liver infiltrating cells (4 dpi)
Unpulsed
Pulsed
Count
CFSE

Fig. 3.2 Identification of putative binding MHCI molecule for SSIEFARL peptide.

Alignment of zebrafish class I MHC molecules with the mouse H-2K^b heavy chain to search for the interacting partners for the anchor residues of SSIEFARL peptide. A. Phylogenetic tree is shown to demonstrate the similarity between H-2K^b and zebrafish class I MHC molecules. the top five homologous sequences for class I MHC molecules of zebrafish with the H-2K^b molecule are in the U lineage HC and are shown in the figure by red boxes. B. Amino acid sequence analysis aimed at finding find out the interacting amino acids in class I HC with HSV1-gB-SSIEFARL peptide in five of the U lineage of class I MHC HC. Uda is shown in lowest line and unique amino acids shared between H-2K^b and Uda molecule crucial for making interaction with SSIEFARL peptide are shown in bold red box. The α1 and α2 domains of Uda is shown in different colored arrow. C. An overlaid image of putative Uda tertiary structure with H-2K^b-SSIEFARL monomer for the presence of SSIEFARL binding pocket in Uda HC.

A

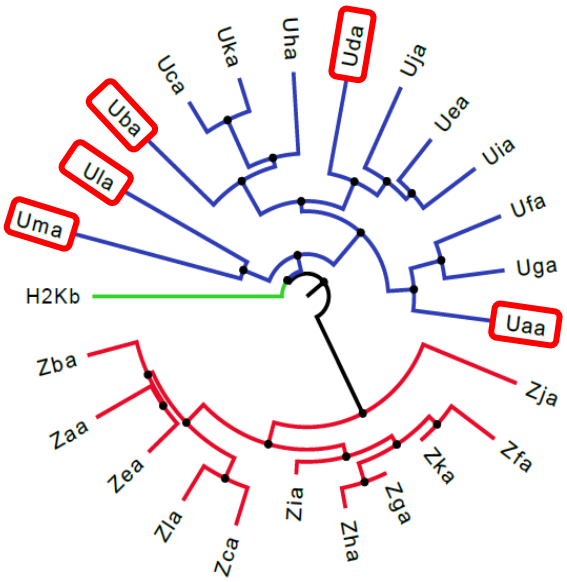

B

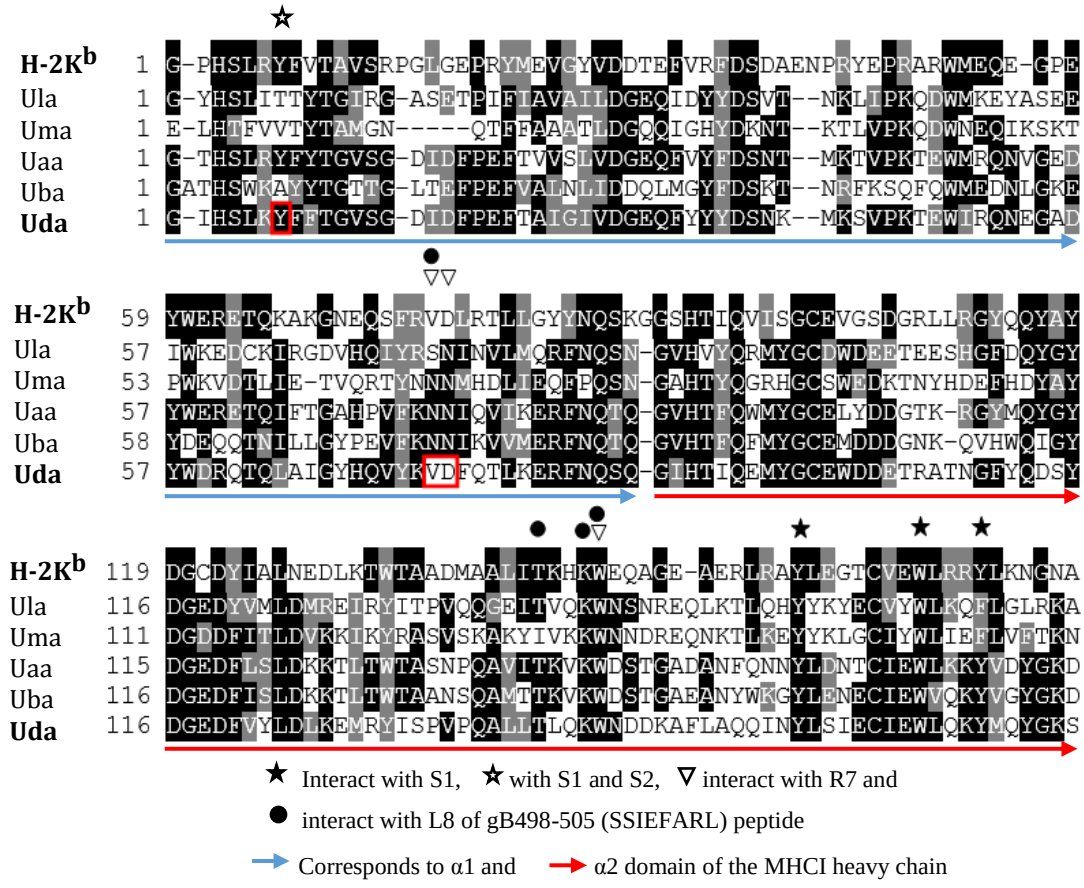

★ Interact with S1, ⛤ with S1 and S2, ∇ interact with R7 and

● interact with L8 of gB498-505 (SSIEFARL) peptide

→ Corresponds to α1 and → α2 domain of the MHCI heavy chain

C

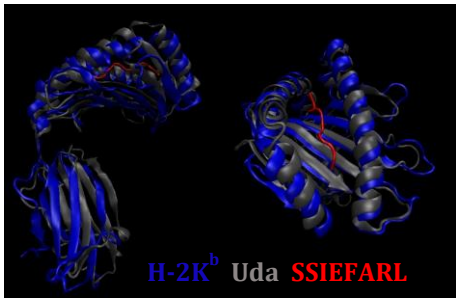

Fig. 3.3 Generation of MHCI tetramer for HSV1 specific T cell detection.

For generating class I MHC tetramers Uda HC and β_2 microglobulin of zebrafish were cloned, expressed and purified. The purified proteins were refolded in presence of HSV1 derived peptide (SSIEFARL) and the refolded monomers were purified using size exclusion chromatography. After biotinylation and fractionation the monomers were tetramerized using streptavidin-PE and the tetramer generation was assessed using denaturing and native PAGE followed by western blotting using streptavidin-HRP (A-L). A. PCR amplification of Uda heavy chain and β_2m. The Uda heavy chain and β_2m were cloned in pET22b plasmid (B and E). MHC class I molecule proteins were expressed in *E. coli* BL21 strain by IPTG induction (C and F). Expressed heavy chain and β_2m proteins were purified from inclusion bodies and the purity was assessed by 12% SDS-PAGE (D and G). The purified proteins were refolded in the presence of SSIEFARL peptide and the monomer were purified using size exclusion chromatography. H. The chromatogram shows the elution profile of different polypeptides collected form the refolding buffer. I. The polypeptides present in different peaks collected from gel filtration column were analysed by 12% SDS-PAGE. J. Circular dichroism spectrum of peak 2 protein (class I MHC monomer) showing the refolded structure. K. Western blotting was performed using streptavidin-HRP for measuring the biotinylation efficiency of purified monomer before tetramerization. L. Western blotting was performed to measure the Uda-SSIEFARL-tetramer by native-PAGE using streptavidin-HRP.

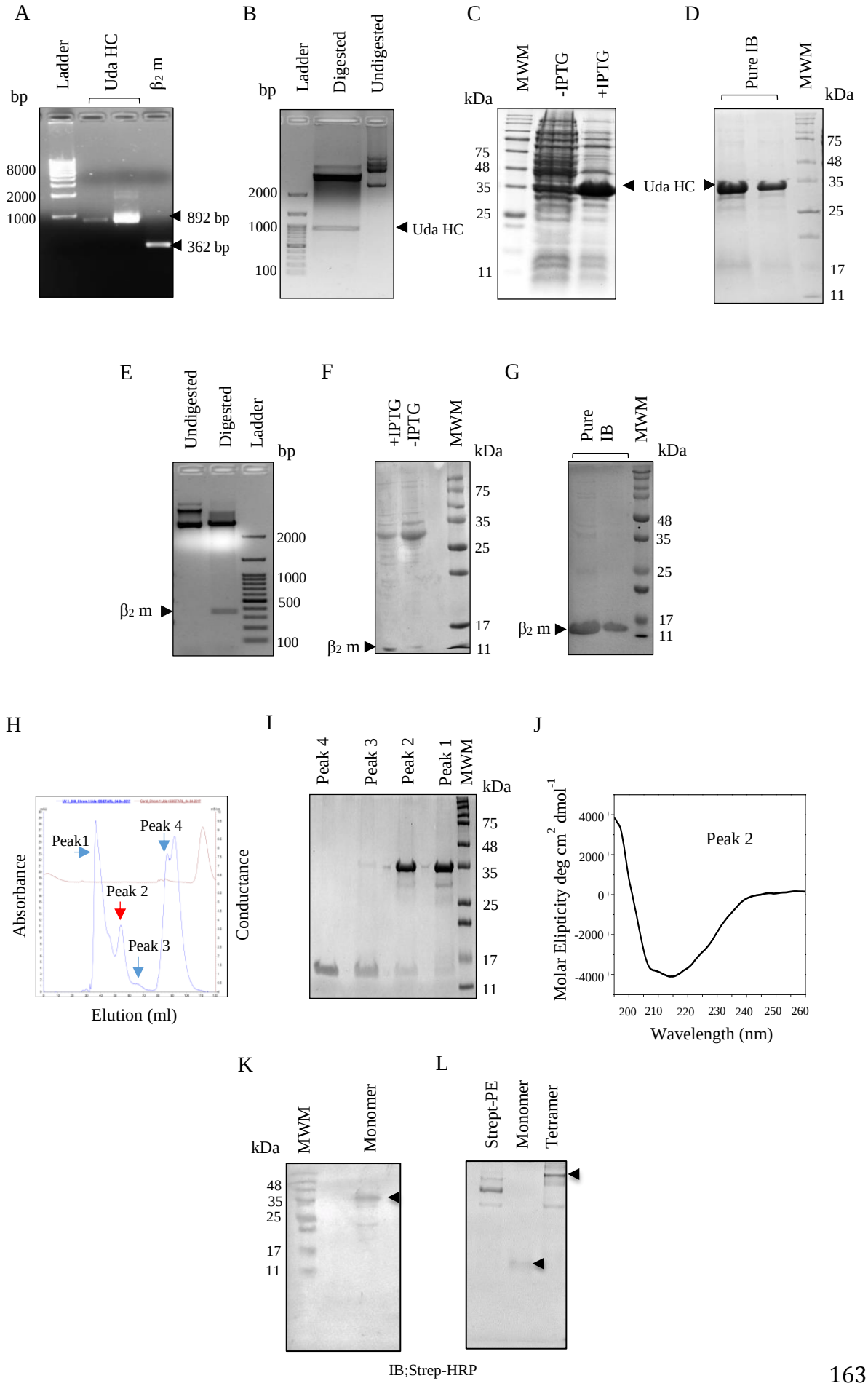
A
Ladder
Uda HC
β2 m
bp
8000
2000
1000
892 bp
362 bp
B
Ladder
Digested
Undigested
bp
2000
1000
100
Uda HC
C
MWM
-IPTG
+IPTG
kDa
75
48
35
25
11
Uda HC
D
Pure IB
MWM
kDa
75
48
35
25
17
11
E
Undigested
Digested
Ladder
bp
2000
1000
500
100
β2 m
F
+IPTG
-IPTG
MWM
kDa
75
35
25
17
11
β2 m
G
Pure IB
MWM
kDa
48
35
25
17
11
β2 m
H
Absorbance
Conductance
Peak1
Peak 4
Peak 2
Peak 3
Elution (ml)
I
Peak 4
Peak 3
Peak 2
Peak 1
MWM
kDa
75
48
35
25
17
11
J
Molar Elipticity deg cm2 dmol-1
4000
2000
0
-2000
-4000
Peak 2
200 210 220 230 240 250 260
Wavelength (nm)
K
MWM
Monomer
kDa
48
35
25
17
11
L
Strept-PE
Monomer
Tetramer
IB;Strep-HRP

Fig. 3.4 Identifying virus-specific T cells in response to HSV1 infection in zebrafish.

A. Experimental plan for the detection and kinetics of HSV1 specific $CD8^+$ T cell response in HSV1 infected zebrafish. The total splenocytes were collected at indicated time points and stained with Uda-SSIEFARL-tetramer. B. Detection of virus-specific $CD8^+$ T cells in uninfected and HSV1 infected (5 dpi) from the splenocytes of zebrafishes. $tetramer^{+ve}$ cells backgated to identify their source in forward and side scatter plots. C. Representative FACS plots showing $tetramer^{+ve}$ cells in from different groups of animals are shown. The frequencies of the gated $tetramer^{+ve}$ cells is shown in the FACS plots D. Cumulative data is shown for the frequencies of virus-specific T cells in HSV1 infected zebrafishes.

A

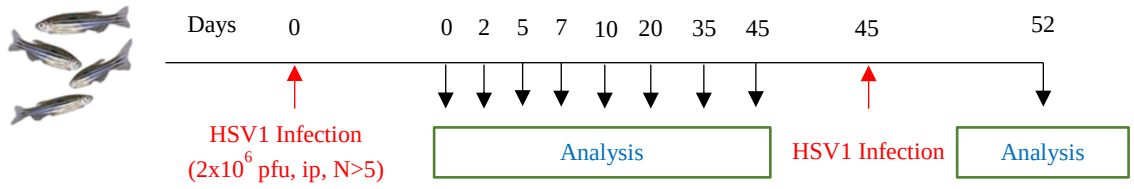
Days
0
0 2 5 7 10 20 35 45
45
52
HSV1 Infection
(2x10^6 pfu, ip, N>5)
Analysis
HSV1 Infection
Analysis

B

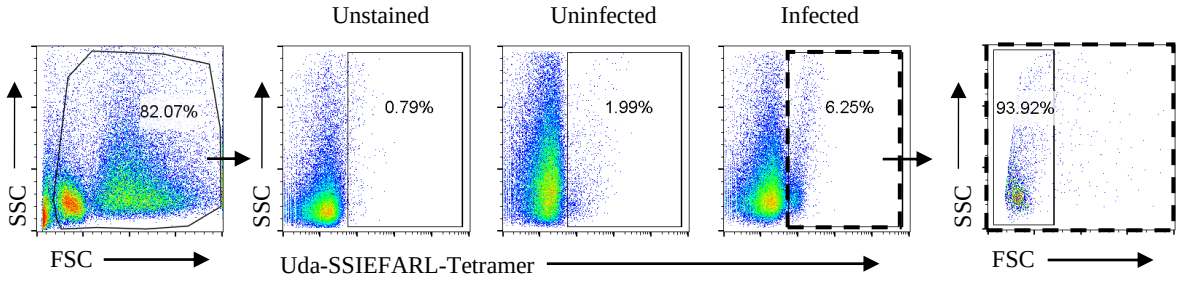
Unstained
Uninfected
Infected
82.07%
0.79%
1.99%
6.25%
93.92%
SSC
FSC
Uda-SSIEFARL-Tetramer

C

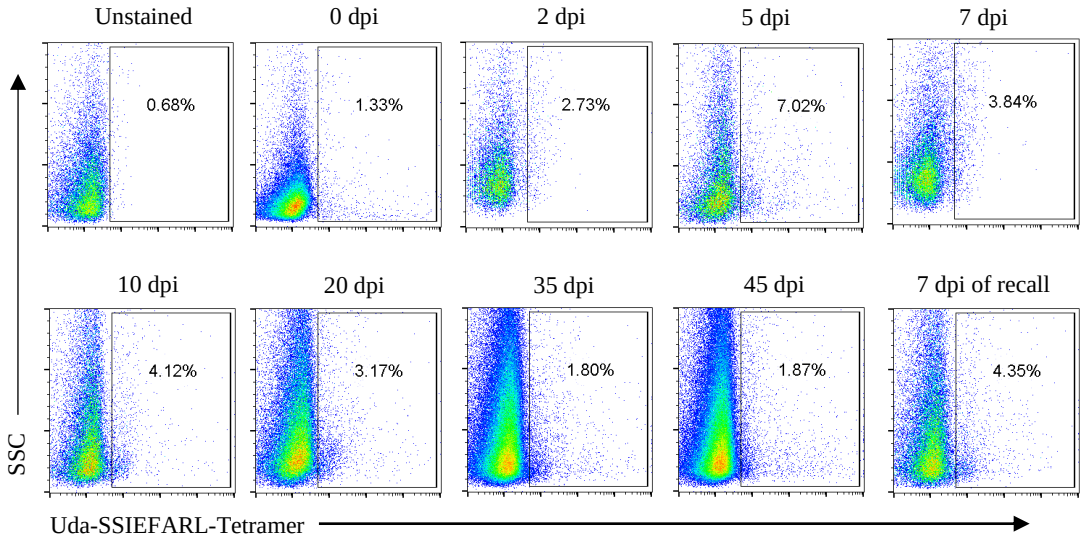
Unstained
0 dpi
2 dpi
5 dpi
7 dpi
0.68%
1.33%
2.73%
7.02%
3.84%
10 dpi
20 dpi
35 dpi
45 dpi
7 dpi of recall
4.12%
3.17%
1.80%
1.87%
4.35%
SSC
Uda-SSIEFARL-Tetramer

D

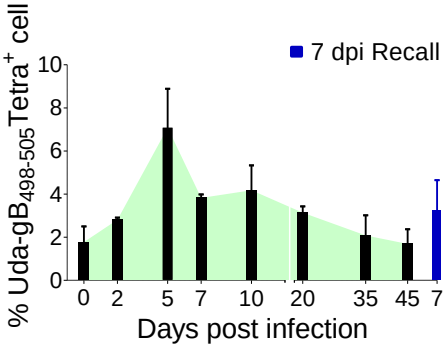
7 dpi Recall
% Uda-gB498-505Tetra+ cell
0
2
4
6
8
10
0 2 5 7 10 20 35 45 7
Days post infection

Fig. 3.5 Cytokines production abilities of lymphocytes isolated from HSV1 infected zebrafish.

The expression of genes encoding for pro-inflammatory cytokines was measured in lymphocytes sorted from uninfected and HSV1 infected animals using quantitative RT-PCR. A. A schematic of the experimental plan for measuring the cytokine level post HSV1 infection is shown. B. After singlet discrimination the total lymphocytes were sort purified on the basis of scattering properties. C. Representative FACS plot show the post sort purity check for sorted cells. D. Cytokines mRNA level in sorted lymphocytes at mentioned time point of HSV1 infection is shown by bar graphs. E. qPCR was performed to measure CD3e and CD8α mRNA molecules in the gated lymphocyte population of sorted cells and the comparative expression for the total live splenocytes is shown. At each time points N>15 animals, where error bars indicate ± SD. ***P < 0.001, **P<0.01, *P<0.05 and NS (P>0.05)- not significant (One way ANOVA, Tukey's test).

A

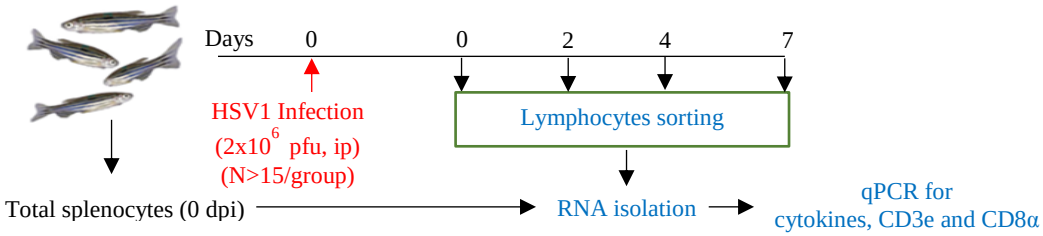
Days 0 0 2 4 7
HSV1 Infection
(2x10^6 pfu, ip)
(N>15/group)
Lymphocytes sorting
Total splenocytes (0 dpi)
RNA isolation
qPCR for
cytokines, CD3e and CD8α

B

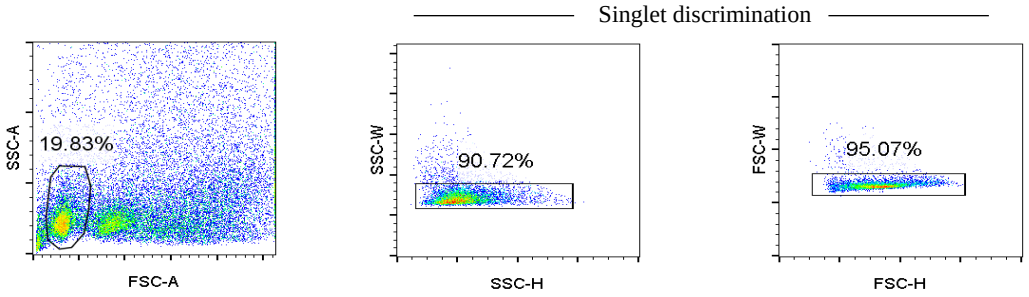
Singlet discrimination
SSC-A
19.83%
FSC-A
SSC-W
90.72%
SSC-H
FSC-W
95.07%
FSC-H

C

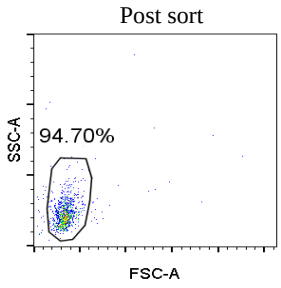
Post sort
SSC-A
94.70%
FSC-A

D

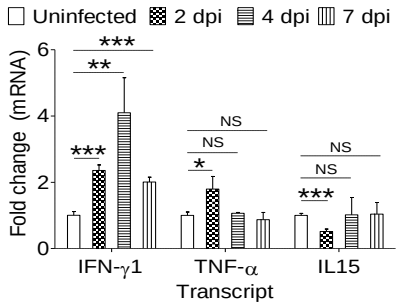
Uninfected
2 dpi
4 dpi
7 dpi
Fold change (mRNA)
IFN-γ1
TNF-α
IL15
Transcript
NS
***
**
*

E

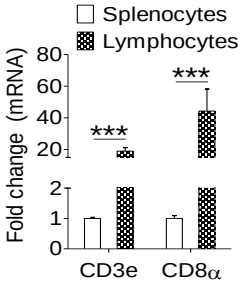
Splenocytes
Lymphocytes
Fold change (mRNA)
CD3e
CD8α
***

Fig. 3.6 Uda monomer generation with other peptides

Different peptides were used for refolding Uda HC and β_2m as using the similar experimental conditions that were used for SSIEFARL peptide. The representative chromatograms show the refolding of Uda with A. FAPG(Anp)YPAL and B. SIINFEKL peptide.

A

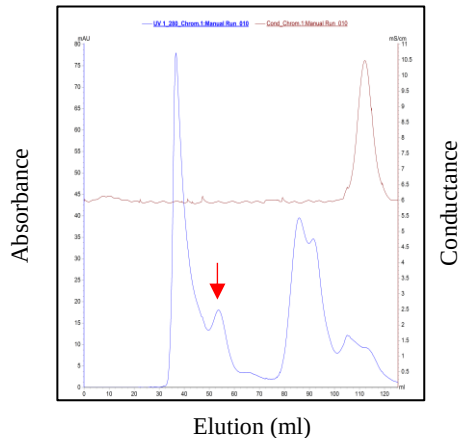

B

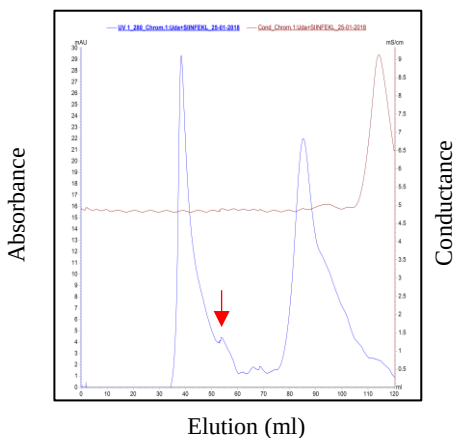

Summary and conclusions

Herpes simplex viruses are neurotropic viruses that belong to the alphaherpesvirinae subfamily under herpesviridae family. More than 75% of human population worldwide is infected with these viruses and many develop one or the other kind of overt diseases as the virus reactivates from the latent sensory neurons. Two types of α-herpesviruses, HSV1 and HSV2 infect humans. HSV1 causes skin, oral, ocular and genital infections, whereas HSV2 is predominantly responsible for genital infections. As the herpesviruses can alternately switch between two modes of life cycles these viruses are considered as the most successful pathogens. Depending on the immune status of host, the virus could adopt either a lytic or a latent life style. $CD8^+$ T cells are critically involved in either clearing the virus or keeping it in the latent stage in sensory neurons. The immune response generated by other immune cells such as $CD4^+$ T cells and neutrophils is considered as a major contributor to tissue damaging immunoinflammatory reactions. Infected individuals developing immunopathologies are generally treated with glucocorticoids but how do these regimens affect the differentiation of $CD8^+$ T cells is not well understood. The experiments were planned to investigate the influence of a transient therapy with a synthetic analogue of glucocorticoid, dexamethasone, in influencing the differentiation of herpesvirus-specific $CD8^+$ T cells in a mouse model as the first part of the dissertation. In the second part, the feasibility of using zebrafish as a model system for measuring the differentiation and dynamics of HSV1 expanded cytotoxic T cell response was explored. Zebrafish could allow for real time *in vivo* tracking of immune cell during herpesviral infections.

Glucocorticoids cause immunosuppression and their synthetic analogues are generally administered in patients not only to control inflammations caused by infections, autoimmune diseases but also to ensure the success of tissue transplantations procedures.

This is because of their enhanced bioavailability as such analogues are resistant to the enzyme, β-hydroxysteroid dehydrogenase 2 (11β-HSD2). Some of the known immunosuppressive effects of corticosteroids include a modulation of cytokine production by immune cells, an altered cellular trafficking, the promotion of phagocytosis as well as the enhancement of regulatory T cell functions. How corticosteroids dictate the fate and function of virus-specific $CD8^+$ T cells still remain ill explored and this issue was investigated in the current study. $CD8^+$ T cells are critically involved in controlling viral infection. Therefore, the effect of an immunosuppressive corticosteroid therapy was investigated on differentiating $CD8^+$ T cells during HSV1 infection.

A transient dexamethasone therapy differentially affected the counts of immune cells as well their functionality during HSV1 infection. Although the treatment of infected mice reduced the total leukocytes ($CD45^+$ cells) in the host but myeloid cells remained unaffected. The drug treatment reduced the count of leukocytes as well as naïve $CD8^+$ T cells, but more frequency of the antigen activated $CD8^+$ T cells persisted. This observation further led us to decipher divergent effects of dexamethasone therapy in various subsets of $CD8^+$ T cells. Dexamethasone exerts its effect via genomic and non-genomic mechanisms. The genome mechanisms are likely to exert enhanced and a wide varieties of regulatory functions. So we focused to elucidate the role of the genomic pathway that require the ligation of glucocorticoid receptor (Nr3c1) in the cytosol. The complex then translocates to the nucleus to alter gene expression.

The results show that the expression of Nr3c1 is tightly regulated during the differentiation of naïve $CD8^+$ T cells into effector and memory generation during herpesvirus infections. Both α- (HSV1) and γ- (MHV68) herpesvirus infection-expanded $CD8^+$ T cells (activated) down regulated their Nr3c1 expression in the acute phase of the response. Nr3c1 expression levels in $CD8^+$ T cells enhanced their susceptibility to

dexamethasone-induced apoptosis that led to a skewed virus-specific $CD8^+$ T cell response in the acute phase of infection. Dexamethasone mediated preferential killing of quiescent $CD8^+$ T cells led to an inefficient anti-virus $CD8^+$ T cell immunity during a subsequent infection. The residual cells preferentially however preferentially homed to inflammatory tissue sites due to their enhanced expression of molecules such as CD103 and CXCR3 as well as the transcription factor, Tbet that regulates CXCR3 and IFN-γ expression in $CD8^+$ T cells. Surprisingly the transient drug treatment induced an activation of surviving $CD8^+$ T cells in the absence of an overt TCR stimulation and additionally enhanced memory precursor generation potential as well as their proliferation. Therefore the dexamethasone exposed activated $CD8^+$ T cells survived longer as memory cells and exerted an enhanced protective potential to clear the viral infection upon a challenge. Our study therefore calls into question the logic of corticosteroid therapy for managing persistent inflammatory conditions but at the same time also describes the strategy to harness untapped potential of corticosteroids in promoting differentiation of immune memory cells.

In the second half of the dissertation, the feasibility of using zebrafish as a model organism to explore the differentiation of virus-specific $CD8^+$ T cells was investigated. Zebrafish (*Danio rerio*) has been extensively used as a model system to study development and regeneration, haematopoiesis and to also elucidate different immunological phenomena in lower vertebrates. Despite some data to demonstrate the presence of immune cells by transgenesis approaches, the immunophenotyping, the functionality and differentiation of cytotoxic T cells have not been described in zebrafish.

Visual transparency of the developing zebrafish provides unmatched advantages for cellular tracking in real-time, efficient visualization of cellular interactions and migratory potential of cells from the immune inductive sites to infection sites. The other

attributes which make adult zebrafish a better biological model system is its smaller size, relatively short life cycle, ease of handling, the requirement of smaller doses of inoculum as well as the availability of a growing list of molecular tools and reagents to manipulate its genome. Zebrafish has been used as a valuable model for elucidating events involved in innate immune responses and inflammation. A demonstration in some recent studies that the cells of adaptive immune system such as γδ T cells and Treg-like cells occurs in zebrafish further provides support to our studies aimed at exploring their potential as a model system to investigate cytotoxic T cells dynamics during viral infections.

The unavailability of reagents to detect antigen-specific $CD8^+$ and $CD4^+$ T cells in zebrafish however still remains a major hurdle in utilizing the optimal potential of this model and to study the differentiation and function of T cells. Therefore, the investigation focused to first generate class I MHC tetramers to identify antigen-specific $CD8^+$ T cells and then to measure their kinetics during a herpesvirus infection. Understanding events involved in the activation and differentiation of cytotoxic $CD8^+$ T cells that contribute to the eradication of pathogens and capturing such events in live animals is topical. Therefore class I MHC tetramers as fluorescent probes for zebrafish were generated to detect and characterize antigen-specific $CD8^+$ T cells during herpesvirus infection. These tetramers were then used to measure the kinetics of HSV1 specific $CD8^+$ T cells and their ability to produce effector molecules such as IFN-γ and TNF-α in experimentally infected zebrafishes. These studies pave the way for extensive utility of zebrafish as a model system for elucidating the differentiation pathways of antigen-specific $CD8^+$ T cells responses.